2013

The Metabolic Transitions Regulated by the Estrogen-related Receptor (ERR) in Drosophila melanogaster

Yan Li
Virginia Commonwealth University

THE METABOLIC TRANSITIONS REGULATED BY THE ESTROGEN-RELATED RECEPTOR (ERR) IN *DROSOPHILA MELANOGASTER*

A dissertation submitted in partial fulfillment of the requirements for the degree of Doctor of Philosophy at Virginia Commonwealth University.

by

YAN LI
B.S., Shandong University, P. R. China, 2007

Director: KEITH D. BAKER
ASSISTANT PROFESSOR, DEPARTMENT OF BIOCHEMISTRY AND MOLECULAR BIOLOGY

Virginia Commonwealth University
Richmond, Virginia
December, 2013

Acknowledgement

This dissertation could not have been written without Dr. Keith Baker who not only served as my mentor but also encouraged and challenged me throughout my academic program. I am very much impressed and influenced by his high standard of scientific integrity, enthusiasm in basic science, extensive knowledge and creative ideas in research, and the way of enjoying life. Keith had been and always will be an inspiration to me as a true scientist. I would like to give sincere gratitude to Keith for all his great help and support on my research.

I must dedicate my special thanks to all the individuals who contribute to this dissertation. Dr. Catherine Dumur from Department of Pathology in VCU performed all microarray analyses and helped analyzing data. Metabolon Inc. at Durham, NC performed all the GC/LC-MS to make our metabolic analysis possible. Dr. Leon Avery from Department of Physiology and Biophysics in VCU helped me with the principle component analysis. Dr. Jessica Bell from Department of Biochemistry and Molecular Biology in VCU provided me with purified GST recombinant protein. Dr. Tomek Kordula also from Department of Biochemistry and Molecular Biology in VCU taught me many techniques in person. Without them, my research could not have been completed.

I would also like to give my thanks to my thesis committee members, Dr. Andrew Larner, Dr. Frank Fang, Dr. Joyce Lloyd, and Dr. Michael Grotwiel. They provided me

with advice and encouragement that helped me to improve the quality of my research.

My deepest gratitude goes to Dr. Andrew Larner, Dr. Youyang Jai, Dr. Leon Avery, Dr. Tomek Kordula, and all the lab members in their labs, who provided many interesting thoughts and suggestions to my project in our group meeting and journal club discussion.

My special thanks also go to Luciana Gentile who supported me emotionally as my dear friend and also helped me to collect GC-MS sample as my lab member. I am also indebted Jiang Yang and Xinping Xu from Department of Physiology, who endeared me as a good friend and also gave me helpful advices for protein purification.

Last but not least, I can never achieve what I have accomplished without the care and unconditional love from my family and my husband, Wenan Chen. Their trust in my capability will always be my source of strength.

Table of Contents

Page

B Appendix table 2 Metabolic analysis of carbohydrates by GC/MS and LC/MS.

C **Author contributions:** Keith D. Baker conceived and designed the experiments. Yan Li performed most experiments, Catherine Dumur performed all the microarray analyses, Metabolon Inc. performed the GC/LC-MS, and Keith D. Baker performed the yeast two hybrid analysis and the GST pull- down experiments. Yan Li and Keith D. Baker analyzed the data, and performed statistical analysis. Leon Avery performed the principle component analysis. Contributed reagents/materials/analysis tools: Bloomington Stock Center provided several fly strains, and Jessica Bell provided the purified GST recombinant protein.

List of Tables

Page

List of Figures

Page

List of Abbreviations

ERR	Estrogen-related receptor
ATP	Adenosine triphosphate
HIF	Hypoxia inducible factor
CoA	Coenzyme A
L1 larvae	1st instar larvae
L2 larvae	2nd instar larvae
L3 larvae	3rd instar larvae
NRs	Nuclear receptors
GRs	Glucocorticoid receptors
ARs	Androgen receptors
ERs	Estrogen receptors
DNA	Deoxyribonucleic acid
PPAR	Peroxisome proliferator-activated receptor
LXR	Liver X receptor
FXR	Farnesoid X receptor
RXR	Retinoid X receptor
LXRE	LXR response element
FXRE	FXR response element

ERRE	ERR response element
ERE	ER response element
DR	Direct repeat
TR	Thyroid hormone
RAR	Retinoic acid
VDR	Vitamine D
EcR	Ecdysone
DBD	DNA-binding domain
LBD	Ligand-binding domain
AF-1	Activation function region-1
Ad	Autonomous transactivation domain
AF-2	Activation function-2
20E	20-hydroxyecdysone
JH	Juvenile hormone
HNF4	Hepatocyte nuclear receptor 4
MODY	Early onset type 2 diabetes
LCFAs	Long chain fatty acids
NTD	N-terminal domain
PGC-1	PPARγ coactivator-1
RIP140	Receptor-interacting protein 140

BAT	Brown adipose tissue
TCA cycle	Tricarboxylic acid cycle
OXPHOS	Oxidative phosphorylation
MCAD	Medium-chain acyl-CoA dehydrogenase
FAO	Fatty acid oxidation
ROS	Reactive oxygen species
IFN	Interferon
T2DM	Type 2 diabetes
AIB 1	Amplified in breast 1
VEGF	Vascular endothelial growth factor
OPG	Osteoprotegerin
CCNE1	Cyclin E 1
NADPH	Reduced nicotinamide adenine dinucleotide phosphate
IDH	Isocitrate dehydrogenase
miR	MicroRNA
LDH	Lactate dehydrogenase
ARNT	Aryl hydrocarbon recptor nuclear translocator
Asn	Asparagine
CAD	C-terminal activation domain
ODD	Oxygen-dependent degradation domain

PHD	Prolyldehydroxylase
VHL	von Hippel-Lindau
Pro	Proline
FIH-1	Factor inhibiting hypoxia inducible factor-1
CBP	CREB-binding protein
PCA	Principle component analysis
GFP	Green fluorescent protein
Hr/hrs	Hour/hours
RTP	Relative to the onset of pupariation
SAM	The significance analysis of microarray
ANOVA	Analysis of variance
PBS	Phosphate buffered saline
EDTA	Ethylenediaminetetraacetic acid
PFK	Phosphofructokinase
AEL	After egg laying
FDR	False discovery rate
HI	HIF-independent
HD	HIF-dependent
RNA	Ribonucleic acid
GO category	Gene ontology category

GC/LC-MS	Gas and/or liquid chromatography
MEFs	Mouse embryonic fibroblasts
Ru5P:Xu5P	Ribulose 5 phosphate : Xylulose 5 phosphate
S7P	Sedoheptulose 7-phosphate
GST	Glutathione S-transferase
ED	dERR-dependent
DM	Double-mutant-dependent
NMNAT	Nicotinic Acid Mononucleotide Adenylyltransferase
GAPDH	Glyceraldehyde 3-phosphate dehydrogenase
cAMP	Cyclic adenosine monophosphate
eEF2	Elongation factor 2
UTR	Untranslated region
eIF4E2	Eukaryotic translation initiation factor 4E type 2
DHAP	Dihydroxyacetone phosphate
HRE	HIF response element
IDF	International diabetes federation
FAs	Fatty acids
SCFAs	Short-chain fatty acids
MCFAs	Medium-chain fatty acids
VLCFAs	Very-long-chain fatty acids

TGs	Triglycerides
mβ-ox	Mitochondrial β-oxidation
ACS	Acyl-CoA synthetase
CPT-I/II	Carnitine palmitoyltransferase I/II
CAT	Carnitine-acylcarnitine translocase
pβ-ox	Peroxisomes β-oxidation
ER	Endoplasmic reticulum
ACC	Acetyl-CoA carboxylase
AMPK	5'-AMP-activated kinase
PPRE	PPAR response element
IGF	Insulin-like growth factor
PP	Prepupa
RT-PCR	Reverse transcription polymerase chain reaction
DMSO	Dimethyl sulfoxide
AMP	Adenosine monophosphate
ACSBG1/2	Acyl-CoA synthetase bubblegum family member 1/2
CHIP	Chromatin Immunoprecipitation
CHIP-seq	Chromatin Immunoprecipitation-sequencing
EMS	Ethyl methanesulfonate
RNAi	RNA interference

mRNA	Messenger RNA

Abstract

By Yan Li

A dissertation submitted in partial fulfillment of the requirements for the degree of Doctor of Philosophy at Virginia Commonwealth University.

Virginia Commonwealth University, 2013

Major Director: Dr. Keith D. Baker
Assistant Professor, Department of Biochemistry and Molecular Biology

In multicellular organism, bioenergetic metabolism is strictly regulated toward efficient generation of ATP. However, in certain situations, such as in limiting oxygen or in the rapidly proliferating system like growing juvenile or cancer cells, organisms apply the metabolic strategy that favors the production of biomass (e.g., nucleotides, amino acids, and lipids) over efficiency of ATP generation. The conserved estrogen-related receptors (ERRs) are master regulators in controlling metabolic homeostasis, and good candidates for mediating the metabolic transition induced by hypoxia and development.

First, we investigate how dERR influences hypoxic adaptation in *Drosophila melanogaster*. We find that dERR is required for a competent hypoxic response alone, or together with hypoxia inducible factor (HIF), which is the main transcription factor modulating the hypoxic adaptation. We show that dERR binds to dHIFα and participates in the HIF-dependent transcriptional program in hypoxia. In addition, dERR acts in the absence of dHIFα in hypoxia and a significant portion of HIF-independent transcriptional responses can be attributed to dERR actions, including up-regulation of glycolytic transcripts. These results indicate that competent hypoxic responses arise from complex interactions between HIF-dependent and -independent mechanisms, and that dERR plays a central role in both of these programs.

Secondly, we examine how dERR modulates metabolic transition toward the fatty acid oxidation at late L3 larva stage. We show that dERR is essential for the expression of an uncharacterized long-chain-fatty-acid acyl-CoA synthetase, CG4500, which is subject to induction by starvation. Furthermore, late L3 larvae of *dERR* mutants exhibit altered lipid profiles with elevated medium-chain and long-chain fatty acids. Together, with the previous finding that ERR directs an early switch toward glycolysis in the embryo, our studies indicate that ERR is a master regulator of programmed metabolic shifts through *Drosophila* development.

CHAPTER 1 Introduction

1.1 Molecular mechanism of nuclear receptor function

Nuclear receptors (NRs) are a superfamily of ligand-inducible transcription factors that control diverse processes, including metabolic homeostasis, detoxification, cellular differentiation and embryonic development. NRs are responsible for sensing small molecules that include steroid and thyroid hormones, vitamins, and many metabolites. Unlike convoluted signal-transduction pathways with membrane-bound receptors, like other transcription factors NRs directly bind to DNA and regulate the expression of adjacent genes. Upon stimulation, these receptors, form monomers, homodimers, or heterodimers, and transcriptionally regulate the expression of their target genes, thereby directly controlling biological processes (1-4). There are 48 NRs in human (5), and they can be categorized into three classes, based on their ligand-binding and DNA-binding characteristics (2). The first class is the classical steroid hormone receptors, like glucocorticoid receptors (GRs), androgen receptors (ARs) and estrogen receptors (ERs). The only sources of ligands for this class of receptors are steroid hormones that are regulated by negative-feedback control of the hypothalamic-pituitary axis. The binding affinity between ligand and these receptors is fairly high (dissociation constant K_d = 0.01 to 10 nM) (6). Steroid receptors that are produced in their inactive form reside in the

cytoplasm and/or nucleus and form complex with heat-shock proteins (HSP). Upon binding to hormones, these receptors are dissociated from chaperone protein complexes and are allowed to bind to specific DNA sequence known as hormone response elements (HREs) in target genes, which consist of two inverted repeat half-sites separated by a variable length of DNA (3). The second class of NRs is known as orphan nuclear receptors. They do not have known endogenous ligands and in some cases even function in a ligand-independent manner. A large subset of this category of NRs primarily binds to DNA as monomers, but other members of this group could function as homodimers or heterodimers. Whether or not they form dimers, only a single receptor DNA binding domain attaches to a single half-site response element (2). The next class of NRs are the so-called 'adopted' orphan receptors (also known as type II receptors), including fatty acid receptors (PPARs), oxysterol receptors (LXRs), and the bile acid receptor (FXR). They were first considered as orphan receptors, but naturally occurring ligands were identified subsequently. These receptors form heterodimers with the retinoid X receptor (RXR), and recognize hormone response elements that consist of two direct hexameric repeats separated by varied number of nucleotides for different receptors. For example, PPAR/RXR response element has an interspacing of one basepair (DR1), but LXREs and FXREs have an interspacing of four nucleotides (DR4) (7, 8). They function as lipid sensors by transcriptionally regulating genes that are widely involved in lipid metabolism, storage, transport, and elimination. Ligand binding to these receptors causes

dissociation of co-repressor proteins and recruitment of co-activator proteins, which initiates a feedforward metabolic cascade that maintains lipid homeostasis (4). In addition to the adopted orphan receptors, four NRs also form a complex with RXR, but cannot be fit in to either feedforward or feedback models precisely. They are thyroid hormone (TR), retinoic acid (RAR), vitamin D (VDR), and ecdysone (EcR) receptors as a *Drosophila* NR. Their ligands and target pathways engage elements of both the endocrine and lipid-sensing receptor pathways. For example, EcR not only acts as endocrine receptors in regulating development and reproduction in *Drosophila*, but also functions as a lipid sensor, because its ligand, ecdysone, is converted from cholesterol that is essential dietary lipids. These four receptors may fill the evolutionary gap between steroid receptors and adopted orphan receptors (4).

NRs consist of typical structural elements, including a variable amino N-terminal activation domain, a highly conserved DNA-binding domain (DBD) and a relatively conserved C-terminal ligand-binding domain (LBD). N-terminal domain containing at least one activation function region (AF-1) and several autonomous transactivation domains (Ad) is highly variable in length and function (9). DBD often consist of two zinc-fingers. The first zinc-finger has a stretch of five amino acids called the P-box, which mediates the binding between DNA and DBD (10). The second zinc-finger contains a moderately weak dimerization interface that permits DBDs to form dimers when exposed to a target DNA molecule (11). The relatively conserved LBD is the

largest domain in NR protein. The 12 α-helix secondary structure of LBD is better conserved than the primary sequence (12). As its name suggests, LBD bears the function of interacting with ligands. But other than ligand binding, the LBD participates in several other NR functions, such as forming homo- and/or heterodimers, nuclear localization, formation of heat-shock protein complexes (steroid receptors only), and, most importantly, transcriptional activation or repression (3). LBDs mediate transcriptional up-regulation or down-regulation through interacting with either co-activator or co-repressor proteins, respectively. Generally, binding to ligands causes the conformational changes in an α-helical region in the C terminus of LBD, also known as activation function2 (AF2). These structural changes facilitate the binding with co-repressor or co-activator proteins that often contain a consensus sequence LXXLL in their interaction motif (12, 13).

1.2 *Drosophila melanogaster* as a model for nuclear receptor biology

Drosophila melanogaster, also known as the fruit fly, is a widely used model organism. It features easy to care for, low cost, fast development, and well-established genetic and genomic tools. It is a species in the family of *Drosophilidae*. The developmental period for fruit fly varies with temperature. At 25°C, eggs normally take 24 hours to hatch as first-instar larvae (L1). L1 and second-instar larvae (L2) generally grow 24h until molting to the next stage, and third-instar larvae (L3) normally grow 48h until pupariation. Metamorphosis is about 5 days long, after which the adults emerge. L2

larvae need to reach a critical mass of about 0.3mg to pupariate. Until mid-L3, larvae are burrowed in food and eat constantly. After mid-L3, larvae exit the food and start to wander. The larvae reach their highest wet weight and dry weight in mid-L3. In the four days of development from embryos to mid-L3, the fruit fly larvae experience a 200-fold increase in mass (14).

Although studies in mammals have revealed the molecular mechanism of how NRs transcriptionally regulate target genes, their biological roles in many processes, including development and energy homeostasis, still require further investigation. In addition to a well-established model organism, the fruit fly has other special advantages to study NRs biology. Firstly, the hormone signaling pathways in *Drosophila* is less complex compared to humans. Only two physiologically active lipophilic hormones, the steroid hormone 20-hydroxyecdysone (20E) and the sesquiterpinoid juvenile hormone (JH), have been identified in fruit fly. Furthermore there are only 18 nuclear-receptor genes found in *Drosophila* genome, versus 48 genes in humans. Secondly, NRs in fruit flies still represent all the main NR superfamilies (1). Furthermore the structure and operating function of NRs are also conserved between fly and humans. For example, ultraspiracle (USP), an ortholog of the vertebrate RXR, works as an heterodimeric partner for many fly NRs, just as its vertebrate counterparts (15). Hepatocyte nuclear receptor 4 (HNF4) is a good example of the functional similarity of NRs between flies and humans. HNF4 has two paralogs in mammals, HNF4α and HNF4γ. In humans, it has been shown that

HNF4α is associated with MODY (early onset type 2 diabetes), whose patients show defects in the expression of genes involved glucose and lipid metabolism genes. But the function of HNF4γ is not very well understood (16, 17). Genetic mutation of HNF4 in flies revealed reduced ability to generate energy from stored fat under starvation through significant down-regulation of genes involved in lipolysis and β-oxidation. Together with the fact that long chain fatty acid (LCFAs) can tightly bind with and activate HNF4, it suggests that HNF4 is activated by fatty acids released from triglycerides, and then induces genes involved in fatty acid oxidation for energy production. This is a feed-forward model; similar to the model of adapted orphan receptors introduced previously (18). Lastly, I want to point out that our work on the estrogen-related receptor (ERR), which is the main focus of this document, is another great example of using fruit fly as an ideal system for investigating the regulation and function of NRs in vivo.

1.3 Estrogen-related receptors (ERRs) control metabolic gene networks in mammals

Estrogen-related receptors (ERRs) were the first orphan nuclear receptors found in the NR superfamily. There are three paralogs (ERRα, β, and γ) in mammals. ERRα (NR3B1) and ERRβ (NR3B2) were first discovered in a screen to identify genes encoding proteins closely related to estrogen receptor α (ERα, NR3A1) from kidney and heart (19). ERRγ (NR3C3) was found later by several studies (20-22). In addition to the

three isoforms, several splice variants of ERRβ and ERRγ were also identified in humans, but their function is not currently understood (23).

Each of these ERRs has the typical structural elements of NRs, including a non-conserved NTD, a highly conserved DBD, and a fairly conserved LBD. Unlike the other NRs, the three ERRs share appreciable amino acid similarity in their NTDs. Posttranslational modification, including mainly phosphorylation and sumoylation, can affect the transcriptional activities of ERRs. Phosphorylation on serine 19 subsequently results in sumoylation of lysine 14 in ERRα and γ, leading to inhibition of the transcriptional activity of both receptors via a functional phospho-sumoyl switch motif (24, 25). Interestingly, PPARγ also has a phospho-sumoyl switch motif within its NTD (26), which suggests that phosphorylation-dependent sumoylation might play an important role in the transcriptional control of energy metabolism by nuclear receptors. ERRs recognize the ERR response element (ERRE) containing the consensus sequence TCAAGGTCA, as monomer, a homodimer, or heterodimer (27). In addition to recognizing an ERRE, that is a single core motif preceded by three nucleotides, ERRs can also interact in tubes with estrogen response element (ERE) that is an inverted repeat of AGGTCA with three nucleotides in between (28). However, investigations have revealed that ERRs tend to regulate their target genes, and also ER targets via ERREs, rather than an ERE. Studies done in breast cancer showed that ERRα is preferentially recruited to ERRE enriched regions, and binding to EREs happen infrequently and mostly when

combined with an ERRE (29). It suggests that ERRα regulates transcription in an ERα-independent manner in breast cancer cells. So the overlapping function between ER and ERRs is not as important as it was anticipated. Although ERRs are orphan NRs, their LBD has a conserved AF-2 helix motif and can interact with synthetic molecules like 4-hydroxytamoxifen, co-activator such as PPARγ coactivator-1α and β (PGC-1α/β), and co-repressor proteins such as RIP140 (30, 31). Notably, the AF-2 motif stays in an active configuration even in the absence of a ligand, which suggests that ERRs are capable of binding to co-activators no matter the presence of ligands (32). In fact, full transcriptional activity of ERRs depend on PGC-1α/β in most cellular contexts, which makes PGC1s function as alternate protein ligands for the ERRs (33).

The expression pattern for ERR isoforms is not uniform. However, all three of them are abundantly present in organs maintaining high metabolic needs, including the heart and kidneys. ERRα is expressed in most tissues and in more abundant quantities than the other two isoforms. Other than heart and kidney, ERRα is also highly expressed in the intestinal tract, skeletal muscles, and brown adipose tissue (BAT), but ERRβ and ERRγ tend to be expressed in organs associated with basal metabolic functions. This distribution hints that three ERR isoforms collectively play key roles in regulating networks of energy metabolism (34).

The ERRs are recruited to the promoter regions of nearly all enzymes involved in each step of the tricarboxylic acid (TCA) cycle, all parts of the oxidative phosphorylation

(OXPHOS) apparatus, lipid, glutamine, amino acid, nucleic acid and pyruvate metabolism and energy sensing in metabolic tissues (35-41). ERRs also bind to the regulatory region of more than 700 nuclear genes encoding mitochondrial proteins in many tissues and function collectively with PGC1 α and β to regulate mitochondrial biogenesis (42). Although all ERR isoforms are involved in controlling metabolic homeostasis, the specific function for each isoform is distinct and sometime even conflicting. ERRα, together with PGC-1α, transcriptionally regulates medium-chain acyl-coenzyme a dehydrogenase (MCAD), which is the rate-limiting enzyme of tissue FAO. Other studies have found a more profound role for ERRα in metabolic regulation. In SAOS2 cells, the ERRα/PGC-1α complex up-regulates 151 nuclear genes that encode proteins involved in many aspects of mitochondrial functions (mitochondrial protein synthesis and transport across the mitochondrial membrane, FAO, the TCA cycle, and OXPHOS) (43). However, ERRα null mice are lean and resistant to diet-induced obesity, display substantial impaired lipid absorption in the intestine and are incapable of adapting to cold temperatures (44-46). These phenotypes are unexpected considering that ERRα up-regulates genes involved in FAO and mitochondrial energy expenditure. It has been hypothesized that ERRα might be important in fat absorption in intestine, but this idea needs further investigation. Furthermore, ERRα is responsible to adjust energy imbalance induced by physiological pressures. For example, ERRα is essential for inducing mitochondrial reactive oxygen species (ROS) production in response to IFN-γ in bone

marrow-derived macrophages, as well as the adaptive bioenergetic response to hemodynamic stressors in heart (41, 47). These phenomena propose that ERRα could be a crosslink between metabolism and inflammation. Unlike ERRα null mice, mice lacking ERRγ present a lethal phenotype shortly after birth, due to their failure to switch from primarily depending on glycolysis to oxidative metabolism as a newborn pup. ERRγ also plays a role in promoting myogenesis. Overexpressing either constitutively active ERRγ or wild-type ERRγ in skeletal muscle enhances mitochondrial enzyme activity, exercise capacity, and expression of genes involved in fat metabolism. And overexpressing ERRγ promotes a switch toward more oxidative fiber types and vascularization in muscle (48, 49). In contrast, muscle specific loss of function of ERRγ form immature myotubes with reduced mitochondrial content and altered distribution, increased rates of medium-chain FAO, decreased rates of glucose oxidation and oxidative stress (50). These phenotypes suggest that the ERRγ, but not ERRα, is crucial for establishing and keeping a basal oxidative metabolic gene program (40). The function of ERRβ is not studied as extensively as the other two isoforms. This is probably because ERRβ null mice are embryonic lethal due to abnormal differentiation of the trophoblast lineage (51). However, the phenotypes of ERRβ null and ERRγ null mice also support the idea that the ERRs also control cell growth and differentiation during development.

1.4 ERRs is a potential therapeutic target in human diseases

ERRs are excellent drug target candidates, because the tertiary structure of their ligand-binding domains often permit binding of full and partial agonists, antagonists and inverse agonists (52). Emerging studies show that pharmacologically targeting ERRs could have a beneficial impact on human diseases, including breast cancer and metabolic disorders (obesity and type 2 diabetes).

As discussed previously, ERRα null mice are lean and resistant to high fat induced obesity (44). But the underlying molecular mechanism for this phenotype is not understood. It is not clear whether using a potent ERRα antagonist will lead to a similar phenotype. One epidemiological study in 703 Japanese individuals observed that a higher ERRE copy number was associated with a higher body mass index (53).This result would agree with the lean phenotype observed in the ERRα-null mice because more ERRα expression would lead to a higher body weight. However, a genome wide association study (GWAS) done in 334500 Danish white individuals revealed that ERRα is not associated with obesity, type 2 diabetes, or related quantitative traits (54). However, recent studies found that fasting and diabetes conditions induce hepatic ERRγ expression, which leads to increased expression of gluconeogenic genes and blood glucose in wild type mice. Also, ablation of hepatic ERRγ gene expression decreases gluconeogenic genes expression and normalizes blood glucose levels in mouse models of T2DM (55, 56). Interestingly, another epidemiological study found that the levels of bisphenol A, which has been shown to bind ERRγ with high affinity, in humans are linked with type 2

diabetes and metabolic dysfunction (57). However, further investigations still need to be done to address the specific molecular mechanisms that individual ERR isoforms affect the pathology of metabolic disorders including obesity and type 2 diabetes.

ERRs have also been found to be associated with cancer progression. ERRα has been found to be correlated with recurrence and adverse clinical outcomes; however, ERRγ is associated with favorable prognosis. In ovarian cancer cells, ERRα is expressed at high levels and correlates with advanced tumor stages and grades (58). In colorectal cancers, another study found that the mRNA level for ERRα is higher in the cancer mucosa than in the surrounding normal mucosa (59). In a breast cancer model, ERRα is not only inversely associated with ERα and the progesterone receptor (PR), which are markers of good prognosis and hormone sensitivity, but also found to be positively correlated with ERBB2 (a marker of aggressive tumor), Myc oncogene, the proliferation marker Ki-67 and the NR co-activator AIB1 (60-63). In contrast, ERRγ is positively linked with ER and ERBB2 that are marks of favorable prognosis in breast cancer (60). ERRα also has been shown to regulate the proliferation and migration of cancer cells. In a mammary gland xenografts model, ERRα can promote proliferation through inducing the expression of vascular endothelial growth factor (VEGF) and osteoprotegerin (OPG) (64). VEGF and OPG can function together to stimulate angiogenesis. Also, another study showed that down-regulation of ERRα would result in decreased proliferation and migratory capacity through down-regulating the expression of WNT11 and CCNE1 (65).

Importantly, because ERRs stand at the center hinge of the metabolic network, it would be surprising if ERRs did not regulate the distinct metabolic profile in cancer pathology. To support the fast growing profile, cancer cells undergo metabolic reprogramming that features a metabolic shift from oxidative respiration to an aerobic glycolytic profile. This phenomenon is called the Warburg effect (66, 67). The regulatory role of ERRs on metabolic transitions in fast growing system will be discussed extensively in the following manuscript. Lastly, I want to point out that ERRs can interact with functional HIF-1 and stimulate HIF-induced transcription, which also contributes to cancer pathology from not only metabolic perspectives (68). However, only a few HIF-1α target genes were tested in vitro in this study. The physiological role that the ERR/HIF complex plays under hypoxic conditions has not been tested. The regulatory role of dERR under hypoxia will be extensively discussed in chapter 2.

1.5 ERR regulates the metabolic transitions in fast growing programs (Warburg effect in cancer and *Drosophila* development)

In the first four days of development from embryos to mid-L3, *Drosophila* larvae experience a dramatic increase in mass as discussed in section 1.2. The fast-growing programs of larvae and cancer cells have similar metabolic needs. A large number of nucleotides, amino acids and lipids are needed to either grow (larvae) or proliferate (cancer). When larvae need to grow rapidly, they primarily depend on aerobic glycolysis

instead of OXPHOS, a program that resembles the Warburg effect during development. Again as mentioned previously, the Warburg effect refers to the phenomenon that most proliferating cell, including cancer cells but not limited to them, primarily rely on glycolysis rather than mitochondrial OXPHOS even under aerobic conditions (69, 70). However, normal differentiated cells depend primarily on mitochondrial OXPHOS to generate the energy needed for their function and growth. OXPHOS is aerobic, *i.e.* it uses oxygen. Later research found that the lower the OXPHOS capacity of tumor cells, the more aggressive they are (71). OXPHOS generates ATP more efficiently than does glycolysis. Catabolizing one mole of glucose by TCA cycle and OXPHOS can produce approximately 36 moles of ATP. But catabolizing one mole of glucose by aerobic glycolysis can only generate 2 moles of ATP. This raises the question why fast-proliferating tumor cells prefer glycolysis as their major way to produce energy. Originally, Warburg hypothesized that cancer cells have a defect in their mitochondria which leads to impaired aerobic respiration. However, later studies showed that many cancer cells largely maintain their mitochondrial function (72, 73). Alternative explanations of the Warburg effect are required to better understand this phenomenon. One possible explanation is that ATP production is not an issue when resources are abundant. Normal cells do not take up nutrients such as glucose unless they are stimulated by growth factors. But cancer cells have altered receptor-initiated signaling pathways and constitutively take up nutrients. This provides sufficient energy for the

survival and growth of tumor cells (74, 75). Proliferating cells have metabolic requirements in addition to their need for ATP. They must replicate all the cellular contents to produce daughter cells in mitosis. Thus, they need a large number of nucleotides, amino acids and lipids to produce new cells. For most mammalian cells, glucose and glutamine provide most of the carbon, nitrogen, free energy, and reducing equivalents. A glucose molecule can produce 36 ATPs (full oxidation), or 30 ATPs and 2 NADPHs (which go into the pentose phosphate pathway), or 6 carbons for macromolecular synthesis. From this perspective, ATP is not the only material needed for growth by cancer cells, but acetyl-CoA for fatty acids, glycolytic intermediates for nonessential amino acids, and ribose for nucleotides are all necessary as macromolecular precursors to support the proliferation of cancer cells (76). Cancer cells therefore need to catabolize glucose in such a way to provide all these resources, not just ATP. For example, a study showed that glioblastoma cells in culture convert about 90% of glucose and 60% of glutamine they take into lactate or alanine, and meanwhile NADPH is actively generated and important for fatty acid synthesis (77). Lactate dehydrogenase (LDH) is a key enzyme involved in converting glucose and glutamine to lactate. Possibly, LDH activity is required for generating enough NADPH which is needed by the fast proliferation. In many breast cancer cell lines and tissue sections, LDH activity has been found to be increased. More interestingly, later studies showed that inhibiting LDH activity in cancer cells stimulated their mitochondrial respiration and impaired their

proliferation (78). Furthermore, several studies showed that mutations of metabolic enzymes can directly assist carcinogenesis. Mutations in genes of the TCA cycle enzymes succinate dehydrogenase and fumarate hydratase have been found in a variety of cancers (79, 80). Mutations in cytosolic isocitrate dehydrogenase-1 and 2 (IDH 1 and 2) have been found in several human brain tumors (81-83). It becomes crucial to understand the molecular mechanism that directs this metabolic reprogramming not only in cancer cells but also in proliferating cells, in order to develop new anti-cancer therapies.

Accumulating evidence suggests that ERRs control the Warburg effect in proliferating cells such that ERRα assists in setting an aerobic glycolytic profile, but ERRγ rather tries to maintain the oxidative metabolic program. This hypothesis corresponds with the observations that ERRα is linked with poor prognosis but ERRγ is associated with better prognosis. ERRα is expressed in aggressive tumors that often display an increase in glucose uptake (84). Furthermore, ERRα not only up-regulates enzymes that are involved in the glycolysis pathway in breast cancer cells, but is also indispensable for the switch from oxidative to glycolytic metabolism in hepatocarcinoma cells (37, 85). On the other hand, the expression of ERRγ is inhibited by miR-378, which directs a metabolic reprogramming to an aerobic glycolytic phenotype in breast cancer cells (86). In spite of the fact that ERRα and ERRγ are recruited to the same set of target genes, can readily form heterodimers, and share a capability to regulate genes governing both the glycolytic and the oxidative mitochondrial respiration phenotype, the opposing

roles of the two isoforms in the establishment of a Warburg-like profile illustrate the complexity of metabolic reprogramming by ERR proteins in cancer cells (27). So it becomes very important to understand how ERRs control metabolic shift in a physiological context.

Drosophila is a great tool to study ERR biology. There is only one ERR in *Drosophila*, making it an excellent tool to study ERR function. ERRs are well conserved from flies to mammals. The dERR DBD and LBD are approximately 85% and 35% identical to mERR DBD and LBD. In 2011, *Tennessen et al.* showed that the expression of active dERR protein triggers a coordinate switch from OXPHOS toward glycolysis at late embryogenesis in flies, which is also considered as developmental Warburg effect (87). This report demonstrates that the role of the ERRs as regulators of carbohydrate metabolism and metabolic programs associated with proliferating cells is highly conserved from flies to humans. As discussed in previous sections, *Drosophila* undergoes massive proliferation during the first four days of development from embryos to mid-L3. Starting around day one after L3 onset, the larvae will go out of the food and start to wander and be prepared for pupariation. Then in the next 4 days, pupae undergo a total reconstruction of all body parts to form adult fly. During this period, they have to depend on burning the fat that was accumulated in their fast growing phase (the time from embryo to mid-L3), which is also considered as developmental starvation. Eventually, an adult fly will be emerge and run a metabolic program that very much resembles

differenciated mammalian cells. These phenotypes suggest flies trigger two switch-like metabolic reprogrammings. They have to turn on glycolysis in late embryogenesis to facilitate massive fat storage and turn it off right before pupariation in order to stop storing and start consuming fat. There is a study that showed that dERR governs the first transition, and hopefully our work here will provide evidence the dERR controls the second transition, but also control metabolic transitions induced by physical stress, like hypoxia. I hope my work in this thesis will provide a molecular context to understand the close association between mammalian ERR family members and human diseases, such as metabolic syndromes and cancer.

CHAPTER 2 HIF-and Non-HIF-Regulated Hypoxic Responses Require the ERR in *Drosophila melanogaster*

2.1 Introduction

Hypoxia is a condition in which the body or a region of the body is deprived of adequate oxygen supply. Hypoxia plays an essential role in the pathology of many disease, including heart disease, stroke, chronic lung disease, and especially cancers. Although in the past oxygen sensing was thought to be limited to certain cells, it is now been recognized that all nucleated cells in the body can respond to hypoxia (88). One important way that cells adapt to limiting oxygen is by transitioning from oxidative metabolism toward glycolytic lactate production for energy production. Specifically, cells convert glucose to pyruvate by glycolytic enzymes, and subsequently pyruvate will be derived either to acetyl coenzyme A (CoA) for oxidation in the tricarboxylic acid cycle (TCA) in the present of oxygen or to lactate by lactate dehydrogenase (LDH) as a glycolytic end product under hypoxia (89). Complementing this strategic change of metabolism are complex shifts in the transcriptome, which add durability to the initial hypoxic response. Hypoxia-inducible factor 1 (HIF-1) regulates the expression of genes that mediate the adaptive response to hypoxia. The HIF transcriptional complex is comprised of an oxygen-labile HIF-1α subunit and its stable partner HIF-1β. This

pathway is central to the hypoxic response and is highly conserved from worms to human (88). HIF-1 complex has been found to be important in the etiologies of many diseases, including cancers and heart disease (90-92); these conditions have a hypoxic component- and therefore an altered metabolic component - that is critical to disease progression.

In mammals, HIF-1α belongs to the family of basic-helix-loop-helix (bHLH)/PAS transcription factors. It forms a heterodimer with the constitutively expressed HIF-1β (aka aryl hydrocarbon receptor nuclear translocator or ARNT). Together they bind to the HIF response elements (HREs) in the promoter regions of their target genes to regulate transcription. Under normoxia, HIF-1α expression is tightly regulated and quickly degraded in the cytosol. Two prolyl residues in the oxygen-dependent degradation domain (ODD) of HIF-1α are Fe(II)- and O_2-dependently hydroxylated by prolyl dehydroxylase (PHD) (93). Then, HIF-1α binds to the von Hippel-Lindau (VHL) protein which can be recognized by the E3 ubiquitin ligase complex, leading to HIF-1α degradation by the proteasome. In mammals the two prolyl sites are Pro^{402} and Pro^{564} (94-96). Additionally, to fully function, HIF-1α needs to bind to the coactivator protein p300/CBP. Under normoxia, an asparagine site (Asn^{803}) in its C-terminal activation domain (CAD) is hydroxylated by FIH-1, which prohibits HIF-1α from interacting with p300. Without binding to p300, HIF-1α is not capable of completely up-regulating its target genes (97-99).

The number of transcripts impacted by HIF-1α is large and ontologically diverse. Despite this, a few affected pathways generally characterize HIF-mediated adaptation responses, including upregulation of angiogenic (100, 101), erythropoietic (102) and glycolytic transcripts (103, 104). The total hypoxic response, however, is not entirely dependent on the HIF pathway. For example, *Shen et al.* found 110 hypoxia response genes in C. elegans, 47 of which were induced in the absence of HIF (105). Although HIF-independent hypoxia-induced activities have also been identified in other organisms, these pathways remain poorly understood, though even in mammalian cells, HIF-1α is dispensable for hypoxic upregulation of a number of transcripts (106–108). These results suggest that HIF-independent hypoxic signaling mechanisms may act in concert with, or even supplant, the HIF response pathway in a context-dependent manner.

Drosophila melanogaster deal with no/low oxygen conditions well when compared to mammals, and can survive anoxic challenge for hours at a time (109, 110). This phenomenon is possibly due to the highly efficient gas exchange systems in flies. Flies maintain the three fundamental components of the HIF pathway: 1) the HIF prolyl hydroxylase (Fatiga); 2) dVHL; and 3) both components the HIF complex-dHIFα (encoded by sima) and Tango (dHIFβ). As in mammals, dHIFα has an ODD domain that is sufficient to direct oxygen-sensitive degradation when hydroxylated (111). While previous studies have examined hypoxic responses in adult flies (112, 113), the precise input that dHIFα has in this process has not been examined. In contrast, detailed studies

have shown that dHIFα plays a vital role in directing hypoxia-driven terminal branching of the tracheal system during development (114, 115). The Drosophila tracheal network serves as the fly respiratory system, and it is noteworthy that its developmental branching bears a striking resemblance to processes controlling mammalian angiogenesis (116). In addition, similar hypoxia-induced metabolic transitions have been reported in flies and mammals (117), although these remain poorly defined.

As thoroughly discussed in Chapter 1, the highly conserved dERR nuclear receptor directs a developmentally-regulated transcriptional switch towards glycolytic metabolism that supports developmental growth (87). This function is similar to that described for ERRα in vertebrates, which is associated with glycolytic metabolism and breast cancer (62, 118). Importantly, mammalian ERRs are also active participants in HIF-mediated hypoxic responses. They are directly recruited by HIF-1α to HREs and are required for a complete transcriptional response at specific promoters (68), suggesting that ERRs play a critical role in hypoxic responses.

Principal component analysis (PCA) is a widely used technique to transform a number of possibly correlated variables into a smaller number of uncorrelated variables called principal components. In general terms, PCA uses a vector space transform to reduce the dimensionality of large data sets. Using mathematical projection, the original data set with many variables can often be interpreted in just a few variables (the principal components). It is therefore often the case that an examination of the reduced dimension

data set will allow the user to spot trends, patterns and outliers in the data (119). In this study, we wanted to use PCA detect the general trends of the high-throughput GC-MS analysis that carried out on four experimental conditions (w^{1118} N, w^{1118} H, *sima* N, *sima* H). In our data, N is the number of metabolites and p is 4 (number of conditions). The mathematical background of principal component analysis will be explained briefly here. Let X denotes the $N \times p$ data matrix, where N is the number observations and p is the dimension of each observation. PCA first find the average metabolites m which is a 4×1 vector across all metabolites. It is the center of the N data points. PCA then subtracts the mean from all data points to form a centered data matrix X_c. Then PCA seeks the first projection direction v_1 onto which the variance of the projected data points has the maximal variance. This projection direction v_1 is called the first PC loading vector. The projected values from data point's $Xc \times v_1$ are called the first PC scores. The second PC loading vector v_2 is orthogonal to the first PC loading vector and maximizes the variance of projected data points. Correspondingly, the projected values from data points $Xc \times v_2$ are called the second PC scores. The kth PC loading vector v_k is orthogonal to the first (k-1) PC loading vectors and maximized the variance of projected data points. The associated projected values $Xc \times v_k$ are called the kth PC scores. In our application, the maximal number of PC loading vectors/PC scores is the dimension of the data points p. With the all the PC loading vectors and PC scores, the original data point x can be reconstructed as $x = m + PC_1 * v_1 + PC_2 * v_2 + \ldots + PC_p * v_p$.

In this Chapter, we wanted to investigate hypoxic responses in *Drosophila* and assess the influence of dHIFα on transcriptional and metabolic adaptation. We report here that the hypoxic transcriptional response segregates into distinct HIF-dependent and HIF-independent pathways. These pathways are differentially sensitive to hypoxic challenge in a temporal fashion during development, but both pathways are most sensitive prior to metamorphic onset and least active in the immediate hours following pupariation. Contrary to expectations, we find that upregulation of glycolytic transcripts is HIF-independent. Our metabolic analysis suggests that loss of dHIFα has a profound and wide-ranging effect on all aspects of carbohydrate catabolism when unchallenged in normoxia. In hypoxia, however, *dHIF (also called as sima)* mutants remain unable to mobilize glycogen, which is preferentially depleted under hypoxic conditions. We additionally show that dERR is required during hypoxia, in that it controls a unique set of hypoxia-regulated dERR-dependent transcripts that include HIF-independent glycolytic genes. Altogether, our studies raise important questions regarding the breadth of HIF involvement in hypoxic transitions and identify dERR as an essential factor that complements HIF-dependent and -independent responses.

2.2 Methods

2.2.1 Fly strains and hypoxic treatments

Flies were maintained on regular cornmeal-molasses-yeast media at 25°C. *sima* mutants (*sima*^{07607}) (120) were obtained from Bloomington Stock Center. w^{1118} animals were treated as controls. dERR mutants ($dERR^1/dERR^2$) are described elsewhere (87). *dERR,sima* double-mutants were generated by recombination of the *sima*^{07607} allele with each of the individual $dERR^1$ and $dERR^2$ mutations. Embryos were collected at 25°C for 14 hrs onto egg caps (molasses-agar media in 35 mm×10 mm dishes) with yeast paste. Mid-L2 larvae were transferred to a fresh egg cap with blue yeast paste (0.3% bromophenol blue), and allowed to develop until achieving the partial clear-gut L3 stage (-10 to -4 hrs RTP). Staged animals were moved to fresh agar plates and allowed to age an additional 6 hours at 25°C (normoxic treatment); or, animals were placed in an airtight Modular Incubator Chamber (Billups-Rothenberg, Inc., Del Mar, CA) for 6 hours at 25°C after a gas mixture containing 4% oxygen balanced with nitrogen was flashed into the chamber (hypoxic treatment). The *sima*^{07607} chromosome was carried over a TM3, twi-GFP (green fluorescent protein) balancer chromosome. Homozygous mutant larvae were sorted for the absence of GFP expression using a Zeiss Discovery V.8 dissecting stereoscope with fluorescence at mid-L2. For lethal phase analysis in Figure 2.8B, 0–4 hr post-hatch L1 larvae were sorted for fluorescence to assign genotype. Larvae were placed in vials containing fresh yeast paste and were then exposed to 21% (normal air) or 4% oxygen for 48 hrs and scored for lethality or completion of L1.

2.2.2 Microarray analysis

Microarray analyses were performed on at least three biological replicates of w^{1118} animals, *sima* mutants, *dERR* mutants, and *sima,dERR* double-mutants at the partial clear-gut L3 stage and treated for 6 hrs in normoxia or 4% O_2. For each biological replicate, at least 10 larvae were collected and washed with 1×PBS before homogenization in TRIzol (Invitrogen, Carlsbad, CA) using a VWR disposable pellet mixer. Total RNA was isolated using a TRIzol/RQ1 DNase hybrid extraction protocol (Promega, Madison, WI). Template labeling was done using the GeneChip 3' IVT Express Kit according to the manufacturer's specifications (Affymetrix, Santa Clara, CA). Hybridizations to Affymetrix GeneChip Drosophila Genome 2.0 arrays were performed using the manufacturer's recommendations. Every chip was scanned at a high resolution by the Affymetrix GeneChip Scanner 3000 according to the GeneChip Expression Analysis Technical Manual procedures (Affymetrix, Santa Clara, CA). Raw data were normalized with RMA (121) and analyzed with the significance analysis of microarray (SAM) program (122). No changes below 1.5-fold were considered significant. Additionally, the following false discovery rate percentages were imposed: 0.733% for w^{1118} normoxia vs. w^{1118} hypoxia; 0.414% for *sima* normoxia vs. *sima* hypoxia; 0.721% for w^{1118} hypoxia vs. *sima* hypoxia; 7.84% *dERR* normoxia vs. *dERR* hypoxia; 0.619% for w^{1118} hypoxia vs. *dERR* hypoxia; 0.662% *dERR,sima double-mutant* normoxia vs. *dERR,sima double-mutant* hypoxia; 0.703% for w^{1118} hypoxia vs.

dERR,sima double-mutant hypoxia. Microsoft Access was used to compare data sets. Microarray data from this study can be accessed at the Omnibus website (http://www.ncbi.nlm.nib.gov/geo) with the accession number GSE33100.

2.2.3 Quantitative RT-PCR

Total RNA samples were isolated as described above. RNA was reverse transcribed with the High Capacity cDNA Reverse Transcription Kit (Applied Biosystem, Carlsbad, CA) using the manufacturer's specifications. For real-time PCR, premixed primer-probe sets were purchased from Applied Biosystems, with the exception of the primer set used for *amylase*. For *amylase*, a standard SYBR Green (Bioline, Taunton, MA) protocol was used with the primer sets: 5' AACTACAACGACGCCAACGAG 3' and 5' TGGTCGGTGTTCAGGTTCTTG 3'. All amplifications were carried out on a CFX96 real-time PCR system (Bio-Rad, Hercules, CA). Experimental values were normalized to values obtained for the *Rp49* probe set. Data are reported as the mean ± SEM. All values reported represent experiments performed on at least three biological replicates.

2.2.4 Metabolic analysis

Analyses were performed on partial clear-gut L3 larvae treated for 6 hours in normoxia or 4% O_2. After treatment, animals were washed twice in PBS pH 8.0 and immediately frozen at -80°C. For glycogen measurements, 45 animals were split into

three pools and the assay was performed essentially as described (18). Color intensity was measured using a Bio-Tek Elx800 absorbance microplate reader at 540 nm. Glucose and glucose+glycogen amounts were determined using a standard curve. The amount of glycogen was determined by subtracting the glucose from the glucose+glycogen total. Glycogen amounts were normalized to protein content in each homogenate using a Bradford assay (Bio-Rad). For ATP measurements, larvae were homogenized in 300 µl of 6M guanidine-HCl extraction buffer (100 mM Tris and 4 mM EDTA, pH 7.5). The homogenate was heated at 70°C for 5 min and centrifuged in at 3000×g for 1 min. The supernatant was diluted 1:750 in dilution buffer (25 mM Tris and 100 mM EDTA, pH 7.5) and spun at 14000×g for 3 min, after which 10 µl supernatant was transferred to a 96-well white opaque plate and mixed with 100 µl of luminescent solution (Invitrogen, Molecular probes). Luminescence was immediately measured by a Bio-Tek Synergy 2 SL luminometer. The amount of ATP was determined using a standard curve. Amounts were normalized to total protein. For lactate measurements, 300 first instar larva, 60 third instar larva or 30 1-day-old males were split into three pools and measured as described *Monserrate et al.* (2012) using Lactate Assay Kit (Biovision Milpitas, CA,) (123). For metabolomics, analyses were performed by Metabolon, Inc. (Durham, NC). Replicates were normalized by protein content (Bradford analysis). Recovery standards were added to samples prior to extraction using a proprietary series of organic and aqueous solutions. Extracts were divided into two fractions, one for GC and one for LC. Organic solvent

was removed using a TurboVap (Zymark). Briefly, for LC/MS, split samples were dried and reconstituted in acidic or basic LC-compatible solvents containing standards. Positive and negative ion-optimized sample conditions were analyzed in separate injections. For acidic reconstitutions a gradient of water and methanol containing 0.1% formic acid was used, and for basic extracts a water/methanol gradient with 6.5 mM NH_4HCO_3. Analysis was performed on a Thermo-Finnigan LTQ mass spectrometer with an electrospray ionization source and linear ion-trap mass analyzer. For GC, samples were re-dried under vacuum prior to derivatization under nitrogen using bistrimethyl-silyl-trifluoroacetamide. The column was 5% phenyl with a temperature ramp of 40˚ to 300°C over 16 minutes. Samples were analyzed using a Thermo-Finnigan Trace DSQ fast-scanning single-quadrapole mass spectrometer with electron impact ionization. Refer to Appendix table 2 for normalized data of each replicate and *p*- and *q*-values. Extensive quality control care was applied to minimize variability between days. The Metabolon platform has been described elsewhere (124, 125). Data values were imputed in the following way when values fell below the threshold level of detection: when all six replicates were undetectable, each was assigned the minimum detectable value of across all compounds tested; when five or less replicates were undetectable, sample values were assigned the minimum value obtained among those that were detected for a given compound.

2.2.5 Yeast two-hybrid screen and GST-pull down

A yeast two-hybrid screen was conducted using the Invitrogen ProQuest Two-Hybrid System. For this purpose, three cDNA prey libraries were simultaneously prepared using the CloneMiner cDNA Library Construction Kit (Invitrogen). All the libraries (a, b, c) were made from poly-A-selected RNA that was extracted from w^{1118} animals at -4, +0, or +4 RTP, which was reverse transcribed and pooled in equal proportions before library construction. Each library differs by only a single base pair in the adapter sequence to facilitate expression of clones in all three frames. Extensive procedures, provided by the manufacturer, were followed to capture clones into the pDONR222 vector. Clones in the donor vector were subsequently recombined into the pDEST22 vector. Libraries were titered (a=7.18E6 CFU, b=4.44E6 CFU, c=14.28E6 CFU) and sampled for average insert size (a=1.64 kb, b=1.25 kb, c =1.60 kb) before transformation into ElectoMax cells (Invitrogen). Transformed cells for each library were pooled (total of 6.4E6 CFU) and grown for 22 hrs at 30°C for preparation of library DNA by standard techniques. 22lg of library DNA was transformed into the yeast bait strain containing the LBD of dERR (L193-R496) that had been recombined into the pDEST32 vector. A total of 5.28E5 clones were screened by auxotrophic selection. All positive hits were sequenced. GST-pulldown experiments and the expression of GST-fused ERR constructs in pGEX-4T1 were performed as described (126).

2.2.6 Statistical analysis

A one-way ANOVA *F*-test was applied to test for the differences in glycogen levels, followed by Tukey's HSD method. For developmental qRT-PCR analysis, delta CT values were used to perform statistical analysis, whereby a two-tailed unpaired student's t-test was applied for the differences in gene expression using a Bonferroni correction. Following log transformation and imputation, a one-way ANOVA with contrasts was used to identify significance for metabolites in the mass spec analysis (See Appendix table 2). Cumulative hypergeometric probability was used to determine significance between overlapping gene sets. For PCA analysis, the original scan data of metabolites in each experiment condition (w^{1118} normoxia, w^{1118} hypoxia, *sima* normoxia, *sima* hypoxia, *dERR* normoxia, *dERR* hypoxia) measured by GC/LC-MS were averaged and normalized by protein concentration. For missing data, the global minimum of the non-missing average was imputed. Then we take a logarithm with base 10 of the data. For *sima* hypoxia and normoxia, there are 243 metabolites, so the final data matrix is 243×4. All statistical analysis was performed using R 3.0.2.

2.3 Results

2.3.1 Robust transcriptional response to hypoxia in late third instar larvae

To better understand the contribution of dHIFα in the hypoxic adaptation response, we wanted to determine the developmental time point when dHIFα was most active. To start, we examined the wild-type expression of two known hypoxia-responsive transcripts

in *Drosophila*, *lactate dehydrogenase* (*LDH*, known also as: *ImpL3*, *CG10160*), and the HIF prolyl hydroxylase, *fatiga* (*CG31543*) (127, 128). We also examined the rate-limiting enzyme of glycolysis, phosphofructokinase, encoded by *Pfk* (*CG4001*) as a potential hypoxia-responsive gene. We surveyed three times points, late embryo, mid-second instar (mid-L2) larvae, and late-L3 larvae by qRT-PCR to examine transcriptional responses of whole animals that were allowed to develop in normoxia (21% O_2) and then challenged with a 4% O_2 treatment for 6 hours – hereafter referred to as H-treatment (Figure 2.1A). This level of oxygen, and this time course, has previously been shown to mobilize the fly HIF pathway (129). As seen in Figure 2.1D, the late-L3 time point of wandering larvae [-10 to -4 hours relative to the onset of pupariation (RTP)] is a period where each of the three genes is significantly induced by H-treatment. This expression profile is different from responses observed in embryos 18–24 hr after egg laying (AEL) (Figure 2.1B) and mid-L2 larvae (Figure 2.1C), when *LDH* and *Pfk* were unresponsive to treatment, indicating that hypoxic responses are developmentally tempered.

2.3.2 Identification of HIF-dependent and HIF-independent hypoxic transcripts

To establish the identity of the full complement of H-regulated transcripts, RNA samples were prepared from N- and H-treated pools of control w^{1118} animals and *sima* mutants at the late-L3 time. The *sima* mutant line ($sima^{07607}$) contains a lethal P-element insertion in the first intron in the *sima* locus, which eliminates detectable expression of

the transcript, rendering the animals incapable of directing expression of an oxygen-sensitive murine *LDH*-reporter and, importantly, unable to respond competently to hypoxic challenge (120, 130).

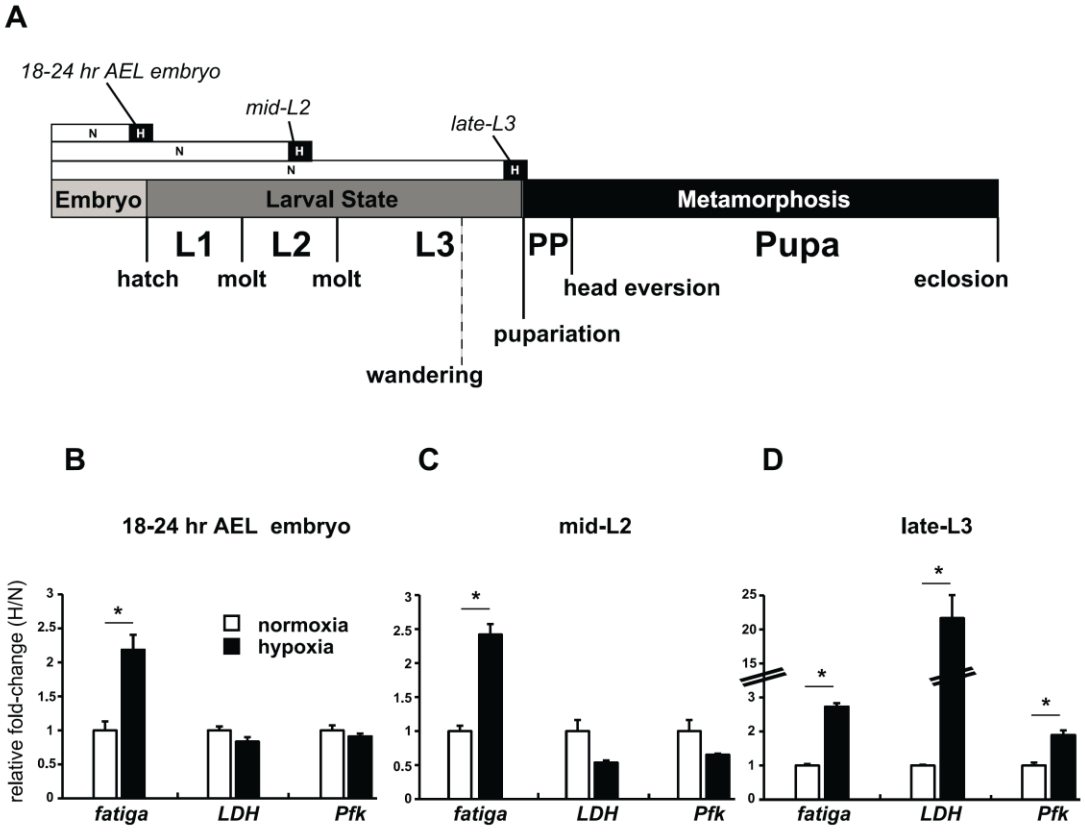

Figure 2.1 Temporal-dependent hypoxic responses. (A) Hypoxic treatment regimen of w^{1118} animals that were allowed to develop in normoxia (N) until they reached one of three developmental stages, at which point they were treated for 6 hours in N or hypoxia (H) (4% O_2). (B-D) qRT-PCR analysis was performed to assess the espression of *fatiga*, *LDH*, and *Pfk* at 18-24 hr AEL, mid-L2, or partial clear-gut larvae in late-L3. All experiments of H/N. Error bars are SEM. * = *p*-value<0.05 (statistically significant).

As expected, H-treatment resulted in a pronounced change in the transcriptome. Using the microarray scheme outlined in Figure 2.2, we extracted a series of significantly altered gene sets (Appendix table 1). We were primarily concerned with identifying two mutually exclusive H-regulated gene sets – HIF-independent (HI) and HIF-dependent (HD). Transcripts that did not exhibit at least a 1.5-fold change in expression, and which did not have a false discovery rate (FDR, *q*-value) of less than 1%, were not included in any set. This high stringency means that we have likely excluded genuinely H-regulated transcripts from our final sets, be they HD or HI. Despite this, we classified 254 transcripts as HI and 171 as HD. It is important to note that the HI and HD categorizations reflect the hypoxic responsiveness of individual transcripts at the late-L3 time alone. The top 20 affected transcripts from the HIF-dependent and -independent categories are listed in Table 2.1.

Gene ontology (GO) analysis (130) was performed on the hypoxia genes sets (Figure 2.3A and 2.3B). Notably, the HI gene set, and not the HD gene set, contain glycolytic transcripts that are up-regulated in hypoxia, which was the single most statistically impacted process in either the HD or the HI sets (Figure 2.3A). Instead of glycolytic genes, significant GO categories were identified for HD genes involved in translational control and RNA processing (Figure 2.3B). However, among the HD H-regulated

transcripts are *fatiga* and *dVHL*. This suggests that dHIFα participates in a feedback regulatory loop that attenuates its own activity.

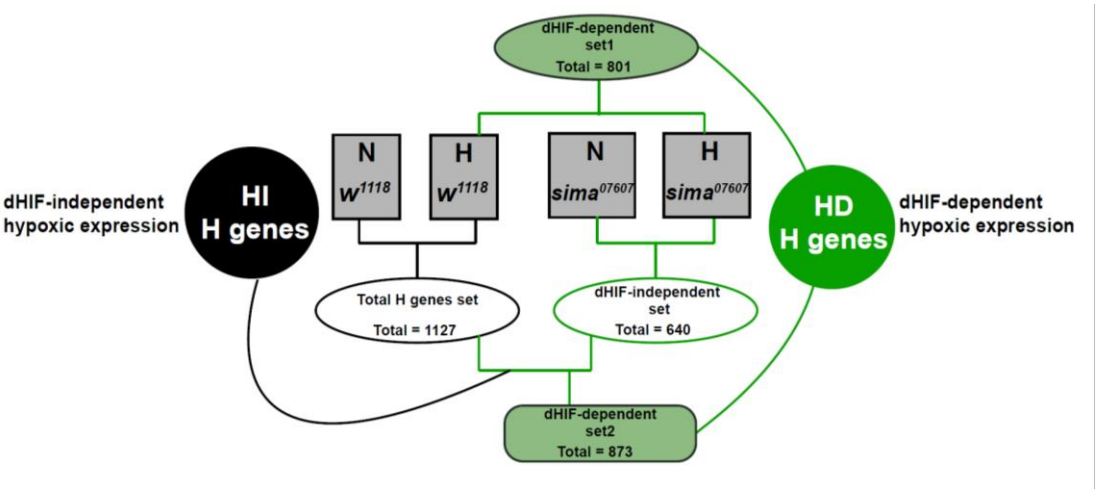

Figure 2.2. Scheme to identity dHIF-independent (HI) and dHIF-dependent (HD) hypoxia-regulated genes. The dHIF-independent set (640 genes), represents the direct comparison of N- or H-treated samples from *dHIF* mutants. The Total H genes set (1127 genes) represents the direct comparison of N- or H-treated samples from w^{1118} animals. The HI H genes set (red circle), represents the overlap of the Total H genes set with the dHIF-independent set. The dHIF-dependent set2 (873 genes), represents the subtraction of the dHIF-independent H genes set from the Total H genes set. The dHIF-dependent set1 (801 genes), represents the direct comparison of H-treated samples from w^{1118} animals and *dHIF* mutants. The HD H genes set (green circle), represents the overlap between the dHIF-dependent sets1 and 2. All genes in any of the sets are up- or downregulated at least 1.5-fold and have a FDR of less than 1%. See Appendix table 1 for gene set lists.

Table 2.1. List of 20 top transcripts whose expression changes in response to hypoxic challenge in a dHIF-dependent or –independent fashion.

Top 20 HIF-Dependent Hypoxia Response Genes					
Probe Set ID	CG	Gene Title	Process/Function	W^{1118} hypoxia vs. *sima* hypoxia	W^{1118} hypoxia vs. *sima* hypoxia
1639737_at	CG34330	---	---	-67.60	4.82
AFFX-Dm-U46493-1_s_at	---	---	---	-22.19	2.47
1625173_s_at	CG11652	dDPH1	diphthamide synthesis	-16.82	10.91
1626857_at	CG4408	---	carboxypeptidase	-11.90	-2.93
1627135_at	CG4608	Branchless	FGF receptor	-9.51	10.87
1637758_at	CG7737	---	spermine oxidase	-7.93	8.56
1638797_a_at	CG31543	Fatiga	HIF prolyl hydroxylase	-7.91	7.70
1637182_at	CG9503	---	choline dehydrogenase	-6.85	2.51
1624497_at	CG2676	---	---	-6.44	4.28
1634786_at	CG7106	Lectin-28C	mannose receptor	-6.01	1.80
1628705_at	CG31022	PH4alphaEB	prolyl hydroxylase	-5.62	3.08
1636482_at	CG14005	---	---	-5.34	5.69
1639555_at	CG17724	---	---	-4.66	4.23
1629753_at	CG3340	Kruppel	Transcriptional repression	-4.47	-1.76
1632203_at	CG31706	---	---	-4.26	6.16
1628428_at	CG12389	dFPP	geranyltransferase	-4.25	3.79
1635558_s_at	CG17724// CG32904	---//sequoia	---	-4.19	4.31
1627535_a_at	CG1333	Ero1L	protein disulfide isomerase	-3.79	5.91
1636145_at	CG7219	Serpin 28D	serline-type endopeptidase inhibitor	-3.78	3.87
1626844_at	CG5748	HSF1	transcriptional activator	-3.54	2.98
Top 20 HIF-Independent Hypoxia Response Genes					
1631533_at	CG10240	Cyp6a22	E-class cytochrome P450	7.82	5.38
1638182_at	CG5999	---	UDP-glucuronosyltransferase	7.49	5.89
1635227_at	CG10160	ImpL3	lactate dehydrogenase	7.38	14.16
1626324_at	CG9964	Cyp309a1	E-class cytochrome P450	6.48	3.57
1628758_at	CG1774	dACOT	acyl-CoA thioesterase	6.36	4.39
1632021_at	CG10245	Cyp6a20	E-class cytochrome P450	6.30	2.79
1629061_s_at	CG32041	Hsp22//Hsp67Bb	response to stress	5.83	6.01
1628052_at	CG10241	Cyp6a17	E-class cytochrome P450	5.20	5.67
1632343_at	CG3017	Alas	5-aminolevulinate synthase	5.07	3.82
1631637_a_at	CG11567	Cpr	NADPH-Cyp reductase	4.91	4.36
1639495_at	CG4485	Cyp9b1	E-class cytochrome P450	4.80	5.44
1628660_at	CG7130	Hsp40	dnaJ homolog	4.18	3.05
1624156_at	CG18578	Ugt86Da	UDP-glucuronosyltransferase	4.02	3.06
1632639_at	CG13941	Arc2	synaptic plasticity	3.94	3.44
1631611_at	CG33983	obstructor-H	chitin-binding	3.94	2.39
1641169_s_at	CG11050	---	phosphoric diester hydrolase	3.71	3.68
1634072_s_at	CG4311	Hmgs	HMG-CoA synthase	3.68	2.53
1625134_at	CG10873	p53	tumor suppressor	3.57	2.36
1630885_at	CG12534	Alr	flavin-linked sulfhydryl oxidase	3.52	1.97
1628657_at	CG17534	GstE9	glutathione S transferase	3.38	3.89

A

dHIF-Independent (HI) H genes

GO Category	Number of Genes (total)	P-Value
Up-Regulated ≥ 1.5-fold, FDR < 1% -- 130 total		
- glycolysis	4 (11)	6.6 e-4
- vesicular fraction	7 (84)	6.6 e-4
- carbohydrate catabolism	5 (32)	6.6 e-4
- glucose catabolism	4 (16)	6.6 e-4
- electron carrier activity	9 (166)	6.6 e-4
- membrane fraction	7 (93)	7.7 e-4
- cell fraction	7 (96)	8.7 e-4
- transferase activity	18 (851)	1.6 e-3
- glucose metabolism	4 (22)	1.6 e-3
- carbohydrate metabolism	4 (26)	2.9 e-3
- telomere maintenace	3 (10)	2.9 e-3
- hexose metabolism	4 (37)	0.01
Down-Regulated ≥ 1.5-fold, FDR < 1% -- 124 total		
- vitamin binding	4 (18)	6.5 e-3
- retinoid binding	3 (9)	9.0 e-3

B

dHIF-Dependent (HD) H genes

GO Category	Number of Genes (total)	P-Value
Up-Regulated ≥ 1.5-fold, FDR < 1% -- 68 total		
- ribosome biogenesis and assembly	4 (33)	3.4 e-3
- ribonuclearprotein complex biogenesis and assembly	5 (100)	6.0 e-3
- solute:sodium symporter activity	4 (52)	6.0 e-3
- rRNA processing	3 (20)	6.0 e-3
- rRNA metabolism	3 (21)	6.0 e-3
- solute:cation symporter activity	4 (66)	9.0 e-3
Down-Regulated ≥ 1.5-fold, FDR < 1% -- 103 total		
No Significant Categories	--/--	

C

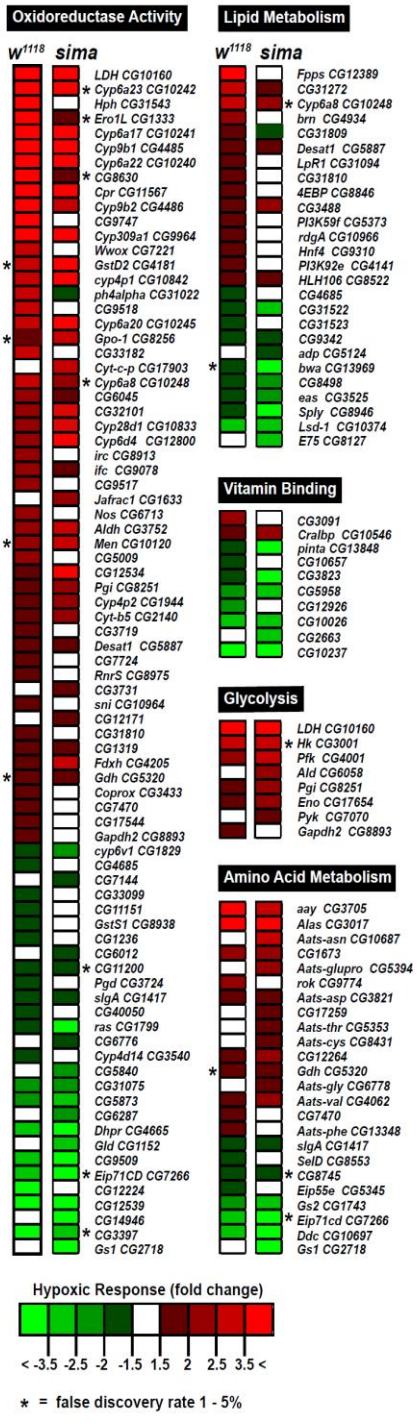

Figure 2.3 HIF-dependent and HIF-independent hypoxic response genes. (A-B) Gene ontology (GO) analysis was performed on sima -independent (HI) and sima -dependent (HD) gene sets that were derived from microarray analysis of H- or N-treated control (w^{1118}) animals or *sima* ($sima^{07607}$) mutants collected at the partial clear-gut late-L3 time. See Figure S1 for the analysis scheme. GO categories are listed in order of statistical significance. The numbers of H-regulated genes affected are shown along with the total number of genes in each category. All transcripts are up- or downregulated at least 1.5-fold and have a false discovery rate (FDR) of <1%. (C) A heat map was created to illustrate the similarity or dissimilarity of hypoxic responses observed in control and *sima* mutant animals for major GO categories impacted by H-treatment. Red (up-regulated), green (down-regulated), or white (no significant change) values represent hypoxic responses observed in the backgrounds indicated. For this analysis, FDR stringency was <1%, unless otherwise noted with * for a particular genotype, where a relaxed gate was used (1-5%), also means that false discovery rate equals to 1-5%.

Ontology-focused heat maps were generated to compare hypoxic transcriptional responsiveness. In addition to glycolytic genes, comparisons were made for other metabolic categories where GO significance was identified, including oxidoreductase activity, lipid metabolism, vitamin binding, and amino acid metabolism (Figure 2.3C). With the exception of lipid metabolic genes, when hypoxic responsiveness is seen (up- or down-regulated) in the control background, the majority of genes also respond in-kind in the *sima* background, and usually with a similar fold change increase. These results suggest that HIF-independent, H-sensitive mechanisms account for a large percentage of the hypoxic response.

2.3.3 Temporal-dependent hypoxic responses

The unexpected breadth of contribution of the HI pathway in the hypoxic response led us to reconsider our initial observations made in Figure 2.1, where *fatiga* displayed a similar response profile across each of the times assayed, and *LDH* and *Pfk* displayed a hypoxic response at only the late-larval time. Indeed, *fatiga* is a HD gene, whereas *LDH* and *Pfk* are HI genes (Appendix table 1). Were *LDH* and *Pfk* unresponsive at earlier developmental times because the HI pathway was not active until just prior to metamorphic onset? To address this question, we collected RNA from control animals and *sima* mutants staged at times that spanned development. In all, twelve samples were gathered: 4 embryonic times (0–6 hrs AEL [w^{1118} background only], 6–12 hrs AEL, 12–18 hrs AEL, and 18–24 hrs AEL); 4 larval times (mid-L1, mid-L2, mid-L3, and -4 hr RTP); 3 metamorphic times (0 hr RTP, +12 hr RTP, +72 hr RTP); and 1 adult time (1 day-old males). qRT-PCR was used to assess H responses of 13 select genes that displayed varying levels of H-sensitive expression. Of those genes analyzed: five were classified as HD genes – *fatiga*, *spermine oxidase* (*CG7737*), *sequoia* (*CG17724*), *branchless* (*CG4608*), and *Peroxiredoxin 2540-2* (*Prx2540*, *CG11765*); seven were classified as HI genes – *LDH*, *Pfk*, *NMNAT* (*CG13645*), *Alas* (*CG3017*), *Cyp9b1* (*CG4485*), *Cyp6a17* (*CG10241*), and *Cyp6a22* (*CG10240*); and one was highly affected by H, but did not meet the stringency requirements for H set inclusion –*CG31769*, which had a largely HIF-dependent expression profile in late-L3.

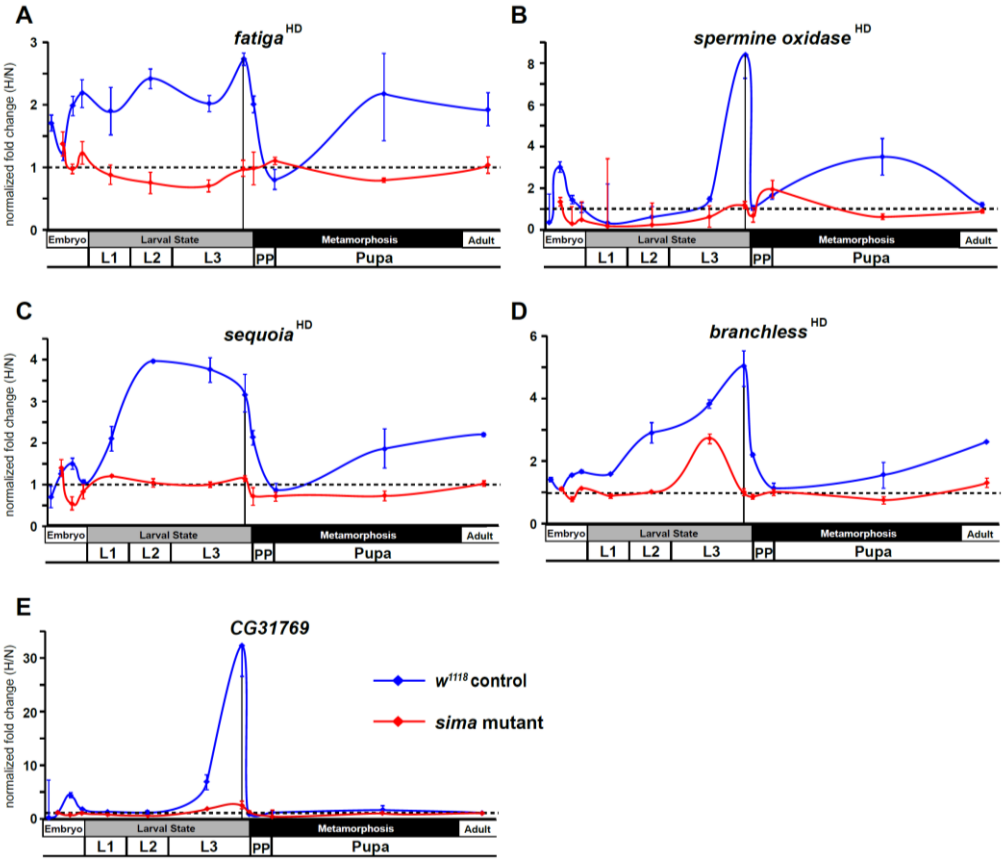

Figure 2.4 Temporal expression of HIF-dependent hypoxic response genes. (A-E) Developmental hypoxic response profiles from qRT-PCR analyses are shown for transcripts that display HIF-dependent (A - *fatiga*, B - *spermine oxidase*, C - *sequoia*, D - *branchless*) or largely HIF-dependent expression (E - *CG31769*). Control (w^{1118}) animals or *sima* mutants were challenged for 6-hrs with 4% O_2. Animals were challenged at 0-6 hr after egg laying (AEL) (not from mutant), 6-12 hr AEL, 12-18 hr AEL, 18-24 hr AEL, mid-L1, mid-L2, mid-L3, -10 - -4 hr relative to pupariation (RTP) L3, 0 hr RTP, +12 hr RTP, +72 hr RTP, and 1-day old males. All values are from experiments performed in triplicate from pools of biological replicates. Values are normalized to *rp49* expression and are reported as the relative fold-change of H/N. The dotted line represents no net change in response, or a value of 1.0. The vertical black line in late-L3 is when microarray analysis was performed. Error bars are the SEM.

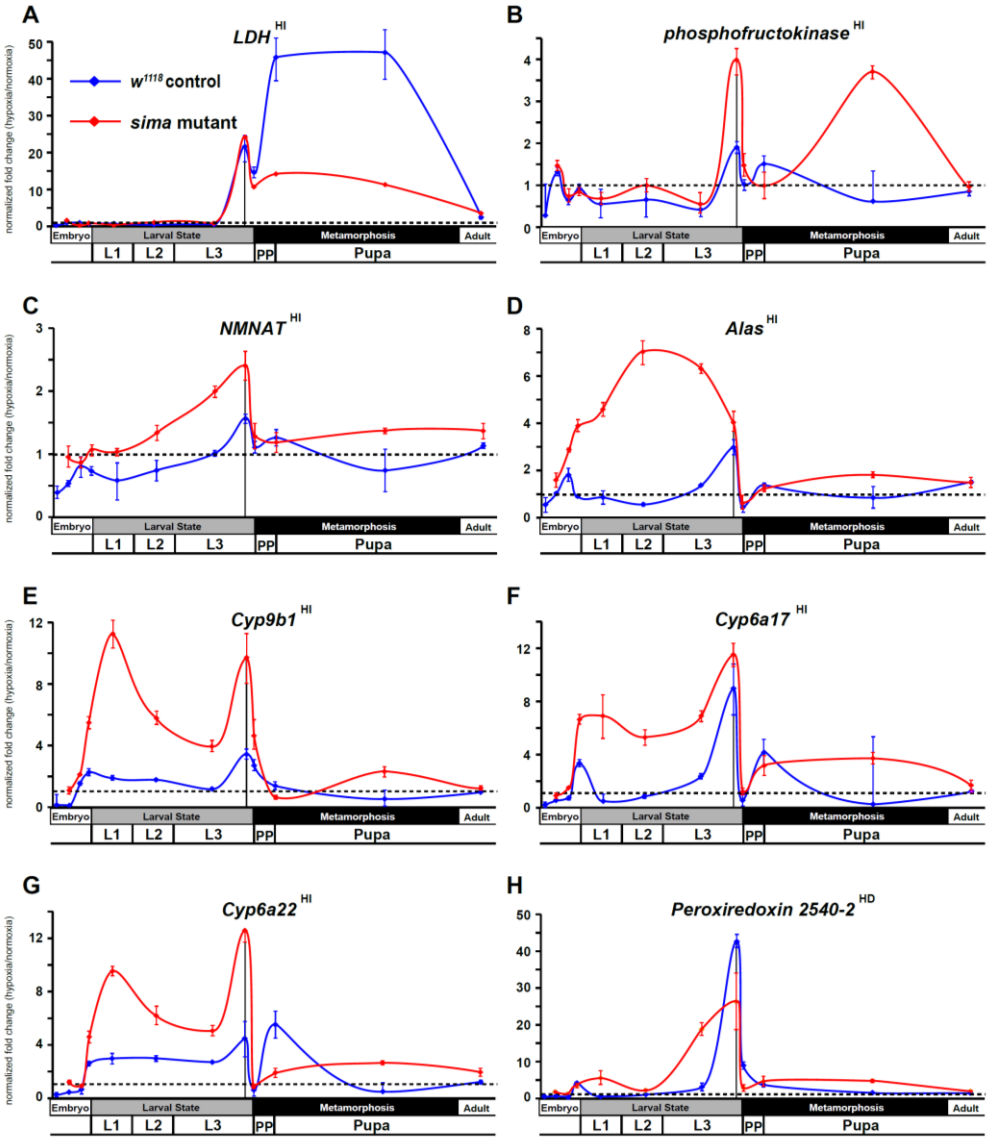

Figure 2.5. Temporal expression of HIF-independent hypoxic response genes. (A-H) Developmental hypoxic response profile from qRT-PCR analyses are shown for transcripts that display HIF-independent (A - *LDH*, B - *phosphofuctokinase*, C - *NMNAT*, D - *Alas*, E - *Cyp9b1*, F - *Cyp6a17*, G - *Cyp6a22*) or largely HIF-independent expression (H - Peroxiredoxin 2540-2 – we note that Prx2540-2 displays HD expression for probe set 1631628_s_at in the microarray and is thus classified as such; however, a second, non-overlapping probe set, 1633471_at, which is much more robustly induced in H appears to be from HI action, although its variability is too great to classify in this

manner (Appendix table 1). Our qPCR primer set favors HI expression.) Control (w^{1118}) animals or *sima* mutants were challenged for 6-hrs with 4% O_2. Developmental challenge times are identical to those from Figure 2.4. All values are from experiments performed in triplicate from pools of biological replicates. Values are normalized to *rp49* expression and are reported as the relative fold-change of H/N. The dotted line represents no net change in response, or a value of 1.0. The vertical black line in late-L3 is when microarray analysis was performed. Error bars are the SEM.

Several patterns emerged from the developmental analysis. First, hypoxic transcriptional induction is most evident at the late-L3 time for each gene assayed. Second, without exception, HD and HI genes display marked drops in H responsiveness just after metamorphic onset. In most cases, H responsiveness is eliminated during the hours surrounding head eversion, which is the initiation of the pupal phase. Among the transcripts examined, HD genes were not induced in hypoxia in a *sima* background at any developmental time, with the notable exception of a single point in mid-L3 for *branchless* (Figure 2.4D). Finally, in the absence of dHIFα, HI genes tend to be hyper-responsive to H challenge throughout development – this was true for all genes examined except *LDH* (Figure 2.5A). The *LDH* profile was unique amongst those assayed, in that late-L3 expression was HI, while pupal expression appears to be dominated by HD expression. The super-activation of LDH during the pupal phase in the w^{1118} background (vs. *sima*) suggests that both the HD and HI pathways are capable of converging simultaneously at the same locus to contribute to its overall expression. Collectively, these developmental

expression data indicate that hypoxic responses are comprised of a patchwork of HD and HI activities throughout life-stage progression.

2.3.4 *sima* mutants are metabolically disturbed in normoxia and are unable to mobilize glycogen in hypoxia

The observation that glycolytic transcripts are effectively up-regulated in *sima* mutants challenged with hypoxia raised the question of how metabolism was affected under these conditions. As before, we concentrated on the late-L3 time because of its particularly robust transcriptional response to H-treatment. We found that glycogen was significantly depleted by control w^{1118} animals in H, in addition to a near 50% reduction in the level of ATP (Figure 2.6A and 2.6B).

We tested for additional HIF-dependent metabolic defects in carbohydrate catabolism using mass spectrometry tied to gas and/or liquid chromatography (GC/MS, LC/MS). Extracts were prepared from animals subjected to N- and H-treatments and 243 metabolites in all major metabolic processes were measured. At first, we applied PCA analysis on the 24 normalized metabolite data sets (6 replicates in each four experimental conditions as w^{1118} N, w^{1118} H, *sima* N, *sima* H) to see whether the majority of metabolites in the replicates clustered in each different conditions. We see indeed nicely clustering of data in all four experimental conditions without obvious outliers (data not shown). Next, we carried out PCA analysis on the raw data sets as described in section

2.2.6 to detect the changing patterns in the four experimental conditions (w^{1118} N, w^{1118} H, *sima* H, *sima* H). Unsurprisingly, we see that many metabolites do not change at all within any conditions. However, if we exclude those unchanged metabolites and only consider those do change statistically significantly, we observed an interesting phenomenon that there is a genotype-dependent component that accounts for 71% of the variance and an oxygen-dependent component that accounts for 25%. This result suggests that the genotype has more influence on the change of metabolites than the oxygen concentration.

Here, we measure 32 carbohydrate metabolites measured (Appendix table 2). The metabolites correspond to four broad categories: 1) aminosugar metabolism; 2) fructose, mannose, galactose, starch, and sucrose metabolism; 3) glycolysis, gluconeogenesis, and pyruvate metabolism; and 4) nucleotide sugars and pentose metabolism (Figure 2.6C). We found that the control response to hypoxia is characterized by a remarkable level of metabolic stability for carbohydrate catabolites (third column in Figure 2.6C). Among those compounds that do display significant H-induced depletions are oligomeric forms of glucose (maltose, maltotriose, maltotetraose, and maltopentaose), which are catabolic products from glycogen and starch breakdown (Figure 2.6C and 2.6E). These sugars feed into the glycolytic cascade by replenishing glucose. They are successively depleted in H the larger they are, and their reductions are consistent with a depletion of total glycogen

seen in the w^{1118} response (Figure 2.6A), as well as the HIF-dependent up-regulation of amylase in H in the same background (Figure 2.6D).

In contrast to the effects that H-treatment has on w^{1118} animals, *sima* mutants cannot deplete glycogen in H (Figure 2.6A). Instead, they adopt a profile for the maltose oligomers in normoxia that resembles the hypoxia-mobilized profile in control animals (Figure 2.6C and 2.6E). This is likely a combination of two factors- the *sima* mutant's inability to effectively up-regulate amylase in H and its constitutively elevated expression profile for amylase in normoxia that is greater than w^{1118} expression in hypoxia (Figure 2.6D, Appendix table 1).

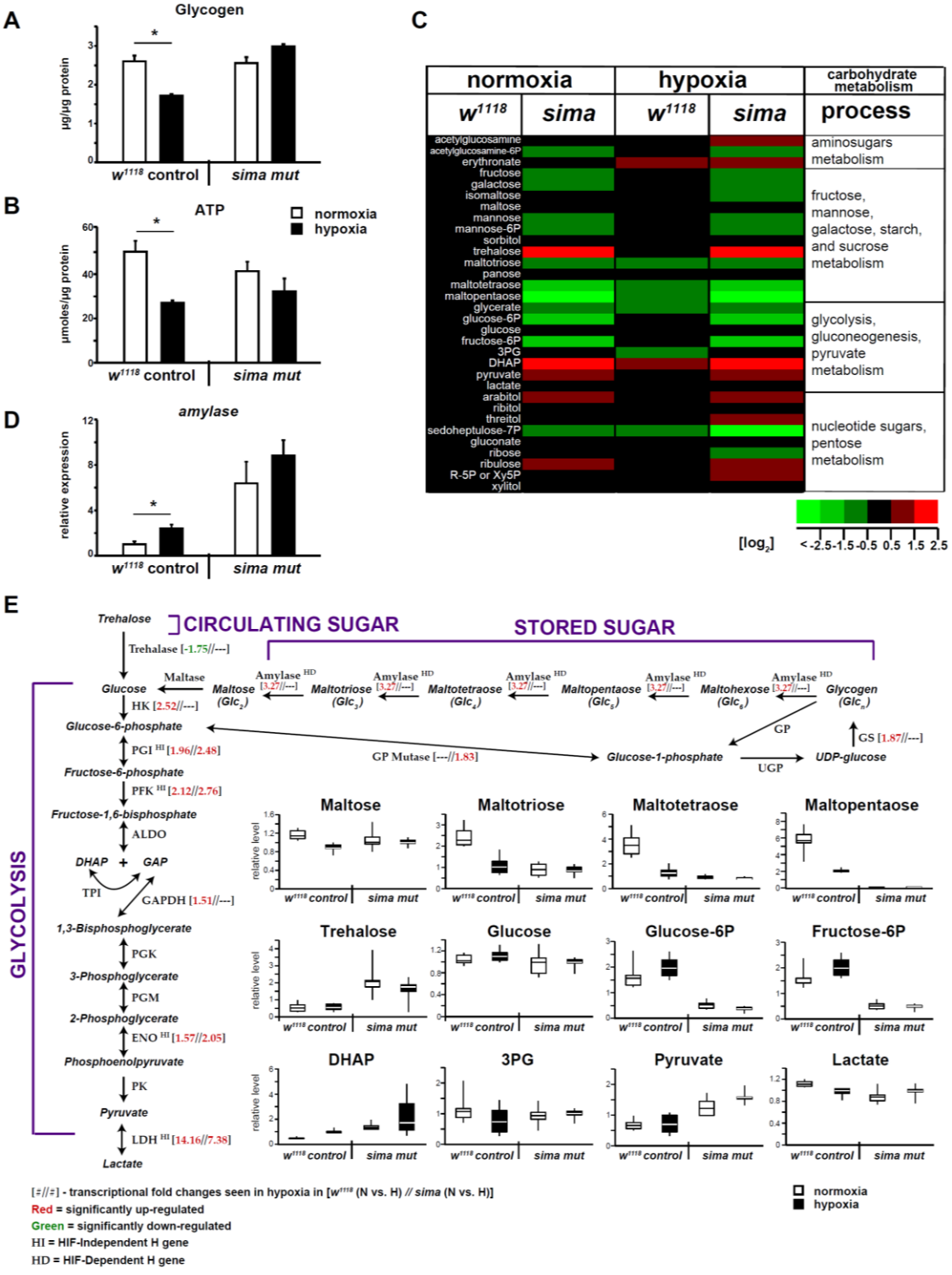
A
Glycogen
µg/µg protein
w1118 control
sima mut
B
ATP
normoxia
hypoxia
µmoles/µg protein
C
normoxia
hypoxia
carbohydrate metabolism
process
aminosugars metabolism
fructose, mannose, galactose, starch, and sucrose metabolism
glycolysis, gluconeogenesis, pyruvate metabolism
nucleotide sugars, pentose metabolism
[log2]
D
amylase
relative expression
E
CIRCULATING SUGAR
STORED SUGAR
GLYCOLYSIS
Trehalose
Glucose
Glucose-6-phosphate
Fructose-6-phosphate
Fructose-1,6-bisphosphate
DHAP + GAP
1,3-Bisphosphoglycerate
3-Phosphoglycerate
2-Phosphoglycerate
Phosphoenolpyruvate
Pyruvate
Lactate
Glucose-1-phosphate
UDP-glucose
Maltose
Maltotriose
Maltotetraose
Maltopentaose
Maltohexose
Glycogen
Maltose
Trehalose
Glucose
Glucose-6P
Fructose-6P
DHAP
3PG
Pyruvate
Lactate
relative level
[≠//≠] - transcriptional fold changes seen in hypoxia in [w1118 (N vs. H) // sima (N vs. H)]
Red = significantly up-regulated
Green = significantly down-regulated
HI = HIF-Independent H gene
HD = HIF-Dependent H gene
normoxia
hypoxia

Figure 2.6. HIF-dependent effects on carbohydrate catabolism. (A) Unlike the w^{1118} response, *sima* mutants are not able to mobilize glycogen stores in response to 6-hr H-treatment in late-L3. (B) ATP levels are significantly depleted upon H-challenge by w^{1118} animals. Although *sima* mutants showed a similar trend, the decrease observed was not significant. Levels of glycogen and ATP are normalized to total protein. (C) Shown is a metabolic heat map of individual metabolites measured by GC/MS or LC/MS from late-L3 w^{1118} animals or *sima* mutants subjects to N (left two columns) or H (right two columns). Six replicates were measured for each treatment group. Each replicate has 250 independently collected and pooled animals. Metabolite levels are expressed as $\log_2$ transformations of the average values, which are plotted relative to the normoxic level obtained in the WT background. The data are normalized to total protein content. Red indicates an elevated metabolite level; green indicates a decreased level, and black no/little change. See Appendix table 2 for further information and statistics. (D) qRT-PCR *analysis* showing amylase expression increases in hypoxia in control animals. Although *sima* mutants have an elevated constitutive level of *amylase* expression, they do not induce expression in hypoxia. (E) Integrated snapshots of the transcriptional and metabolic response to hypoxia at 6-hr. Shown, are the metabolites and enzymes of stored sugar and circulating sugar as they feed into glycolysis. When significant H-induced changes were noted (fold-change > 1.5, FDR < 1%) for transcripts in microarray experiments, those changes are noted in brackets next to the enzyme names. HD or HI status, as classified in Appendix table 1 is also noted. Metabolite levels from mass spec analysis are additionally shown as box and whisker plots. The upper and lower boundaries of the box note the upper and lower quartile values, while the ends of the vertical line indicate the maximum and minimum values. The average value is the noted by the horizontal line within the box. Error bars are the SEM. * = p-value < 0.05.

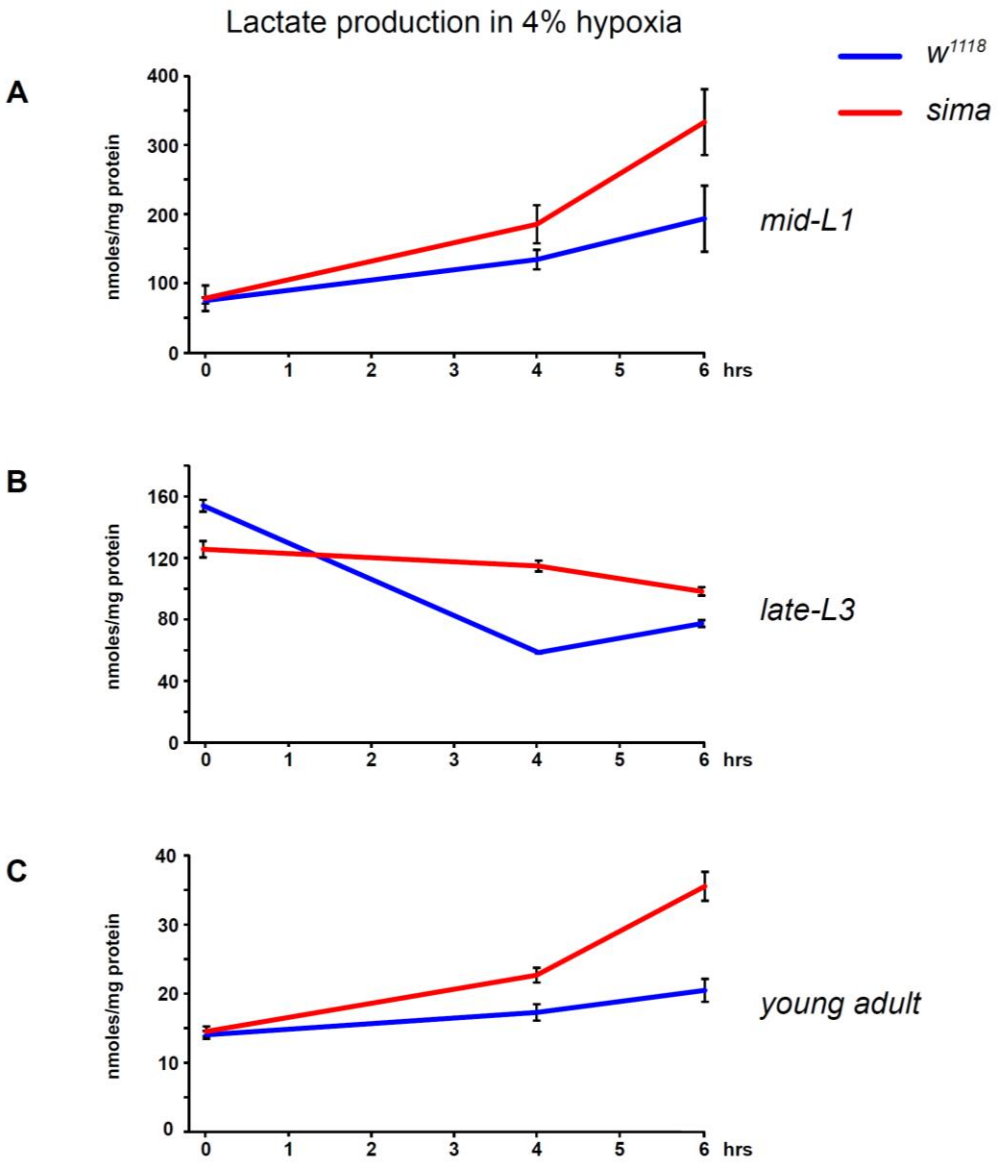

Figure 2.7. Lactate production in hypoxia is life-stage-dependent. Lactate measurements from mid-L1 (A), late-L3 (B), and day-old males (C) from w^{1118} animals and *sima* mutants treated for 0, 4, or 6 hrs in 4% O_2. All measurements were determined in triplicate. Values are normalized to protein content. Error bars are the SEM.

Curiously, despite the clear transcriptional switch toward glycolytic energy production at late-L3, lactate levels remained unchanged for either genotype in H (Figure 2.6C). This failure to generate lactate in hypoxia is a stage-specific block. We independently performed lactate measurements by an enzymatic assay to confirm the late-L3 findings made by GC/MS. Indeed, we find that mid-L1 larvae and young adults from either the w^{1118} or *sima* backgrounds produce lactate in hypoxia, but not late-L3 larvae (Figure 2.7A–2.7C). Notably, early larval and young adult *sima* mutants exhibit an exacerbated hyperlactatemic phenotype when subject to hypoxia (Figure 2.7A, 2.7C) – this does not happen to late-L3 animals. Additionally, though the transcriptional H response profile was largely normal for glycolytic genes in the *sima* mutant, profound depletions were still observed for glucose-6-phosphate and fructose-6-phosphate in H (Figure 2.6C and 2.6E). This is because the normoxic levels for these compounds, rather than H-induced changes, dominate their metabolism. We also observed a HIF-dependent increase for pyruvate in N and H. This is consistent with findings in HIF-1α-/- MEFs, which maintain higher levels of ATP in hypoxia than WT MEFs do in normoxia (131). Finally, the elevated level of Ru5P:Xu5P and ribulose, coupled with the depleted levels of S7P, reveal that *sima* mutants display a clear split in the oxidative (NADPH-generating) and non-oxidative phases of the pentose phosphate pathway in normoxia, which is exacerbated by H-treatment.

2.3.5 dERR binds to dHIFα

The only factor known to transcriptionally regulate glycolytic transcripts in *Drosophila* is dERR (87). Our lab identified this orphan nuclear receptor as a potential factor that may participate in hypoxic signaling when the dERR ligand-binding domain (LBD) was used to repeatedly isolate *sima* clones in a large-scale yeast two-hybrid screen. Of the 20 positive clones recovered in the screen, seven encoded different C-terminal fragments of dHIFα. These findings are consistent with a previous report that demonstrated HIF/ERR interactions between the *Drosophila* proteins and their mammalian homologs (68); however, there are two important aspects about HIF/ERR complexes that we note differentiate the fly and mammalian complexes. First, we find that the dERR DBD is dispensable for interaction with dHIFα, whereas the Ao report showed that interaction occurs between the mammalian ERR DBD and the HIF-1α/β heterodimer. Second, unlike in mammals (68), HIF-1β (tango) is not required for dERR association with dHIFα in *Drosophila* – tango was not present in the screen. In this respect, our findings are consistent with the findings made by Ao et al. Their two-hybrid screen of *Drosophila* components also did not have a HIF-1β (68).

We validated our two-hybrid screen findings by performing a GST-pulldown with GST-fused dERR LBD protein with full-length dHIFα, which confirmed a robust interaction (Figure 2.8A). The C-terminal AF-2 helix of nuclear receptors often mediates interaction with transcriptional coregulators through an LXXLL motif that is found on the

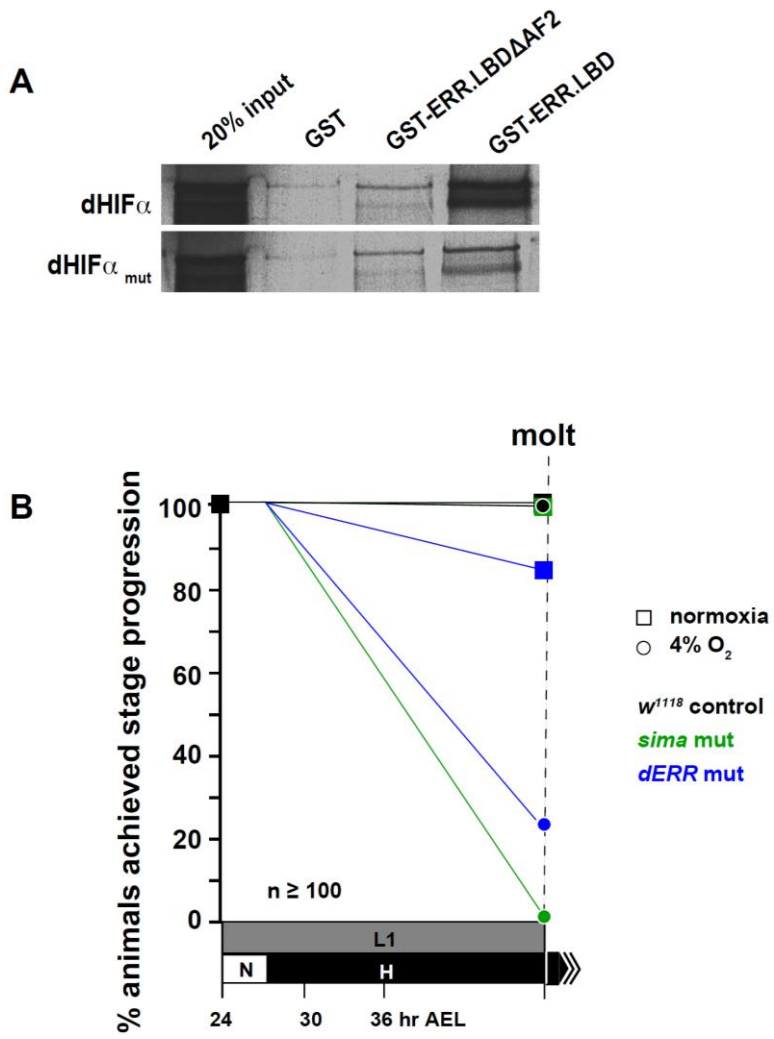

Figure 2.8. dERR binds to dHIFα and is essential to hypoxia survival. (A) GST-pulldown experiment showing GST-fused dERR LBD association with full-length dHIFa, which is diminished when the final 11 amino acids of the LBD are deleted (ΔAF-2). Similarly, when the LXXLL motif in dHIFα is mutated, binding with the ERR LBD and ΔAF-2 proteins is lessened, but not eliminated when compared to GST alone. (B) *dERR* mutant animals are sensitive to H exposure and fail to successfully progress to the molt when challenged with 4% O_2. Shown also are the results of w^{1118} animals and *sima* mutants. The L1 stage takes ~24 hrs to progress through in N at 25°C, but the allotted time was extended to 48 hrs to account for developmental delays that are caused by H treatment. For more details and additional data, see Appendix table 3.

interacting protein (132). A single such sequence resides within dHIFα, at amino acids 1289–1293 (LKNLL). When the last two leucines of this sequence were mutated to alanine and/or when the last 12 amino acids of the dERR LBD were deleted, spanning the AF-2 helix (479–491), the interaction between the proteins was severely reduced, but not eliminated (Figure 2.8A). These data indicate that the dERR AF-2 helix mediates a docking point with the dHIFα LXXLL motif, but that at least one additional point of contact is maintained between dERR and dHIFα.

2.3.6 *dERR* mutants are hypoxia-sensitive

We have recently shown that the orphan nuclear receptor dERR is essential for triggering the pro-growth glycolytic program during *Drosophila* development (86). Without the dERR-initiated metabolic switch, development cannot successfully proceed. Many of the same metabolic genes that exhibit H-sensitive regulation are also mis-regulated in the *dERR* mutant. If dERR is important in the hypoxic response, as suggested by its association with dHIFα, then the mutants should be sensitive to H-treatment. To test this, we challenged *dERR* mutants and compared their H-sensitivity with *sima* mutants and control animals. Indeed, 24–30 hr AEL L1 larvae challenged with constant hypoxia resulted in *sima* mutant lethality (Figure 2.8B). The *dERR* mutants were also H-sensitive, but not to the same extent as *sima* embryos. Nevertheless, less than 25% of

dERR mutant animals survived as compared to 97% survival for the w^{1118} background. These data indicate that dERR is essential for hypoxic adaptation.

2.3.7 dERR is essential for HIF-dependent and HIF-independent responses

Using the same analytic framework that was used to assess *sima* involvement in the late-L3 larval hypoxic response, we collected RNA samples from *dERR* mutants and *dERR,sima double*-mutants for microarray analysis to determine how loss of ERR alone or ERR and dHIFα together would affect hypoxic responses (Figure 2.9). Through these analyses, we identified 282 dERR-dependent (ED) transcripts and 207 double-mutant-dependent (DM) transcripts whose expression changed in hypoxia (Figure 2.10A, Appendix table 1). The ED and DM H-genes sets encompass a variety of highly significant GO categories, including H-induced kinases and transferases that specifically require dERR, and a host of nucleolar and RNA processing transcripts that are coordinately up-regulated in hypoxia due to the lack of both dERR and dHIFα (Table 2.2, Appendix table 1).

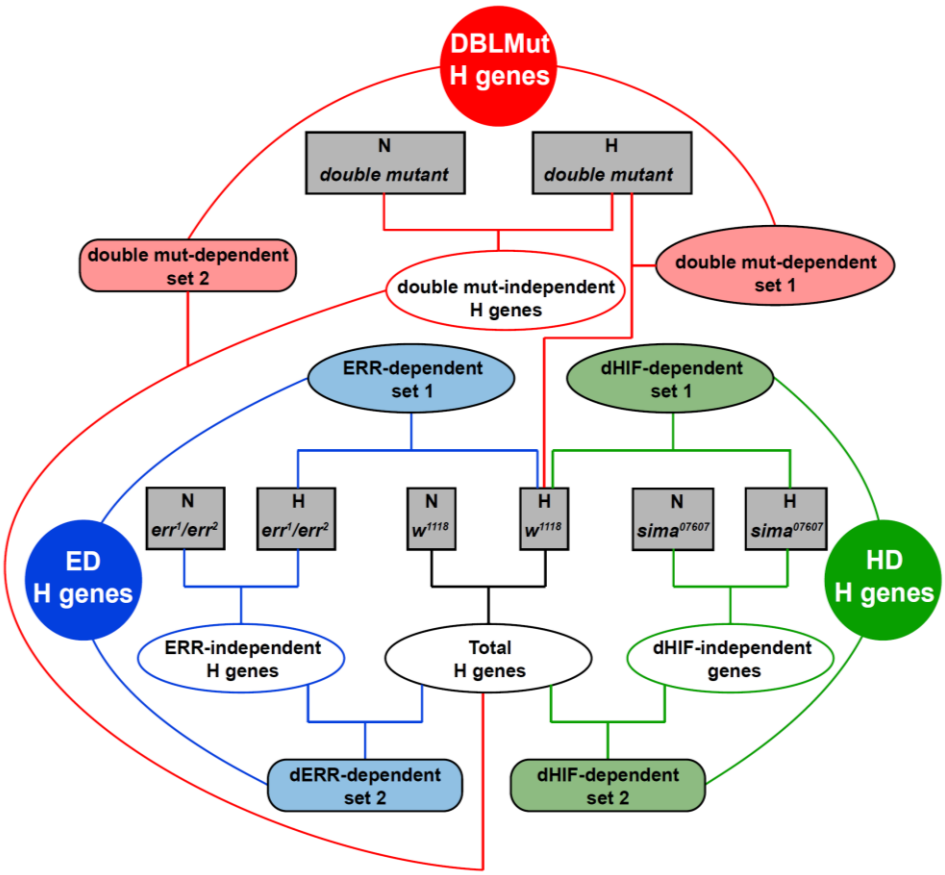

Figure 2.9. Scheme to identity ERR-dependent (ED) and ERR&HIF-dependent (DM) hypoxia-regulated genes. The HD H-genes (green circle) were determined as outlined in Figure 2.2. The dERR-independent set (blue outlined oval) represents the direct comparison of N- or H-treated samples from *dERR* mutants. The Total H-genes set (black outlined oval) represents the direct comparison of N- or H-treated samples from w^{1118} animals. The dERR-dependent set 2, represents the subtraction of the dERR-independent set from the Total H-genes set. The dERR-dependent set1 represents the direct comparison of H-treated samples from w^{1118} animals and *dERR* mutants. The ED H-genes set (blue circle), represents the overlap between the dERR-dependent sets1 and 2. The ERR&HIF-dependent H-genes set (red circle) was determined using the same scheme as above, except that the *dERR,sima* double-mutant was used instead of the *dERR* mutant. All genes in any of the sets are up- or downregulated at least 1.5-fold and have a FDR of less than 1%, except for the dERR-independent set (noted with *). FDR constraints were relaxed for this set alone. It includes FDR scores that are elevated to <7%. See Appendix table 1 for gene set lists.

Table 2.2 List of Gene ontology (GO) analysis of ERR-dependent and ERR&HIF-dependent hypoxic genes.

dERR-Dependent (ED) H genes		
GO Category	**Number of Genes (total)**	***p*-value**
Up-Regulated ≥ 1.5-fold --- 56 total		
No Significant Category	--/--	--/--
Down-Regulated ≥ 1.5-fold --- 124 total		
- kinase activity	22 (371)	1.6 e-10
- transferase activity, phosphorus-containing	23 (446)	8.1 e-9
- transferase activity	32 (851)	6.3 e-7
- phosphotransferase activity, alcohol as acceptor	20 (333)	9.0 e-6
- glycolysis	5 (11)	5.0 e-5
- protein kinase activity	16 (275)	2.2 e-4
- hexose catabolic process	5 (16)	2.2 e-4
- protein serine/threonine kinase activity	13 (190)	2.4 e-4
- glucose metabolic activity	5 (22)	9.7 e-4
- IMP biosynthesis	3 (5)	1.6 e-3
dERR & dHIF-Dependent (DM) H genes		
Up-Regulated ≥ 1.5-fold --- 61 total		
- nucleolus	8 (95)	3.8 e-7
-ribosome biogenesis and assembly	5 (33)	1.7 e-5
- nuclear lumen	8 (348)	1.5 e-3
- ribonucleoprotein complex biogenesis	5 (100)	1.5 e-3
- pseudouridine synthesis	2 (13)	2.0 e-3
- rRNA processing	3 (20)	2.1 e-3
Down-Regulated ≥ 1.5-fold --- 146 total		
No Significant Category	--/--	--/--

The numbers of H-regulated genes affected are shown along with the total number of genes in each category. All transcripts are up- or downregulated at least 1.5-fold and have a false discovery rate (FDR) of <1%.

Venn analysis was used to assess the similarity of the independently derived H-gene sets (HI, HD, ED, DM). The overlapping pattern of the ED genes set with the mutually exclusive HI and HD sets demonstrates that dERR significantly affects both HIF-dependent H-genes (71 transcripts) and HIF-independent genes (54 transcripts) (Figure 2.10B). Among the overlap between the HI and ED genes sets are all the glycolytic transcripts that are upregulated in hypoxia. These data reinforce our earlier findings that demonstrate that at metamorphic onset, dHIF is not part of the hypoxic-induced glycolytic shift. They suggest that a portion of the HI response is attributable to dERR.

Given that dERR can interact with dHIFα, and that it can impact hypoxic transcription independent of HIF, we anticipated that the DM H-genes set would significantly overlap the ED and HD genes sets. Indeed, this is the case – as shown by Venn analysis, the DM set has more overlap with the HD and ED sets than not (Figure 2.10C). A listing of the top hypoxia-sensitive transcripts in the various Venn overlapping regions can be found in Figure 2.10D.

To verify that loss of dERR and/or dHIFα selectively eliminates/diminishes hypoxic induction, RNA samples were independently collected from control animals, *sima* mutants, *dERR* mutants, and double-mutants (Figure 7D). Six genes were chosen for further analysis by qRT-PCR. Independent samples were separately collected and prepared for RNA extraction. The results demonstrate that the factor-dependent classification we employed for hypoxic responsiveness is accurate. For example, *Pfk* is

classified as HI, ED, and DM, indicating that hypoxic regulation should be affected in the double-mutant and the *dERR* mutant backgrounds, but unaffected in the *sima* mutant – this is the pattern that is observed (Figure 2.10E). Similar trends also held true for *fatiga* and *spermine oxidase*, which were expected, respectively, to only respond in the *dERR* mutant background, or not in any of the three mutant lines. With the exception of a modest H-induction in the *dERR* mutant for *spermine oxidase* the responses were as expected. Hypoxic responses for *NMNAT*, *LDH*, and *ALAS* were all expected to display the same pattern; which is that only in the *dERR* background will H-responsiveness be significantly reduced/eliminated. Responses were, by-and large, as expected, except for the significant H-induction of *LDH* in the in *dERR* mutants.

These data indicate that dERR and dHIFα have a different activity profile when in the presence of the other, than either protein has by itself, and suggest that promoter-specific actions of different HIF and/or ERR complexes drive a large percent of hypoxic responses at metamorphic onset. In certain cases, loss of one factor does not influence the other's response, as with loss of dHIFα for the dERR-mediated *Pfk* response (Figure 2.10E). In other cases, loss of either dHIFα or dERR renders the H-response incomplete, such as occurs with *spermine oxidase*. And, still in other cases, loss of one factor is more detrimental for H-induction than is loss of both, as with *ALAS*. Responses of this type appear to suggest that, at certain loci, dHIFα acts as a negative regulator of hypoxic transcription in the absence of dERR but not in its presence.

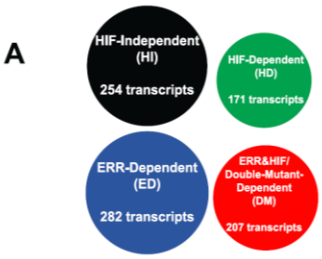

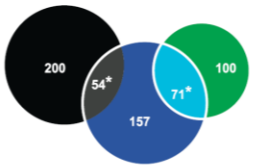

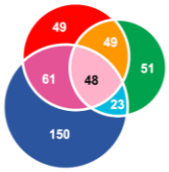

D

CG	Gene Title	Process/Function	mutant background (H) vs. w^{1118} (H) dERR	sima	double mut	(N/H) w^{1118}
ED genes						
CG10160	LDH	glycolysis	-3.40			14.16
CG6687	Spn88Eb	serine-type endopeptidase	-2.99			8.16
CG5164	GST E1	glutathione transferase	-4.52			5.86
CG33474	---	peroxisomal biogenesis	-23.20			5.85
CG11967	CAHβ	carbonic anhydrase	-2.38			5.85
CG8776	nemy	carbon-monoxide oxygenasesynthase	-4.72			5.60
CG4726	MFS3	major facilitator substrate transporter	-2.46			5.43
CG31531	---	LIM domain-containing	-1.74			4.56
CG1774	---	acyl-coenzyme A thioesterase	-4.64			4.39
CG11567	Cpr	cytochrome P450 reductase	-1.95			4.37
DM genes						
CG1113	---				-6.55	3.43
CG7221	Wwox	oxidoreductase			-1.87	3.30
CG4213	---				-1.63	3.27
CG14572	---				-2.02	2.43
CG1148	Osiris 2				-1.97	2.34
CG6531	wengen	cysteine-rich cell surface receptor			-1.59	2.28
CG4934	brainiac	glycosphingolipid biosynthesis			-2.22	2.22
CG17299	SNF4A	AMP-activated protein kinase gamma			-1.54	2.21
CG8808	Pdk	Pyruvate dehydrogenase kinase			-1.78	2.04
CG3091	CG3091	retinaldehyde binding/tocopherol transport			-2.30	2.01
DM/HD genes overlap						
CG11652	DPH1	diphthamide synthesis		-16.82	-11.54	10.91
CG31543	Fatiga	HIF prolyl hydroxylase		-7.90	-9.68	7.70
CG14005	---			-5.34	-6.70	5.69
CG33254	---			-67.60	-18.62	4.81
CG17724	---			-4.19	-5.21	4.31
CR31541	---	pseudogene		-6.44	-5.34	4.28
CG17724	Kdm4B	histone demethylase 4B		-4.66	-5.24	4.23
CG7219	Spn28D	serine-type endopeptidase		-3.78	-3.58	3.87
CG14401	---			-2.24	-2.24	3.82
CG12389	Fpps	Farnesyl pyrophosphate synthase		-4.25	-3.43	3.79
ED/HD/DM genes overlap						
CG4608	branchless	FGF receptor	-9.51	-2.95	-8.62	10.87
CG7737	---	spermine oxidase	-7.93	-5.13	-7.87	8.56
CG31706	---		-4.26	-2.67	-4.82	6.16
CG32694	---		-2.81	-1.65	-2.95	4.37
CG32369	---	ATP-dependent peptidase	-2.73	-1.70	-2.12	4.25
CG4608	branchless	FGF receptor	-2.93	-2.06	-3.07	3.60
CG9747	---	Fatty acid desaturase	-2.43	-1.62	-2.19	3.59
CG9518	---	choline dehydrogenase	-2.87	-2.45	-2.87	2.98
CG3808	---	uracil tRNA methyltransferase	-2.48	-3.22	-3.43	2.90
CG4608	branchless	FGF receptor	-2.93	-2.19	-3.15	2.70

CG	Gene Title	Process/Function	mutant background (H) vs. w^{1118} (H) dERR	sima	double mut	(N/H) w^{1118}
HD genes						
CG11765	Prx2540-2	thioredoxin peroxidase		-2.09		12.26
CG1333	Ero1L	protein disulfide isomerase		-3.79		5.91
CG7224	---			-2.12		5.25
CG32352	---			-2.28		3.27
CG1681	---	Glutathione S-transferase		-1.59		3.25
CG4241	att-ORFA	mitochondrial substrate/solute carrier		-1.58		2.42
CG11175	Rcd6			-1.64		1.83
CG7106	lectin-28C	mannose receptor		-6.00		1.80
CG13316	dMad	basic helix-loop-helix transcription factor		-1.77		1.73
CG1637	---	purple acid phosphatase		-1.57		1.62
ED/DM genes overlap						
CG5571	---	WD40 repeat-like-containing	-5.58		-3.53	9.43
CG3705	astray	phosphoserine phosphatase	-12.28		-3.33	6.68
CG17534	GstE9	Glutathione S-transferase	1.76		2.59	3.89
CG12826	---		-2.81		-2.84	2.70
CG13868	---		-2.61		-2.38	2.68
CG33138	---	Alpha amylase	-2.72		-3.76	2.49
CG13624	---	basic-leucine zipper transcription factor	-1.66		-1.63	2.46
CG15366	---		-1.84		-1.78	2.44
CG15009	ImpL2	insulin peptide-binding	-2.35		-3.16	2.39
CG17982	---		-1.84		-1.72	2.32
ED/HD genes overlap						
CG11765	Prx2540-2	thioredoxin peroxidase	-4.84	-1.60		6.13
CG14066	La related protein	mitotic chromosome condensation	-1.75	-2.84		4.00
CG3672	Cpr67B	cuticle protein	-2.14	-1.76		3.14
CG10248	Cyp6a8	Cytochrome P450-6a8	2.92	6.98		2.57
CG10076	spire	actin nucleation/zinc-finger protein	-1.88	-1.81		2.55
AFFX-Dm-U4	---		-22.95	-22.19		2.47
CG4107	dGCN5	H3 histone acetyltransferase	-1.54	1.94		2.19
CG18135	---	Phospholipase C-like	-1.52	-2.53		2.17
CG10967	Atg1	negative regulation of TOR signaling	-2.03	-2.82		2.01
CG31349	polychaetoid	Guanylate kinase/L-type calcium channel	-1.69	-1.79		1.94

E

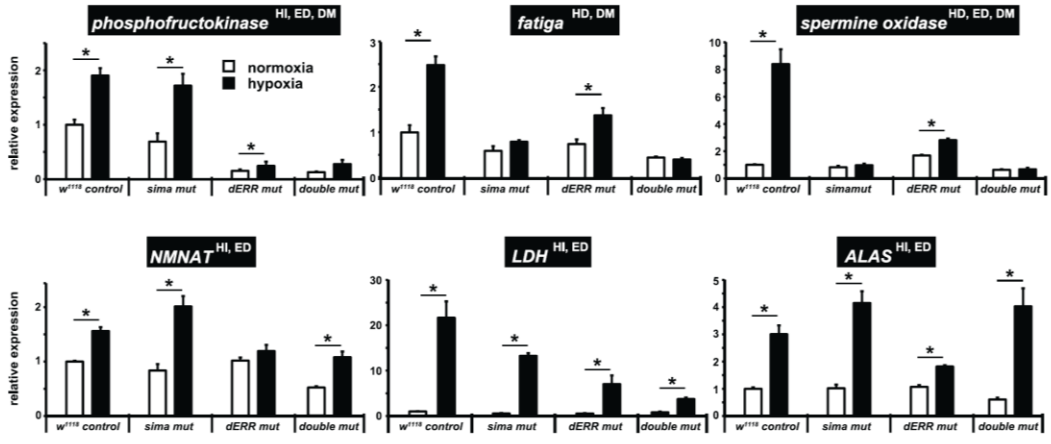

Figure 2.10. The influence of dERR and dHIFα on hypoxic transcripts. (A) HIF-independent (HI), HIF-dependent (HD), ERR-dependent (ED), and ERR&HIF-dependent (DM) gene sets identified by microarray schemes outlined in Figures 2.2 and 2.9. Circles are scaled to size by number of transcripts in each set. (B) A Venn diagram demonstrating the overlap of the HI/HD/ED H-genes sets. Note, HI and HD genes sets are, by definition, mutually exclusive. The asterisks indicate that the overlap is significant (p-value<0.05), as determined by hypergeometric probability. (C) A Venn diagram demonstrating the overlap of the HD/ED/DM H-genes sets. qRT-PCR analysis of hypoxia-regulated genes falling into specific Venn overlaps, as indicated by arrows. (D) The top ten affected transcripts, as assessed by the H-responses measured in the control background, for each of the seven Venn categories shown in Figure 2.10C. Hypoxic expression for each transcript in the different mutant backgrounds (compared to w^{1118}) is reported as fold-change difference. Additionally shown is the N/H ratio obtained for w^{1118} animals. (E) Normoxic and hypoxic expression of each of the six genes (*Pfk, fatiga, spermine oxidase, NMNAT, LDH, ALAS*) was determined using RNA collected from animals of the indicated genotypes at late-L3. Samples were collected in triplicate and are independent from those used in the microarrays. Values are normalized to *rp49* expression and are reported relative to the value obtained for w^{1118} in normoxia.

2.4 Conclusions and Discussions

Our results underscore the complexities of adaptive responses in hypoxia, which are life-stage specific and controlled by multiple H-sensitive pathways. Although our data confirm that HIF is a major transcriptional driver of hypoxic responses, we also define distinct HIF-independent responses. These data raise new questions about dHIFα collaboration and challenge the notion that the HIF complex has little or no normoxic role. In addition, we show that a significant fraction of HIF-independent pathways can be attributed to the ERR nuclear receptor.

Among the HIF-independent genes were numerous glycolytic transcripts that are well-known responders to hypoxia (112, 117, 127). The fact that these genes are as effectively up-regulated in *sima* mutants as they are in a control response was surprising, particularly considering the known role of HIF-1α in this process (133). We find that dERR is the overriding factor that mediates hypoxic up-regulation of glycolytic genes (*Pgi*, *Pfk*, *GAPDH2*, *enolase*) just prior to metamorphic onset.

Our findings, however, do not exclude dHIFα contribution in hypoxic expression of HI genes at other developmental times. The super-induction of *LDH* during metamorphosis in w^{1118} animals versus *sima* mutants is consistent with this scenario (Figure 2.5A). These temporal- and context-specific differences may explain the wide variability in hypoxic responses that have been seen between cell-types (103, 134), despite the ubiquitous presence of the HIF pathway. Furthermore, they may account for discrepancies between our data collected on *Drosophila* and reports on mammalian systems. For example, *LDH* is a HIF-independent hypoxia-regulated gene in late-L3 animals. However, loss of dERR has a greater effect on the diminution of hypoxic induction at this developmental time than does loss of dHIFα (Figure 2.10C). But, this effect is short-lived, because just hours later, when the larva transitions into a pupa, dHIFα appears to work in combination with a non-HIF pathway to elicit hypoxic responsiveness (Figure 2.5A). This combinatorial response during *Drosophila* metamorphosis is consistent with vertebrate studies that show *LDH* expression is the

product of HIF-1 action that also requires the presence a cAMP response element for full hypoxic induction (133, 135). Thus, in addition to different pools of potential co-regulatory molecules that may significantly alter HIF-dependent transcription, entirely different transcriptional pathways, with their own triggers of hypoxic induction, refine the H response. Given the right spatiotemporal setting, HIF-independent pathways may displace (or substitute for) the HIF pathway altogether, a result that is consistent with our data. Further support of this idea is evident in the expression of Alas2, the rate-limiting enzyme for heme production. *Alas2* has been identified as a HIF-dependent and a HIF-independent hypoxia-regulated gene in mammals (136–138). In our hands, *ALAS* is H-responsive, and displays HIF-independent and ERR-dependent up-regulation, which may be subject to dHIFα negative regulation in dERR's absence (Figure 2.10E).

The dynamic patterns of temporal expression of HI and HD genes raise the fundamental question of how hypoxic responses are regulated through development and into the adult. Low-oxygen responses are not one-size-fits-all programs that mitigate oxidative damage and metabolic imbalance; they must be coordinated with developmental progression and metabolic state. In particular, late-L3 wandering larvae exhibit a hypersensitive transcriptional response to hypoxia for HIF-independent/ERR-dependent glycolytic genes. This includes a robust *LDH* induction (Figure 2.5A). Paradoxically, however, late-L3 larvae do not produce lactate in the 6-hr hypoxic challenge (Figure 2.6C, 2.6E, and Figure 2.7). In contrast, at other developmental times

(L1, adult), animals correspondingly produce lactate in hypoxia, even though they remain transcriptionally incompetent to induce *LDH* transcript (Figure 2.7 and Figure 2.5A). We speculate that the atypical transcriptional and metabolic hypoxic profiles of the late-L3 larva are a product of its developmentally programmed energetic state, which at this time is transitioning from low to high efficiency (Pfk expression dramatically decreases in late larvae, Figure 3.3A). Just prior to the wandering L3 time, larvae are prolifically growing, and in a state of metabolism that is fueled by aerobic glycolysis – this metabolic program is ERR-dependent (87). Just after this developmental time, larvae initiate metamorphosis, which will impose 5 days of developmentally forced starvation. During this lipid-driven phase (139), metabolism is characterized by high efficiency OXPHOS.

In contrast to the switch-like hypoxic expression of HIF-independent glycolytic transcripts, the HIF prolyl hydroxylase *fatiga* displays relatively uniform expression throughout development (Figure 2.4A), suggesting that regulation of the HIF pathway, by HIF itself, is equally important at all times for the animal. Such disparities in induction are only understood in context. While our studies here provide a framework with which to view H responses, they indicate that further developmental analysis is needed to more fully appreciate hypoxic response pathways and the mechanisms that specifically support their activities.

Although we have emphasized the transcriptional and metabolic impacts of hypoxia on carbohydrate catabolism, the range of our data sets indicate that many important

hypoxia-induced changes are thus far unappreciated and await further investigation. What is the significance, for instance, of the greater than 10-fold increase of HIF-dependent expression of *dDPH-1* (*CG11652*) in hypoxia (Table 2.1)? DPH-1 is a tumor suppressor that is responsible for the first step of the unique protein modification that occurs on elongation factor 2 (eEF2), which converts a histidine residue to diphthamide. This residue is the target of diphtheria toxin that can shut down protein synthesis through ADP-ribosylation. Although diphthamide formation is conserved from archaea to human, its significance on cellular function is not clear, as it is dispensable for protein elongation (140). However, it has been implicated in translational fidelity (141) and is likely an asset under stress (142). GO analysis performed on HD H-regulated genes indicate that dHIFa is important in replenishing select protein translation/RNA processing transcripts. From this perspective, *DPH-1* induction by dHIFα may be indicative of a regulatory role of hypoxic translation for HIFs. Such a role would be consistent with a recent report from mammals that demonstrates a HIF-2α-dependent association with ribosomal/translational control proteins and the selective hypoxic translation of transcripts containing an RNA hypoxic response element in the 3'UTR via a mechanism involving eIF4E2 (143).

Our analysis of carbohydrate catabolism identifies amylase-mediated breakdown of glycogen as the fuel of first resort in hypoxia (Figure 2.6). This catabolic pathway feeds into glycolysis and supplies needed glucose for increased glycolytic flux, obviating the need to draw on circulating sugar in the form of trehalose, which did not change in the 6-

hr challenge. The strategy of glycogen mobilization allows animals to maintain a remarkably stable profile for a wide variety of carbohydrate catabolites.

Trehalose levels are substantially elevated in *sima* mutants, regardless of oxygen status (Figure 2.6C and 2.6E). These data may indicate a role for dHIFα in the insulin receptor pathway. Numerous studies demonstrate that trehalose levels are altered by genetic disruptions of the insulin-signaling components (144–147). Alternatively, elevated trehalose levels may be the result of constitutively high expression of *amylase* (Figure 2.6D). Although the increased *amylase* expression does not translate into a depleted level of glycogen in the *sima* mutant (Figure 2.6A), it is conceivable that increased glycogen deposition compensates for increased glycogenolysis.

It is important to note that post-transcriptional control mechanisms are well known to impact glycolytic enzymes. Although we did not document them, we consider such influences on hypoxic glycolytic flux likely to have genotype-specific effects.

sima mutants do not mobilize glycogen in hypoxia, but they are able to initiate H-induced changes for other carbohydrates. This is the case for the glycolytic intermediate DHAP, which more than doubles in a control hypoxic response and significantly accumulates in mutants (Figure 2.6C, 2.6E). These findings are consistent with appropriate transcriptional responses we noted for glycolytic transcripts in *sima* animals, which are up-regulated in hypoxia by dERR, not dHIFα. The result for glycogen notwithstanding, it is the widespread derangement of normoxic set points for metabolites

that characterizes the metabolic incompetency of the sima mutant. Our data indicate that dHIFα has it greatest impact on metabolism in the unchallenged normoxic state, rather than in hypoxia.

The mechanism whereby dERR participates in hypoxic responses needs to be explored further. We identified dERR as a potential player in hypoxic responses through its association with dHIFα (Figure 2.8A), suggesting that it acts in a collaborative role with the HIF complex through direct recruitment to HREs. This model was favored by the Ao et al. report for ERR participation in hypoxic responses in vertebrates (68). Additionally, dERR may recruit dHIFα to ERR-specific response elements to facilitate H responses. Another possibility is that dERR actively regulates hypoxic transcription without dHIFα at all; or, in parallel to the actions of dHIFα, which may occur independently, yet simultaneously. Each of these scenarios is consistent with hypoxic expression analysis that we performed to generate HD, HI, ED, and DM gene sets. Moreover, in the presence of dERR, dHIFα may act as a negative regulator of hypoxic responses at select hypoxia-regulated sites (Figure 2.10E, *NMNAT*, *ALAS*). Of further interest also, will be the identification of the triggers for ERR participation in hypoxic-induced responses.

Apart from dERR and dHIFα, our data indicate that at least one more hypoxic-sensitive pathway is active and important for mediating hypoxic adaptation, as we found many H-sensitive transcripts that fall outside the regulation of either factor. The nature of

the alternate pathway(s) is unknown. The results shown here suggest that identifying the sensors and effectors that regulate these HIF- & ERR-independent hypoxic response pathways will have profound impacts on our understanding of hypoxic signaling, and will undoubtedly provide new avenues with which to approach the complex problem of metabolic transition.

CHAPTER 3 The ERR Regulates an Atypical Acyl-CoA Synthetase (CG4500) in *Drosophila melanogaster*

3.1 Introduction

Multicellular organisms from *Drosophila* to mammals need to coordinately maintain system-wide balance between cellular energy consumption and storage. Excessive metabolic consumption or storage will result in devastating consequences. In modern society, due to the advanced development of agricultural and animal husbandry, the contemporary human diet features an overabundance of fat, simple sugars, sodium and chloride, but also accompanies a scarcity of fiber, calcium and potassium (148). This kind of modern diet causes excessive energy storage and subsequent disturbance of lipid metabolism, which is tightly associated with metabolic syndrome that becomes a growing public health concern worldwide. Metabolic syndrome is a group of metabolic abnormalities including obesity as the central factor, as well as hypertension, dyslipidemia (decreased high-density lipoprotein, and elevated serum triglycerides), impaired fasting glucose (type 2 diabetes), and subsequent heart disease (149 - 151). Notably, the prevalence of metabolic syndrome in the United States is over 35% by two separate defining standards, the adult treatment panel (ATP) and the international diabetes federation (IDF) (152). Overall it is hard to overstate the importance of

understanding the molecular mechanism underlying all aspects of lipid storage, mobilization, and oxidation.

Fatty acids (FAs) are a major component of lipids, and key source of high efficiency ATP production through oxidation degradation. FAs are a group of carboxylic acids with a long aliphatic chain, which is either saturated or unsaturated. According to the length of the aliphatic tail, FAs can be categorized as short-chain fatty acids (SCFAs) with chain length of 6 carbons or less, medium-chain fatty acids (MCFAs) with 6 to 12 carbons, long-chain fatty acids (LCFAs) with 14-22 carbons, and very-long-chain fatty acids (VLCFAs) with aliphatic tails longer than 22 carbons. FAs with less than 14 carbons or more than 20 carbons are uncommon, and the predominant FAs in mammals are those of the C16 and C18 species (153). Fatty acid catabolism is a multi-step process. Generally, excess energy is stored in the form of triglycerides (TGs). When energy is needed somewhere in the body, free FAs are initially mobilized from TGs through the activity of lipases. Free FAs can be degraded by several cellular pathways, including α-, β-, and ω-oxidation. In humans, α- and ω-oxidation can only occur in peroxisomes, but both peroxisomes and mitochondria are capable of catabolizeing FAs through β-oxidation. However, the favored path for FAs, including the majority of LCFAs, is through mitochondrial β-oxidation (mβ-ox) (154). Unlike MCFAs that freely penetrate the mitochondrial membrane, LCFAs have to be transferred by means of a carnitine cycle into mitochondrial matrix, where β-oxidation occurs. LCFAs have to first be activated by

coupling to Coenzyme A (CoA) by the acyl-CoA synthetase (ACS) family of enzymes on the mitochondrial outer membrane. The CoA group of the fatty acid-CoA molecule (acyl-CoAs) is next replaced by carnitine to form acylcarnitines by carnitine palmitoyltransferase I (CPT-I). The long-chain acylcarnitines are then exchanged and translocated into the mitochondrial matrix by an integral inner membrane protein, carnitine-acylcarnitine translocase (CAT). Finally, the long-chain acylcarnitines in the mitochondria matrix are converted back to long-chain acyl-CoA by carnitine palmitoyltransferase II (CPT-II) on the inner mitrochondrial membrane. At last, the liberated carnitine is exchanged back to mitochondrial outer membrane and LCFAs are β-oxidized to yield acetyl-CoA, which will enter TCA cycle to generate energy (Figure 3.1A) (153). Essentially, the carnitine cycle is the barrier for LCFAs mβ-ox, because without it LCFAs are not able to go into the mitochondria. And it is not surprising that CPT-I is considered to be the rate-limiting step and a key regulatory site of mβ-ox.

Noteworthy, in addition to mβ-ox, there are also other alternative routes for fatty acid oxidation (α-, β-, and ω-oxidation in peroxisome) (154). FA α-oxidation only occurring in peroxisomes is a process by which 3-methyl-branched-chain FAs like phytanic acid are broken down by removal of a single carbon from the carboxyl end. Compared to mβ-ox, peroxisomes β-oxidation (pβ-ox) is catalyzed by different enzymes encoded by distinct genes. Importantly pβ-ox breaks down a distinct set of FAs, such as VLCFAs, and di-/trihydroxy acid (155). However, pβ-ox is not capable of complete oxidation, but

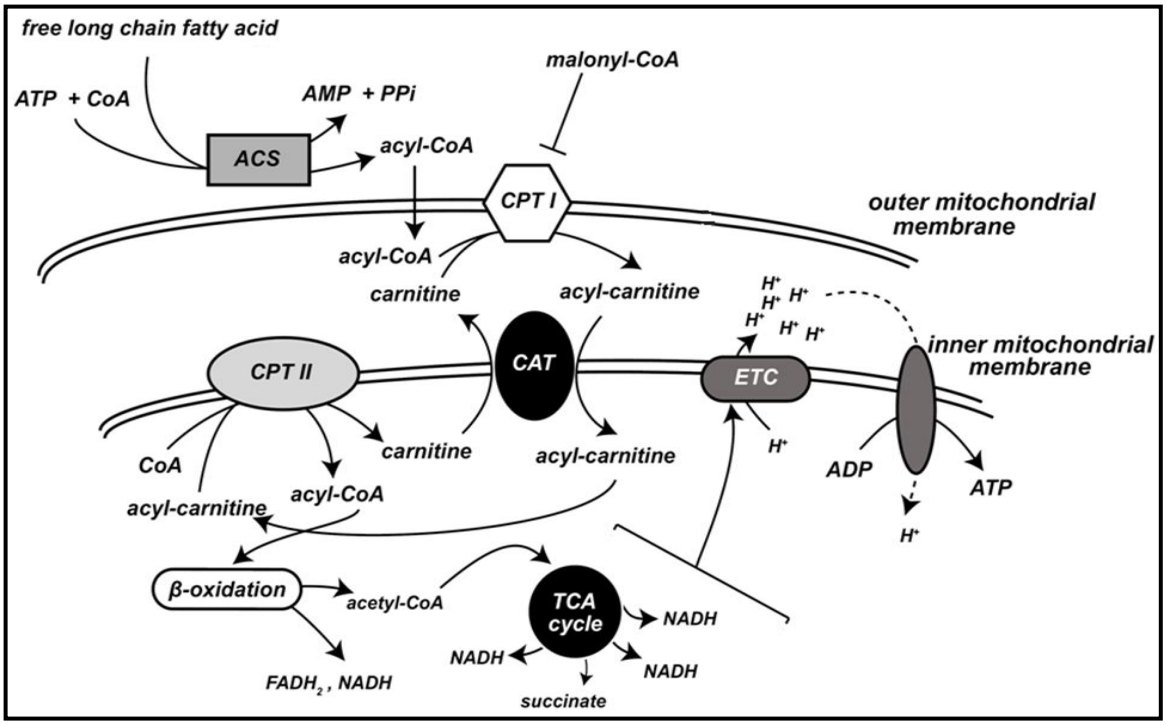

Figure 3.1 A scheme of the conversion of LCFAs into ATP in the mitochondria.

rather truncates the FAs to lengths that can enter the mitochondrial matrix without the need for carnitine, and eventually these chain-shortened FAs are fully oxidized in mitochondria. FA ω-oxidation occurs in the endoplasmic reticulum (ER). The ω-carbon in FAs is the carbon furthest in the alkyl chain from the carboxylic acid, which is progressively oxidized first to an alcohol and then to a carboxylic acid, creating a molecule with a carboxylic acid on both ends in ω-ox. Eventually, the resulting dicarboxylic acids will enter pβ-ox to be catabolized (154). Notably, α- and ω-oxidation

of LCFAs, coupled with pβ-ox, can be vital alternate routes for humans or animals that cannot rely on mβ-ox of FA oxidation, such as CPT-I deficient patients.

Fatty acid catabolism is regulated in many ways. As the rate-limiting step of mβ-ox, CPT-I activity is strictly regulated. Most importantly, it is potently inhibited by the concentration of malony-CoA. The formation of malony-CoA is catalyzed by acetyl-CoA carboxylase (ACC), the activity of which is acutely inactivated or activated by phosphorylation and dephosphorylation, respectively (156). The phosphorylation is achieved by 5'-AMP-activated kinase (AMPK)/AMPK-kinase cascade (157). In addition, the expression of CPT-I is also regulated at the transcriptional level by fatty acid concentration. The transcriptional regulation of fatty acids on CPT-I is very likely mediated through PPARs. A PPRE is found in the regulatory region of the human muscle type CPT-I gene (158). Another study showed that in primary rat neonatal cardiac myocytes, CPT-I mRNA levels are stimulated by oleate through PPARα (159).

Fatty acids catabolism is also regulated through other sites other than CPT-I. The highly conserved insulin/IGF signaling (IIS) pathway is a critical regulator of lipid homeostasis, although the molecular mechanisms by which IIS controls lipid catabolism are only understood in part (160). It has been found that IIS is able to inhibit both expression and activity of lipases (161, 162). Furthermore, IIS also decreases the rate of fatty acid entry into mitochondria partially through FOXO action (163, 164). Interestingly, a recent study conducted in *Drosophila* identified an unconserved ACS,

pudgy, is direct target gene of FOXO in the fly. They also found that in mammalian cells multiple ACSs are regulated by insulin signaling at the transcriptional level (165). Importantly, this study identified fatty acid activation by ACSs as an important, regulated step in FAs oxidation, which has not been considered as a key step in FAs oxidation regulation. Furthermore, NRs and their co-partners, as discussed in Chapter one, are also important regulators of FAs catabolism. PPARs not only directly regulate the expression of CPT-I, but also transcriptionally regulate a broad range of genes involving in many aspects of fat catabolism, such as FAs uptake through membranes, intracellular fatty acid trafficking, FAs oxidation and ketogenesis, and triglyceride storage and lipolysis (166). PGC-1α/β regulate many steps of mitochondrial oxidative metabolism coordinately with lots of transcription factors, including mitochondria biogenesis, OXPHOS, CPT-I expression, FAs oxidation genes, glucogenesis and lipogenesis (167).

Importantly, as discussed extensively in Chapter one, ERRs not only function as a master regulator of almost all aspects of metabolic processes, including glycolysis, FAs oxidation, mitochondrial biogenesis and mitochondrial function (the TCA cycle and OXPHOS), but also likely serves as a switch to metabolic transitions. However, the studies concerning the regulation on FAs catabolism have not focused on the ACS activation of LCFAs, except the one study that showed that the IIS pathway regulates ACS mRNA expression in both fly and human cells (165). This study provides a new perspective that the master regulator of metabolism, ERRs, may transcriptionally regulate

the expression of ACS genes and control the FAs flux into mitochondria in order to manipulate FAs catabolism.

To test this hypothesis, we utilize *Drosophila* development as a platform to investigate lipid oxidation pathways. As discussed previously, the major metabolic processes are very much conserved in *Drosophila*, compared to mammals. Interestingly, *Drosophila* undergoes a programmed Warburg like transition in late embryogenesis (87), but strikingly they turn off the Warburg effect just before metamorphosic onset. These two metabolic switches correspond to the developmental profile that *Drosophila* experience. Figure 3.2 illustrates that flies accumulate lipid from L1 until partial clear gut stage (-10 to -4 hour before pupariation), when in preparation for metamorphosis, larvae finish their growth phase, leave the food, and start a starvation period initiating at the wandering stage and lasting through the pupa stage, which results in a dramatic depletion of fat stores (Figure 3.2). The majority of the liberated FAs are LCFAs, and at this developmental stage the main forms of FAs are myristic acid (14:0), 13.3% of total lipid; palmitic acid (16:0), 24.4% of total; palmitoleic acid (16:1), 24.9% of total; and oleic acid (18:1), 30.8% of total (168). This observation suggests that flies must trigger mβ-ox during this developmental starvation period in order to generate energy to survive. Since the previous study done by Tennessen et al. found that in L2 larvae dERR targets the transcription of glycolysis enzymes rather than enzymes involved in FAs catabolism, we reasoned to make the following hypothesis that dERR is very likely to transcriptionally

regulate FA oxidation at the wandering stage when FAs need to be degraded to produce enough energy for the larvae to survive. In this Chapter, we identify CG4500 as an ACS, which is strongly up-regulated upon fasting in a stage-dependent manner. We find that the expression of CG4500 is almost completed abolished in *dERR* mutant animals, and CG4500 is likely to be a direct target of dERR. Furthermore, we show that the *dERR* mutant is deranged in fatty acid oxidation with dramatically reduced levels of carnitine conjugates of LCFAs and elevated levels of all MCFAs and LCFAs in the C10-15 range. These results suggest that dERR is highly likely to direct the second metabolic switch toward FAs catabolism in late-L3.

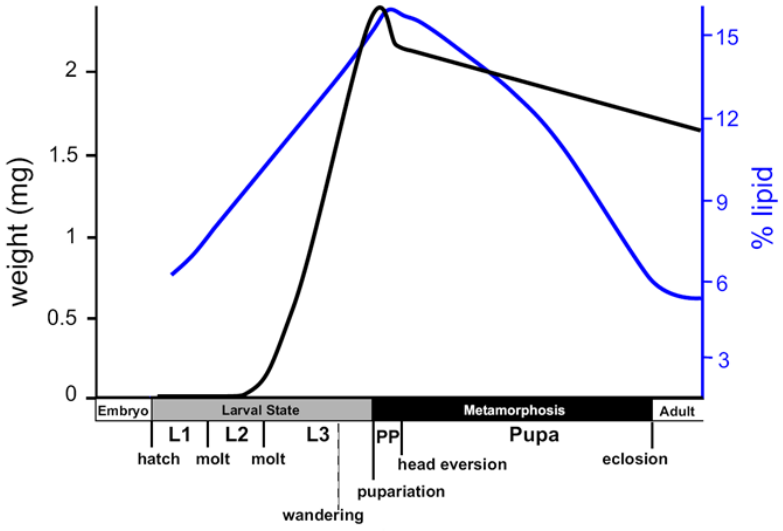

Figure 3.2 The profile of body weight and lipid percentage through *Drosophila* development. The mass (black line) and % lipid (blue line) of *Drosophila melanogaster* plotted with respect to developmental progression. L = instar, PP = prepupa.

3.2 Methods

3.2.1 Fly strains, developmental collection and starvation treatments

Flies were maintained on regular cornmeal-molasses-yeast media at 25°C. w^{1118} animals were treated as controls. *dERR* mutants ($dERR^1/dERR^2$) are described elsewhere (87). The $dERR^1$ and $dERR^2$ chromosomes were carried over a TM3, twi-GFP (green fluorescent protein) balancer chromosome. Homozygous mutant larvae were sorted for the absence of GFP expression using a Zeiss Discovery V.8 dissecting stereoscope with fluorescence at developmental stage between 12hr AEL and mid-L2. For collecting the clear gut L3, embryos were collected at 25°C for 14 hrs onto egg caps (molasses-agar media in 35 mm×10 mm dishes) with yeast paste. Then mid-L2 larvae were either sorted for green fluorescence (*dERR* mutant) or not (wild type), and transferred to a fresh egg cap with blue yeast paste (0.3% bromophenol blue), and allowed to develop until achieving the clear-gut L3 stage (−4 to 0 hrs RTP). For developmental analysis of gene expressions, 12 developmental stages were collected in w^{1118} animal: 6-12 hr AEL, 12-18 hr AEL, 18-24 hr AEL, 0-6 hr L1, mid-L1, mid-L2, mid-L3, -4 to 0 hr RTP (relative to pupariation) L3, 6 hr RTP, +18 hr RTP, +72 hr RTP, and 1-day old males. For starvation treatment in Figure 3.5, mid-L2 of w^{1118} or $dERR^1/dERR^2$ allowed to grow on egg cups as described earlier with yeast paste were sorted for green fluorescence (mutant) or not (wild type), and transferred to a) new egg cups with yeast paste for control; b) kimwipe paper with water for complete starvation, or

c) kimwipe paper with 20% sucrose in water that was sterilized by filtering, treated for 8 hours. For 1-day male starvation experiment, w^{1118} larvae grow on egg cup with yeast paste as described earlier until pupariation, and then pupae were transferred to regular cornmeal-molasses-yeast media until emerge. 1-day old males were picked and treated with a) regular cornmeal-molasses-yeast media; b) kimewipe with water, or c) 20% sucrose prepared as described in this paragraph, treated for 24 hours. All treatment experiments were carried out at 25°C.

3.2.2 Microarray analysis and Quantitative RT-PCR

Microarray analyses were performed on at least three biological replicates of w^{1118} animals and *dERR* mutants at the lear-gut L3 stage. For each biological replicate, at least 10 larvae were collected and washed with 1×PBS before homogenization in TRIzol (Invitrogen, Carlsbad, CA) using a VWR disposable pellet mixer. RNA preparation and microarray analysis were done as described in Chapter 2 Section 2.2.2. No changes below 1.5-fold were considered significant. Additionally, the following false discovery rate percentages were imposed: <1% w^{1118} vs *dERR* mutant. Microsoft Access was used to compare data sets.

For qRT-PCR analysis, cDNA samples were prepared as described in Chapter 2 Section 2.2.3. For real-time PCR, premixed primer-probe sets were purchased from Applied Biosystems. Experimental values were normalized to values obtained for

the *Rp49* probe set. Data are reported as the mean±SEM. All values reported represent experiments performed on at least three biological replicates.

3.2.3 Assay for ACS activity

His-tagged luciferase protein was obtained by cloning the coding sequence into pET16b, expressing it in BL21 E. coli, and purifying it using Ni-NTA Agarose beads (Thermo Fisher Scientific, Waltham, MA). GST-tagged CG4500 protein was obtained by cloning the cDNA sequence into pGEX 4T1, expressed in BL21 E.coli, and purified using glutathione sepharose 4 fast flow beads (GE Healthcare & Life sciences). Purified GST protein was generally given by Dr. Jessica Bell from Department of Biochemistry and Molecular biology of VCU. All FAs (decanoic acid C10:0, lauric acid C12:0, palmitic acid C16:0, palmitoleic acid C16:1, stearic acid C18:0, oleic acid C18:1, arachidic acid C20:0, cerotic acid C26:0) used in this study were obtained from Sigma-Aldrich (St. Louis, MO). All FAs, except cerotic acid, were dissolved in DMSO, aliquot and stored in -20˚C. Cerotic acid was dissolved in chloroform and stored as other FAs.

Adenylation activity for carboxylic acids were carried out as previously described with modification (169). Instead of 50nM of enzyme, 500nM of enzymes were used in our assay. Instead of 0.33µCi, 1.266µCi of [α-^{32}P]ATP was utilized here. The TLC plates were developed in Chloroform/Acetone/Methonal/Acetic acid/H_2O (5:4:3:2:1). The radioactivity of ^{32}P-AMP was measured using a phosphoimager (Molecular Imager FX,

Bio-Rad, Hercules, CA) after exposing overnight. Relative intensity of the radioactivity was obtained by subtracting the background value. The concentration of DMSO and chloroform at 2% in the reaction did not affect the activity (data not shown).

3.2.4 Metabolic analysis by GC/LC-MS

Analyses were performed on clear-gut L3 larvae of w^{1118} and $dERR^{1}/dERR^{2}$animals. Larvae were washed twice in PBS pH 8.0 and immediately frozen at −80°C. The GC/LC-MS analyses and the data analysis method were performed by Metabolon, Inc. (Durham, NC) and extensively described in Chapter 2 section 2.2.4.

3.3 Results

3.3.1 An uncharacterized acyl-CoA synthetase, CG4500, is down-regulated in *dERR* mutant animals.

Previously, it had been shown that *dERR* mutants are unable to initiate the metabolic transition toward aerobic glycolysis to drive biomass production for developmental growth of the larva (87). The phenotypes that were observed in *dERR* mutant mid-L2 larvae were overwhelmingly associated with defects in carbohydrate catabolism, shockingly with little effect on fat catabolism (data not shown and 87). As discussed repeatedly, *Drosophila* larvae need to accumulate fat before the wandering stage, which starts around 24 hours before pupariation. Although only about 48 hrs apart

from mid-L2 in developmental timing, late-L3 animals undergo a very different metabolic plan. We speculated that dERR is likely involved in transcription regulating the late larval-switch toward OXPHOS. To test this hypothesis, we performed microarray analyses on RNA from clear-gut L3 larvae of control (w^{1118}) animals and *dERR* mutant ($dERR^{1}/dERR^{2}$). Clear-gut larvae are in a tight developmental window that is 0-4 hrs prior to pupariation. It takes 14-18 hrs of wandering for larvae to reach clear-gut status. They have been in developmental starvation for quite some time and are rely on fat-derived ATP generation. Although the lipase expression is not changed in *dERR* mutant, encouragingly, we found the expression of several enzymes involved in LCFAs activation are altered significantly (Table 3.1). The most interesting transcript was an uncharacterized gene CG4500, which is predicted to be an acyl-CoA synthetase. The transcriptional expression of CG4500 is down-regulated 8 times in the *dERR* mutant, which is among the top ten most down-regulated genes in all transcripts tested (data not shown, Table 3.1). *CG4500* encodes for an atypical bubblegum-like ACS in *Drosophila*, and is closely related to bubblegum protein in fly (44%), which is an ACS acting on VLCFAs (C22-26) and prevents their build-up (170). However, the human homolog of CG4500 is ACSBG2 that is an ACS acting on oleic acid (C18:1) and linoleic acid (C18:2) but not on other FAs tested (171). Interestingly, a human homolog of bubblegum (ACSBG1) can catalyze both LCFAs and VLCFAs (172).

Table 3.1 Transcriptional fold-changes measured by microarray in *dERR* mutants vs. w^{1118} control animals of LCFA metabolic transcripts at clear-gut L3 larvae

CG	Gene Name	Fold Change in *dERR* mut
Fat Mobilization (ATGL)		
CG5295	brummer lipase	1.00
LCFA Activation (ACS)		
CG8732	ACS long-chain	1.67
CG4501	bubblegum	4.05
CG12512	---	3.22
CG18155	---	-1.52
CG3961	---	-1.18
CG4500	**---**	**-8.03**
CG6178	---	2.77
CG9009	pudgy	-1.37
Carnitine Palmitoyltransferase (CPT)		
CG12891	CPT I	-1.86
CG2107	CPT II	1.19
CG1041	---	1.59
Acyl Carnitine Transporter (CAT)		
CG3057	Colt	1.21
CG3476	---	1.29
CG12201	---	-1.30
CG3790	---	1.16
CG4630	---	1.35
CG6006	---	-1.11
CG8925	---	-1.92

3.3.2 dERR is critical in the programmed expression of *Pfk* and *CG4500*

To further test the possibility that dERR turns on the early metabolic switch toward glycolysis during late embryogenesis, and later initiates a switch toward fatty acid oxidation before pupariation, we examed the expression profile of two representative metabolic enzymes through development. We collected RNA from control animals

and *dERR* mutants at 12 stages of development, including 6-12 hr AEL, 12-18 hr AEL, 18-24 hr AEL, 0-6 hr L1, mid-L1, mid-L2, mid-L3, -4 to 0 hr RTP (relative to pupariation) L3, 6 hr RTP, +18 hr RTP, +72 hr RTP, and 1-day old males. qRT-PCR was used to assess the relative expression of two genes, *Pfk* and *CG4500*. Pfk is the rate-limiting enzyme of glycolysis, and as the detector for glycolytic catabolism. CG4500, as shown earlier, is highly likely to be a LCFA ACS, and serves as the indicator for FAs oxidation. Strikingly, we see that the *Pfk* mRNA amounts dramatically increase from the embryonic stages through mid-L3, when its expression level reaches maximum, and is followed a sharp drop in expression at wandering onset. Thereafter, it is expressed at a low level until adulthood (Figure 3.3 A). In contrast, the *CG4500* mRNA amounts is low from the embryonic stages through clear-gut L3, when its expression increases dramatically and reaches its peak at +18 hr RTP, which is followed by a gradual decrease in metamorphosis, where finally go back to the expression level of the late embryo in adult fly (Figure 3.3 A). Even more strikingly, the expression of *Pfk* and *CG4500* are both almost completely abolished in *dERR* mutant at times, when their expression is still increasing (mid-L2 for *Pfk* and clear-gut L3 for *CG4500*). Collectively, these data suggest that dERR is likely instrumental in the late larval switch toward FAs oxidation, essentially countering its earlier pro-glycolytic activities.

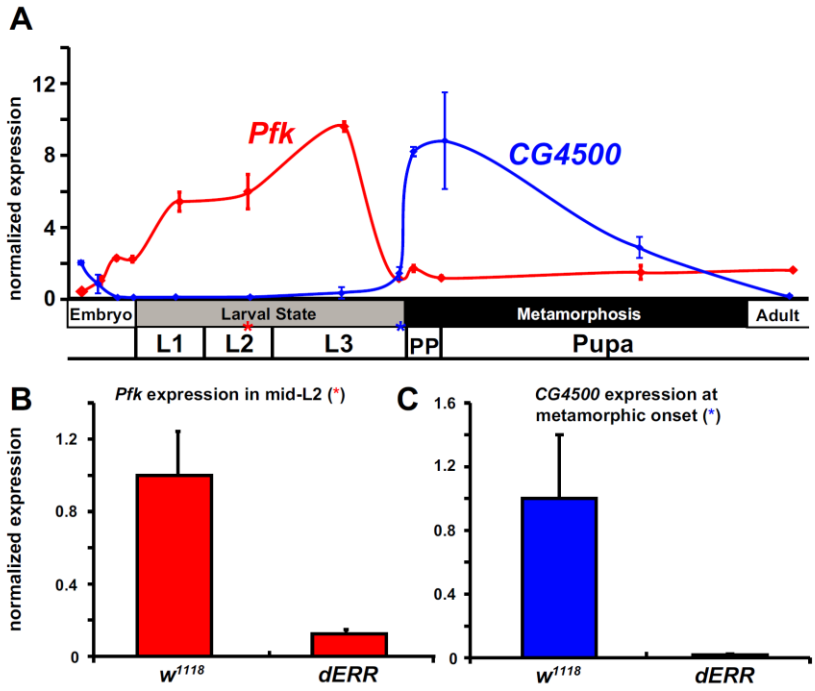

Figure 3.3 qRT-PCR analysis reveals that *Pfk* and *CG4500* exhibit dynamic expression through development (**A**). dERR is required for the pro-growth glycolytic program, represented by Pfk (**B**), and for the late-larval shift to FAs oxidation, represented by the long-chain fatty acid acyl-CoA synthetase, CG4500 (**C**). Collection times for **B** and **C** are noted by *.

3.3.3 CG4500 is an ACS with catalytic specificity on MCFAs and unsaturated LCFAs.

Each ACS has distinct substrate specificity, loading FAs of different lengths or saturation onto CoA. To determine the substrate specificity of CG4500, an acyl-CoA synthesis assay was performed using a series of FAs, including a variety of MCFAs, LCFAs, and VLCFA. Here, firefly luciferase is utilized as a positive control for the assay. It was previously shown that luciferase of *P.pyralis* and *L.cruciata* displayed significant

acyl-CoA synthetase activity on a variety of FAs, including saturated MCFAs (C10:0, C12:0), saturated LCFAs (C14:0), unsaturated LCFAs (C16:1, C18:2, C18:3n-3, C18:3n-6, C20:4, and C20:5) (169). Purified GST protein was used as negative control. Since we use radioactive labeled [α^{32}-P]ATP, recombinant enzymes purified by affinity column were employed in order to avoid high background associated with whole cell extract. Figure 3.4C showed that all three recombinant proteins are relatively pure with > 90% of purity, and, indeed, we see very low or almost no background. As expected, firefly luciferase of P. pyralis exhibits substrate specificity on C10:0, C12:0, C16:0, C16:1, C18:1, which is in accordance with the previous findings (Figure 3.4A and B, and 169). Furthermore, CG4500 acts on both saturated MCFAs and unsaturated LCFAs, including C10:0, C12:0, C16:1 and C18:1 (Figure 3.4A and B). The substrate specificity of CG4500 on C16:1 and C18:1 is encouraging, because its human homolog, ACSBG2, preferentially acts on unsaturated LCFAS (oleic acid (C18:1) and linoleic acid (C18:2)), but not on palmitic acid (C16:0) and linoceric acid (C24:0) (171), suggesting a conserved modality of preference is maintained from *Drosophila* to humans. However, unexpectedly, we observed that CG4500 has higher catalytic activity on MCFAs than on LCFAs. As we discussed in Section 3.3.1, CG4500 is most similar to enzymes that either ACS of LCFAs or VLCFAs; we did not expect it to act on MCFAs. Although CG4500 prefers MCFAs over LCFAs as substrates, because the lipid content of the fat body is overwhelmingly long-chain-triglyceride, it likely still acts mostly on LCFAs.

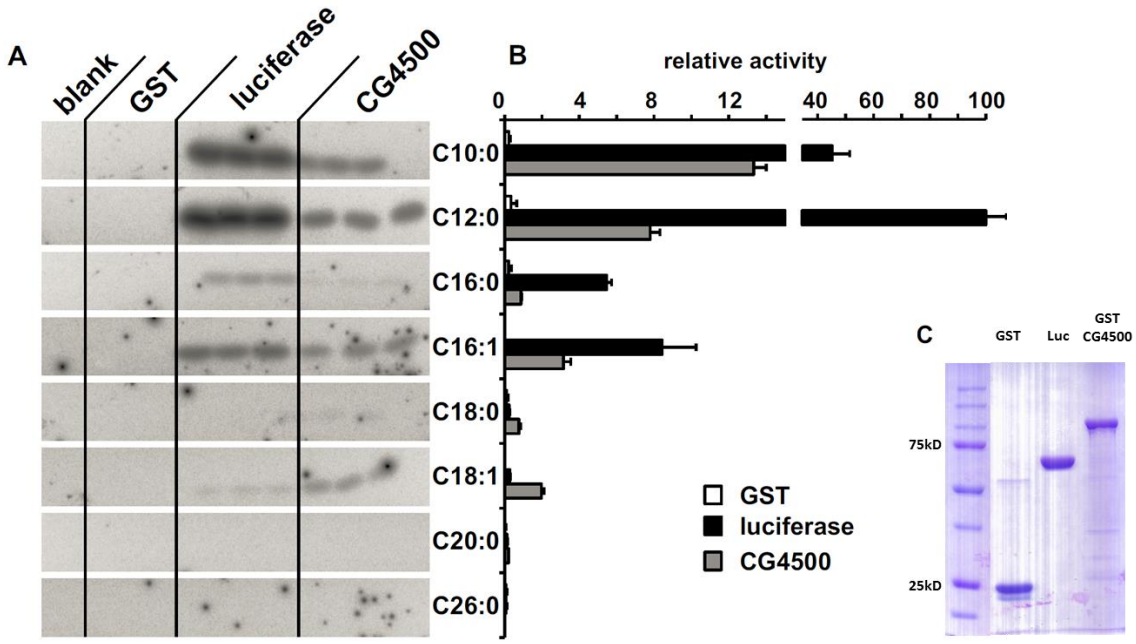

Figure3.4 Substrate specificity of CG4500. A) and B) Fatty acyl-CoA synthetic activity was determined by the formation of acyl-adenylate from a series of FAs. Fatty acyl-adenylate formation was monitored by detection of released ^{32}P-AMP from [α-^{32}P]ATP with TLC analysis. A) shows the TLC scan from Phosphoimager and B) shows the relative activity for each enzyme that is expressed as a percentage with respect to lauric acid. Assays for each FA independently repeated three times and the data represent the means ± SEM. C) Three recombinant protein purified by affinity column were separated by SDS-PAGE. 2.5mg of protein was run for each sample. Abbreviations are as follows: C10:0, decanoic acid; C12:0, lauric acid; C16:0, palmitic acid; C16:1, palmitoleic acid; C18:0 stearic acid; C18:1, oleic acid; C20:0, arachidic acid; C26:0, cerotic acid; Luc, luciferase protein; GST-CG4500, GST tagged CG4500 protein.)

3.3.4 CG4500 expression is induced by water starvation in a temporal-specific fashion.

Next, we wanted to know whether *CG4500* expression could be uncoupled from the developmentally orchestrated induction (Figure 3.3A) and induced by starving animals at developmental times that reach metabolic homeostasis, such as 1-day old males. And, was dERR required at other times? To begin, we tested two different time points, young larvae (at mid-L2) and young adult males (1 days post eclosion) by total nutrient deprivation (H_2O) or through sugar-only feeding (20% sucrose) for an 8-hr period for mid-L2 and 24-hr period for adult fly, and we compared transcriptional responses to animals on a normal diet (yeast for mid-L2 and regular cornmeal-molasses-yeast media for adult males) by qRT-PCR. Because *dERR* mutants do not survive to adulthood we were only able to assay responses in the w^{1118} control. In addition to *CG4500*, we also looked at *CPT-I* responses, reasoning that *CPT-I* may have a similar profile, because it should be active at the same time as CG4500. We found that the expression of *CG4500* is highly sensitive to starvation in young adults (Fig. 3.5A). Interestingly, this induction depends upon a depletion of sugar specifically, as the sucrose-supplemented animals remained unresponsive. We also found that, unlike *CG4500, CPT-I* was induced (albeit to a lesser extent) in animals fed only sugar, which was similar to the H_2O response (Fig. 3.5B). These results indicate that *CG4500* and *CPT-I* are likely controlled through separate nutrient-sensing pathways. In contrast to young adults, young larvae down-regulated *CG4500* expression in response to limiting nutrient conditions, regardless of

genotype (Fig. 3.5C). This response was specific to *CG4500*, because *CPT-I* responded as it did at the later adult time, showing modest induction in the control animals (Fig. 3.5D). However, in the *dERR* background *CPT-I* was not induced, but it did have a much elevated basal expression that was over 10-fold higher than control animals. This phenomenon suggests that dERR not only promotes glycolysis in early *Drosophila* developmental, but also might suppress oxidation of FAs at that time.

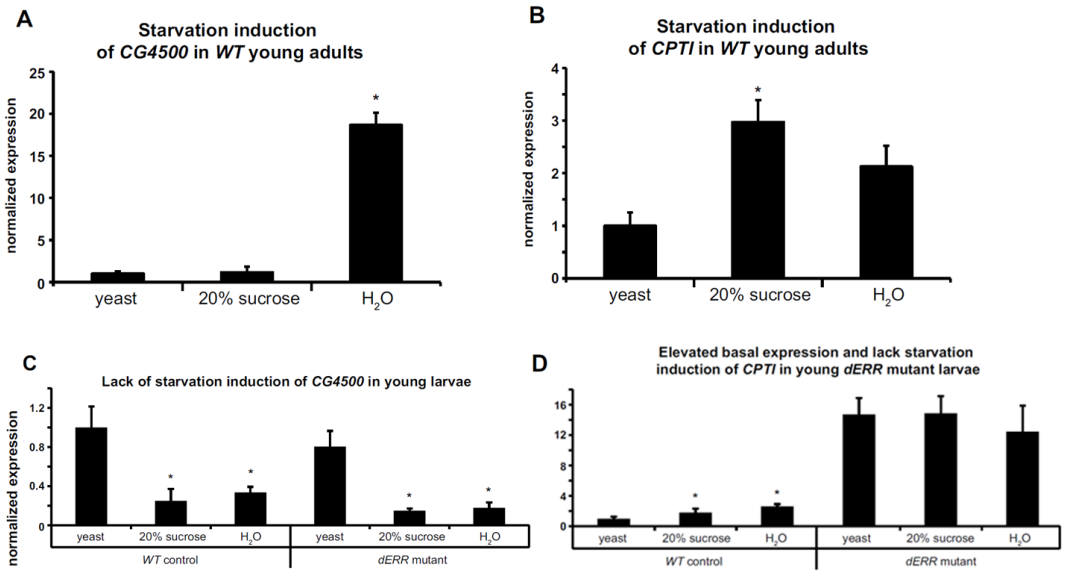

Figure 3.5 The triggers for induced expression of *CG4500* and *CPT-I* are different and temporal-specific. Induction of *CG4500* in day-old control males (A) on water alone but not those fed 20% sucrose, while both conditions elicited similar responses for *CPT-I* (B), though water was not significant. In mid-L2, *CG4500* was repressed in both control and *dERR* mutants (C), while control animals induced *CPT-I* in limiting nutrients and *dERR* mutants showed no change, but had elevated basal (D). Starvation challenges were carried out for 8 hrs for L2 and 24 hrs for adult. Responses measured by qPCR. * = *p*-value < 0.05. Error bars are ±SEM.

3.3.5 *dERR* mutant clear-gut L3 larvae are deranged in FAs metabolism.

We have shown that dERR regulates the expression of CG4500, which is an acyl-CoA synthetase acting on MCFAs and unsaturated LCFAs, just prior to metamorphosis. We next wanted to test whether this regulation has an effect on metabolism in *dERR* mutant. To do this, we measured a host of metabolites by GC/MS and LC/MS/MS in control (w^{1118}) animals and *dERR* mutants ($dERR^{1}/dERR^{2}$) in extracts that were prepared from clear-gut L3 larvae, the same stage of which our microarray analyses were performed. We found that *dERR* mutants are fully competent to mobilize stored fat from triacylglyceride (TAG) stores (Figure 3.6A). Furthermore, they have normal or elevated levels of all LCFAs surveyed, and have elevated levels of all medium-chain FAs measured, with particularly high levels of FAs in the C10-15 range (Figure 3.6A). These results suggested that TAG lipase activity was likely not affected in this background, especially since pre-wandering TAG levels were not significantly different in control and mutant animals (data not shown). These results also correspond to the unchanged expression of *brummer lipase* in *dERR* mutants. In contrast, carnitine conjugates of LCFAs were dramatically reduced altogether, despite having elevated levels of free carnitine available and a two-fold increase in deoxy-carnitine, a marker for carnitine synthesis (Figure 3.6B). These collective results indicated that *dERR* mutants are unable to process LCFAs for mβ-ox at the outer mitochondrial membrane.

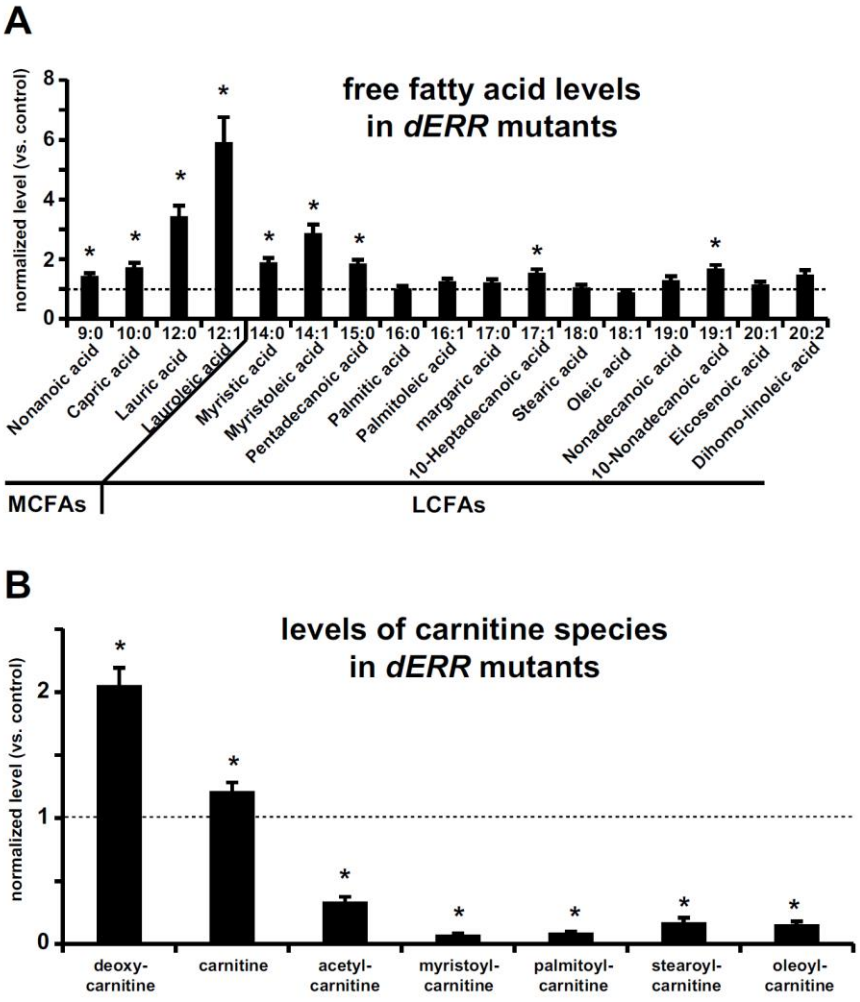

Figure3.6 *dERR* mutants are disturbed in lipid metabolism in clear-gut L3 larvae. Altered free fatty acids levels A) and carnitine species B) in *dERR* mutants as determined by GC/MS and LC/MS/MS. Dotted line shows levels for metabolites in control background. * = *p*-value < 0.05. Error bars are ±SEM.

3.4 Conclusions and Discussions

Here, we identified an uncharacterized acyl-CoA synthetase CG4500, the expression of which is under regulation of dERR right before metamorphosis in *Drosophila*. We showed that CG4500 specifically catalyzes the activation of saturated MCFAs (decanoic acid C10:0 and lauric acid C12:0) and unsaturated LCFAs (palmitoleic acid C16:1 and stearic acid C18:1) (Figure 3.4). In addition, microarray analysis and qRT-PCR experiments both showed that *dERR* mutants have very low-level expression of CG4500 transcripts in clear-gut L3 larvae (Table 3.1 and Figure 3.3). The regulation of dERR on CG4500 could be direct or indirect, however, our evidence favors that it is of a direct nature and that dERR binds to the promoter region to facilitate CG4500 transcription. Firstly, as a transcription factor mammalian ERRs are generally recruited to an ERR-specific response element (ERRE), which is a consensus sequence of AGGTCA as the core motif preceded by a TNA flank (173). We have found multiple potential ERREs (the core element AGGTCA) located in 5 kb upstream of CG4500 translation start site. Furthermore, there is an ERRE with high fidelity to the consensus sequence (TCAAGGTCA) located in the second intron of CG4500, which is conserved in several *Drosophila* species. More importantly, although we have not examined direct binding between dERR and the CG4500 promoter in our lab, a consortium performed CHIP-Seq analysis, and their data suggests that ERR localizes with great enrichment to the CG4500 prompter at three developmental times, including mid/late-embryos and early wandering

L3 (Figure 3.7). In addition, we are in the progress of completing directed CHIP experiments to test the interaction between dERR and the genomic region of CG4500, and identify the dERR regulatory sequence of CG4500 using luciferase reporter gene assay.

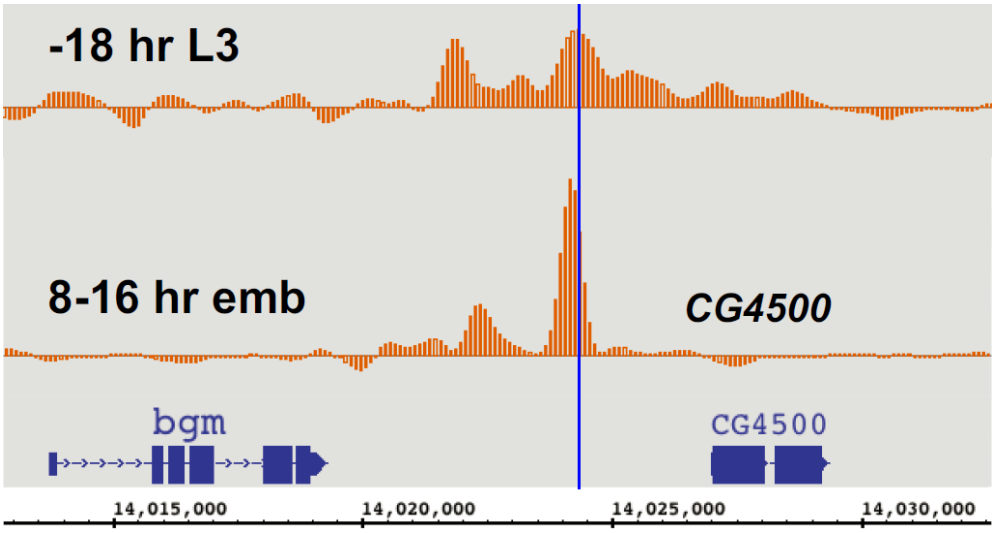

Figure 3.7 ERR-GFP is highly enriched at the CG4500 promoter in mid/late-embryo and early wandering L3. ERRE is indicated by the marked blue line.

Studies of the regulation of FA oxidation has been focused on the step of free FAs liberation (lipase) and the activity and expression of CPT-I considered as the rate-limiting step in lipid oxidation. Nevertheless, emerging evidence has revealed steps other than lipolysis and the carnitine cycle is important regulated events in the fatty acid catabolic pathway. For example, a recent report demonstrated that PGC-1/ERRα axis is involved in

the transcriptional regulation of CAT (carnitine/acylcarnitine translocase), which could be induced by fasting in mouse skeletal muscle (174). Another study which shares great similarity with our study here revealed that the coupling event of fatty acids to CoA via ACSs is an additional important regulated step in lipid catabolism in both fly and mammals (165). Intriguingly, the ACS (*pudgy*) identified in the study performed by Xie et al. is an unconserved gene that is only expressed in *Drosophila*. They observed pudgy is transcriptionally regulated by insulin/IGF. Interestingly, they found that the regulatory relationship between insulin/IGF and ACSs is preserved in mammalian cells, even though the regulated ACS is not conserved (165). The mammalian homolog of the ACS CG4500 we identified is called acyl-CoA synthetase bubblegum family member 2 (ACSBG2). ACSBG2 is primarily expressed in brainstem and testis (171), but not in adipose tissue, liver and muscle. This may raise the concern that the regulation of dERR in lipid oxidation at the level of CoA activation is not applicable to the mammalian system. However, there are two considerations to ease this concern. Firstly, although we did not demonstrate whether the lipid metabolism is disturbed or not in *CG4500* mutant animals due to the availability of the animals, we showed that CG4500 expression is potently induced by starvation, either developmental or applied (Figure 3.3 and Figure 3.5). Additionally, data posted online at flyatlas.org done by Dow *et al.* shows tremendous enrichment of CG4500 expression in the late-L3 fat body relative to any other tissue sampled (175). Fat body is considered as adipose tissue and liver counterpart for flies.

These data suggest that the expression of CG4500 is subject to regulation of nutrition status. Secondly, as mentioned earlier in this paragraph, the regulation relationship rather than the specific molecules seems to be preserved cross spices. We plan to perform starvation experiments in a mammalian adipocyte cell line (3T3-L1) with or without ERRs inhibitor, and examine mRNA level of multiple ACSs, including ACSBG2, by qRT-PCR. Hopefully, these experiments will firmly establish the regulatory role of ERRs on lipid oxidation at the level of fatty acid activation. This new link may be a potential target for drug development for variety of metabolic syndromes.

We observed that *dERR* mutants have imbalanced lipid profile. In clear-gut L2 larvae, they have depleted levels of carnitine conjugated LCFAs (acetyl-carnitine, myristoyl carnitine, palmitoyl-carnitine, stearoyl-carnitine, oleoyl-carnitine), but elevated MCFAs (nonanoic acid C9:0, decanoic acid C10:0, lauric acid C12:0, lauroleic acid C12:1) and LCFAs with carbon between 14 and 20 (myristic acid C14:0, myristoleic acid C14:1, pentadecanoic acid C15:0, 10-heptadecanoic acid C17:1, 10-nonadecanoic acid C19:1) (Figure 3.6). One phenomenon that draws my attention is the much increased MCFAs level in *dERR* mutant animals. As we know, MCFAs can freely penetrate the mitochondria (153). They do not need activation of ACSs or carnitine conjugation as for mβ-ox. If CG4500 is the only lipid metabolic enzyme greatly affected in *dERR* mutant, then MCFAs should not be significantly altered due to the fact that they can still travel into the mitochondria. So this data really suggests that other than CG4500 dERR

probably regulates other enzymes involved in lipid oxidation pathways. Indeed, a mammalian study showed that ERRα transcriptionally regulates the human medium-chain acyl CoA dehydrogenase, which is the enzyme catalyzes the first step of MCFA β-oxidation (173). So without this enzyme, MCFAs cannot be break down through β-oxidation to generate energy. Interestingly, our preliminary result from the microarray analysis done on wild type and *dERR* mutant of the clear-gut L3 exhibits decreased expression level of *CG12262*, which is a probable medium-chain specific acyl-CoA dehydrogenase (data not shown). As the master regulator of metabolic network, in my opinion, it is not shocking that ERR has multiple gene targets no matter in flies or mammals. These findings encouraged us to perform careful analysis on other metabolic enzymes that might be under the control of ERRs, which may provide insights to research performed in other organisms.

Last but not the least, currently we have not been able to measure the level of malonyl-CoA, which can inhibit CPT-I and have the same effect as CG4500 depletion. We want to rule out the possibility that the decreased levels of carnitine-conjugated FAs in *dERR* mutant is a consequence of abnormally high level of malonyl-CoA. We plan to reduce the level of malonyl-CoA by reducing the level of *acetyl-CoA carboxylase* (*ACC*) that converts acetyl-CoA to malonyl-CoA using an available RNAi construct. We consider elevated ACC activity highly unlikely, because we saw that AMPK, which is a potent inhibitor of ACC activity (176), is constitutively activated in *dERR* mutants (data

not shown). If knockdown of *ACC* does not affect the LCFA metabolites in *dERR* mutants, than almost for sure malonyl-CoA is not the problem.

Chapter 4 Conclusions and Future Directions

Metabolic homeostasis is strictly regulated and subject to instant changes under many physiological and pathological conditions, including normal development, where metabolism undergoes approximately series of physiologic changes, in cancer, where a pathological metabolic profile drives physiology, and in hypoxia, as both physiological and pathological conditions control outcomes. Normally, multicellular organisms have limited nutritional uptake, and in that way they need to employ a strategy to produce ATP efficiently. However, in some situations, such as development or hypoxia, cells rely on atypical metabolic strategies that are not necessarily efficient. For example, hypoxic metabolism heavily leans on glycolysis and converts pyruvate to lactate. Interestingly, proliferating cells also shift metabolism from mitochondrial OXPHOS toward glycolysis and lactate generation too, but for a different reason. They need to generate building blocks to provide all the materials for growth as we discussed in Chapter 1.

Our primary goal was to better understand the triggers cells employ and the consequences for different strategies of bioenergetic metabolism, using *Drosophila* as a model. *Drosophila* can respond robustly to hypoxia, and they also experience two programmed metabolic transitions through their development, making them a good model for our studies. Here, we also found that hypoxia-induced adaptation is stage dependent. We saw that hypoxic transcriptional induction is most apparent at the late-L3

time for all genes assayed. Our findings are consistent with previous observation that transient hypoxic exposures during the late larval and early pupal stages had the maximum effects on adult size compared to treatment performed during other stages (177). Altogether, eventually we want to understand the regulatory mechanism that control inducible and programmed metabolic transitions in flies.

First, we find that the molecular mechanisms that control the hypoxic adaptation are more complex than the conventional ideas suggest. We show that hypoxic-induced transcriptional adaptation response is subject to HIF-dependent and HIF-independent regulation. dERR can interact with dHIFα, and transcriptionally modulate hypoxic responses either together with dHIF or alone. Surprisingly, hypoxic responses contributing glycolytic genes are not controlled by the HIF-dependent pathways, but rather are regulated by dERR-dependent mechanisms. Also, a large portion of the hypoxic response cannot be attribute to either dHIF or dERR action. These results demonstrate that unknown pathways modulate hypoxic adaptation. Actually, we have designed a genetic screen to identify those potential pathways, which could provide ideas and perspectives for studying non-HIF hypoxic regulations in mammals. We plan to carry out the recessive EMS screen to identify HIF-independent pathways. We will use the well-established GAL4-UAS system, as well as the antagonizing effect of GAL80 on the activity of GAL4 protein (178, 179). We will generate transgenic flies that express GAL4 in a HIF-dependent fashion by putting *GAL4* gene under the control of HIF-dependent

promoter (HD>GAL4), and flies that express GAL80 in a HIF-independent way by controlling *GAL80* gene by HIF-independent promoter (HI>GAL80). We will detect the GAL4 protein using UAS-GFP strains. So, HD>GAL4 flies will express low GFP signal in normoxia, but light up in hypoxia. Then when we combine the HD>GAL4 chromosome together with the HI>GAL80 chromosome in the same strain by crossing, the new HD>GAL4, HD>GAL80 strain will express low GFP or no GFP signal in both normoxia and hypoxia. Then we chemically mutate the HD>GAL4, HD>GAL80 stain with EMS, and select those gain the ability to express GFP signal in hypoxic treatment, which are those loss the expression of GAL80 (loss the HIF-independence pathway). Hopefully, this strategy will provide us candidacy pathways for the puzzle of hypoxic adaptation response.

Additionally, we also find that loss of dHIFα greatly disturbs all aspects of carbohydrate catabolism under normoxia. This observation suggests that dHIFα might have a role in regulation of metabolic transitions induced by larvae in development. Since dHIFα is regulated in a post-transcriptional way, our wish to exam HIFα protein expression in a series of developmental stages in flies has been hampered by the availability of a good antibody. We made some effort to generate a dHIFα antibody with little success. It is possible that we could conquer this by redesign the part of dHIFα serving as antigen. But protein purification and design strategy for making antibody are not our turf. We plan to collaborate with either another lab or a company to make an

excellent antibody for us. But, overall, because dHIFα is a humongous protein with a molecular weight of 170kD, it will be a hard western to do anyway even with a widely used and commercially available antibody.

Previously, it is been shown that dERR is required to turn on an anabolic program that utilizes aerobic glycolysis (Warburg metabolism) to drive rapid growth at late embryogesis (87). Here, we demonstrate the role of dERR in turning off this aerobic glycolysis and switching on fatty acid oxidation. We find that dERR is essential for the transcriptional expression of CG4500, a previously uncharacterized LCFA acyl-CoA synthetase. We found that the transcription of CG4500 is temporally induced by starvation, and this induction is sugar sensitive. We saw that mid-L2 larvae actually express less amount of CG4500 mRNA under starvation. But the transcription of CG4500 is robustly induced by 24 hours starvation in one-day old male. This result is in accordance with another study done in two wild-derived inbred strains of *Drosophila*. They showed that the expression of CG4500 is induced about 3.5 times after 24 hours starvation in the head by microarray analysis (180). However, we were not able to test whether the starvation induction effect of CG4500 is dependent on dERR, due to the fact that *dERR* mutants do not survive to adulthood. We plan to employ *dERR* RNAi strains and take advantage of the heat-shock induction line, to only knock down dERR in adult fly or other stages desired. Using this system, we could study the function of dERR in adult flies. Because dERR greatly affects sugar metabolism in the earlier stages of larva

development, using the temporal knock down strategy will eliminate the cumulative effects of dERR through development.

Furthermore, we find that the transcription of CG4500 cannot be induced by treatment with 20% sucrose in one-day old males. This is a really interesting finding, because it gives us a hint that sugar metabolites or the products of sugar catabolism might be the signals activating dERR action. ERRα was the first orphan NRs ever found (4). However, even after many years, the signaling pathways that activate ERRs remain elusive. In mammals, co-activators, like PGC-1 or co-repressors, like RIP140, are viewed as protein ligands for ERRs. However, only one PGC-1α-like protein has been found in *Drosophila* (Spargel) but even it is not well conserved (181), and likely does not perform similar functions based on its sequence. Furthermore, there is indeed no evidence to show whether it interacts with or works together with dERR. We would like to study potential binding partners for dERR. Our yeast-two hybrid study has provided several other interesting candidates that may open avenues of investigation. So, our finding that CG4500 induction is sugar sensitive makes us speculate that dERR is activated by molecules involved in sugar catabolism. We plan to take advantage of available genetic tools to knock down major steps in sugar metabolism to see which pathway can block the sugar sensitive phenomenon. Then, we will test whether the metabolites involved in those pathways can activate dERR activity using ERRE reporter. Hopefully, those efforts will

lead us to new that signals stimulate ERR activities, and provide a molecular context for understanding the ERR activation pathways in mammals.

Literature of References

Literature of References

1. King-Jones, K., and Thummel, C.S. (2005). Nuclear receptors--a perspective from *Drosophila*. Nat. Rev. Genet. *6,* 311-323.

2. Glass, C.K., and Ogawa, S. (2006). Combinatorial roles of nuclear receptors in inflammation and immunity. Nat. Rev. Immunol. *6,* 44-55.

3. Evans, R. M. (1988). The steroid and thyroid hormone receptor superfamily. Science. *240,* 889-95.

4. Chawla, A., Repa, J.J., Evans, R.M., and Mangelsdorf, D.J. (2001). Nuclear receptors and lipid physiology: opening the X-files. Science *294,* 1866-1870.

5. Maglich J. M., Sluder A., Guan X., Shi Y., Mckee D. D., Carrick K., Kamdar K., Willson T. M., Moore J. T. (2001). Comparison of complete nuclear receptor sets from the human, Caenorhabditis elegans and Drosophila genomes. Genome Biol. *2,* RESEARCH0029.

6. Shlomo Melmed, Kenneth S. Polonsky, P. Reed Larsen, Henry M. Kronenberg, *Williams Textbook of Endocrinology*, 1955-2011. Philadelphia: Sauders, 2011.

7. Landrier, J.F., Grober, J., Demydchuk, J., and Besnard, P. (2003). FXRE can function as an LXRE in the promoter of human ileal bile acid-binding protein (I-BABP) gene. FEBS Lett. *553,* 299-303.

8. Castelein, H., Declercq, P.E., and Baes, M. (1997). DNA binding preferences of PPAR alpha/RXR alpha heterodimers. Biochem. Biophys. Res. Commun. *233,* 91-95.

9. Robinson-Rechavi, M., Escriva Garcia, H., and Laudet, V. (2003). The nuclear receptor superfamily. J. Cell. Sci. *116,* 585-586.

10. Umesono, K., and Evans, R.M. (1989). Determinants of target gene specificity for steroid/thyroid hormone receptors. Cell *57,* 1139-1146.

11. Renaud, J.P., and Moras, D. (2000). Structural studies on nuclear receptors. Cell Mol. Life Sci. *57,* 1748-1769.

12. Moras, D., and Gronemeyer, H. (1998). The nuclear receptor ligand-binding domain: structure and function. Curr. Opin. Cell Biol. *10,* 384-391.

13. Heery, D.M., Kalkhoven, E., Hoare, S., and Parker, M.G. (1997). A signature motif in transcriptional co-activators mediates binding to nuclear receptors. Nature *387,* 733-736.

14. Michael Ashburner, Kent Golic, R. Scott Hawley, *Drosophila: A Laboratory Handbook,* 2001-2004. New York: Cold Spring Harbor Laboratory Press, 2004.

15. Sutherland, J.D., Kozlova, T., Tzertzinis, G., and Kafatos, F.C. (1995). Drosophila hormone receptor 38: a second partner for Drosophila USP suggests an unexpected role for nuclear receptors of the nerve growth factor-induced protein B type. Proc. Natl. Acad. Sci. U. S. A. *92,* 7966-7970.

16. Stoffel, M., and Duncan, S.A. (1997). The maturity-onset diabetes of the young (MODY1) transcription factor HNF4alpha regulates expression of genes required for glucose transport and metabolism. Proc. Natl. Acad. Sci. U. S. A. *94*, 13209-13214.

17. Shih, D.Q., Dansky, H.M., Fleisher, M., Assmann, G., Fajans, S.S., and Stoffel, M. (2000). Genotype/phenotype relationships in HNF-4alpha/MODY1: haploinsufficiency is associated with reduced apolipoprotein (AII), apolipoprotein (CIII), lipoprotein(a), and triglyceride levels. Diabetes *49*, 832-837.

18. Palanker, L., Tennessen, J.M., Lam, G., and Thummel, C.S. (2009). Drosophila HNF4 regulates lipid mobilization and beta-oxidation. Cell. Metab. *9*, 228-239.

19. Giguere, V., Yang, N., Segui, P., and Evans, R.M. (1988). Identification of a new class of steroid hormone receptors. Nature *331*, 91-94.

20. Eudy, J.D., Yao, S., Weston, M.D., Ma-Edmonds, M., Talmadge, C.B., Cheng, J.J., Kimberling, W.J., and Sumegi, J. (1998). Isolation of a gene encoding a novel member of the nuclear receptor superfamily from the critical region of Usher syndrome type IIa at 1q41. Genomics *50*, 382-384.

21. Heard, D.J., Norby, P.L., Holloway, J., and Vissing, H. (2000). Human ERRgamma, a third member of the estrogen receptor-related receptor (ERR) subfamily of orphan nuclear receptors: tissue-specific isoforms are expressed during development and in the adult. Mol. Endocrinol. *14*, 382-392.

22. Hong, H., Yang, L., and Stallcup, M.R. (1999). Hormone-independent transcriptional activation and coactivator binding by novel orphan nuclear receptor ERR3. J. Biol. Chem. *274*, 22618-22626.

23. Tremblay, A.M., and Giguere, V. (2007). The NR3B subgroup: an ovERRview. Nucl. Recept. Signal. *5*, e009.

24. Vu, E.H., Kraus, R.J., and Mertz, J.E. (2007). Phosphorylation-dependent sumoylation of estrogen-related receptor alpha1. Biochemistry *46*, 9795-9804.

25. Tremblay A.M., Wilson B.J., Yang X.J., Giguère V. (2008) Phosphorylation-dependent sumoylation regulates estrogen-related receptor-alpha and -gamma transcriptional activity through a synergy control motif. Mol. Endocrinol. *22*, 570-84.

26. van Beekum, O., Fleskens, V., and Kalkhoven, E. (2009). Posttranslational modifications of PPAR-gamma: fine-tuning the metabolic master regulator. Obesity (Silver Spring) *17*, 213-219.

27. Dufour, C.R., Wilson, B.J., Huss, J.M., Kelly, D.P., Alaynick, W.A., Downes, M., Evans, R.M., Blanchette, M., and Giguere, V. (2007). Genome-wide orchestration of cardiac functions by the orphan nuclear receptors ERRalpha and gamma. Cell. Metab. *5*, 345-356.

28. Vanacker, J.M., Pettersson, K., Gustafsson, J.A., and Laudet, V. (1999). Transcriptional targets shared by estrogen receptor- related receptors (ERRs) and estrogen receptor (ER) alpha, but not by ERbeta. Embo j. *18,* 4270-4279.

29. Deblois, G., Hall, J.A., Perry, M.C., Laganiere, J., Ghahremani, M., Park, M., Hallett, M., and Giguere, V. (2009). Genome-wide identification of direct target genes implicates estrogen-related receptor alpha as a determinant of breast cancer heterogeneity. Cancer Res. *69,* 6149-6157.

30. Coward P., Lee D., Hull M.V., Lehmann J.M. (2001). 4-Hydroxytamoxifen binds to and deactivates the estrogen-related receptor gamma. Proc Natl Acad Sci U. S. A. *98*, 8880-4.

31. Nichol D., Christian M., Steel J.H., White R., Parker M.G. (2006). RIP140 expression is stimulated by estrogen-related receptor alpha during adpogenesis. J Biol Chem. *281*, 32140-7.

32. Giguere, V. (2008). Transcriptional control of energy homeostasis by the estrogen-related receptors. Endocr. Rev. *29,* 677-696.

33. Kamei, Y., Ohizumi, H., Fujitani, Y., Nemoto, T., Tanaka, T., Takahashi, N., Kawada, T., Miyoshi, M., Ezaki, O., and Kakizuka, A. (2003). PPARgamma coactivator 1beta/ERR ligand 1 is an ERR protein ligand, whose expression induces a high-energy expenditure and antagonizes obesity. Proc. Natl. Acad. Sci. U. S. A. *100,* 12378-12383.

34. Bookout, A.L., Jeong, Y., Downes, M., Yu, R.T., Evans, R.M., and Mangelsdorf, D.J. (2006). Anatomical profiling of nuclear receptor expression reveals a hierarchical transcriptional network. Cell *126,* 789-799.

35. Tremblay, A.M., Dufour, C.R., Ghahremani, M., Reudelhuber, T.L., and Giguere, V. (2010). Physiological genomics identifies estrogen-related receptor alpha as a regulator of renal sodium and potassium homeostasis and the renin-angiotensin pathway. Mol. Endocrinol. *24*, 22-32.

36. Mootha V.K., Handschin C., Arlow D., Xie X., St Pierre J., Sihag S., Yang W., Altshuler D., Pulgserver P., Patterson N., Willy P.J., Schulman I.G., Heyman R.A., Lander E.S., Spiegelman B.M. (2004). Erralpha and Gabpa/b specific PGC-1alpha-dependent oxidative phosphorylation gene expression that is altered in diabetic muscle. Proc Natl Acad Sci U. S. A. *101*, 6579-5

37. Charest-Marcotte, A., Dufour, C.R., Wilson, B.J., Tremblay, A.M., Eichner, L.J., Arlow, D.H., Mootha, V.K., and Giguere, V. (2010). The homeobox protein Prox1 is a negative modulator of ERR{alpha}/PGC-1{alpha} bioenergetic functions. Genes Dev. *24*, 537-542.

38. Dufour, C.R., Levasseur, M.P., Pham, N.H., Eichner, L.J., Wilson, B.J., Charest-Marcotte, A., Duguay, D., Poirier-Heon, J.F., Cermakian, N., and Giguere, V. (2011).

Genomic convergence among ERRalpha, PROX1, and BMAL1 in the control of metabolic clock outputs. PLoS Genet. *7,* e1002143.

39. Dufour, C.R., Wilson, B.J., Huss, J.M., Kelly, D.P., Alaynick, W.A., Downes, M., Evans, R.M., Blanchette, M., and Giguere, V. (2007). Genome-wide orchestration of cardiac functions by the orphan nuclear receptors ERRalpha and gamma. Cell. Metab. *5,* 345-356.

40. Alaynick, W.A., Kondo, R.P., Xie, W., He, W., Dufour, C.R., Downes, M., Jonker, J.W., Giles, W., Naviaux, R.K., Giguere, V., and Evans, R.M. (2007). ERRgamma directs and maintains the transition to oxidative metabolism in the postnatal heart. Cell. Metab. *6,* 13-24.

41. Sonoda, J., Laganiere, J., Mehl, I.R., Barish, G.D., Chong, L.W., Li, X., Scheffler, I.E., Mock, D.C., Bataille, A.R., Robert, F., *et al.* (2007). Nuclear receptor ERR alpha and coactivator PGC-1 beta are effectors of IFN-gamma-induced host defense. Genes Dev. *21,* 1909-1920.

42. Eichner, L.J., and Giguere, V. (2011). Estrogen related receptors (ERRs): a new dawn in transcriptional control of mitochondrial gene networks. Mitochondrion *11,* 544-552.

43. Schreiber, S.N., Emter, R., Hock, M.B., Knutti, D., Cardenas, J., Podvinec, M., Oakeley, E.J., and Kralli, A. (2004). The estrogen-related receptor alpha (ERRalpha)

functions in PPARgamma coactivator 1alpha (PGC-1alpha)-induced mitochondrial biogenesis. Proc. Natl. Acad. Sci. U. S. A. *101,* 6472-6477.

44. Luo, J., Sladek, R., Carrier, J., Bader, J.A., Richard, D., and Giguere, V. (2003). Reduced fat mass in mice lacking orphan nuclear receptor estrogen-related receptor alpha. Mol. Cell. Biol. *23,* 7947-7956.

45. Carrier, J.C., Deblois, G., Champigny, C., Levy, E., and Giguere, V. (2004). Estrogen-related receptor alpha (ERRalpha) is a transcriptional regulator of apolipoprotein A-IV and controls lipid handling in the intestine. J. Biol. Chem. *279,* 52052-52058.

46. Villena, J.A., Hock, M.B., Chang, W.Y., Barcas, J.E., Giguere, V., and Kralli, A. (2007). Orphan nuclear receptor estrogen-related receptor alpha is essential for adaptive thermogenesis. Proc. Natl. Acad. Sci. U. S. A. *104,* 1418-1423.

47. Huss, J.M., Imahashi, K., Dufour, C.R., Weinheimer, C.J., Courtois, M., Kovacs, A., Giguere, V., Murphy, E., and Kelly, D.P. (2007). The nuclear receptor ERRalpha is required for the bioenergetic and functional adaptation to cardiac pressure overload. Cell. Metab. *6,* 25-37.

48. Rangwala, S.M., Wang, X., Calvo, J.A., Lindsley, L., Zhang, Y., Deyneko, G., Beaulieu, V., Gao, J., Turner, G., and Markovits, J. (2010). Estrogen-related receptor

gamma is a key regulator of muscle mitochondrial activity and oxidative capacity. J. Biol. Chem. *285,* 22619-22629.

49. Narkar, V.A., Fan, W., Downes, M., Yu, R.T., Jonker, J.W., Alaynick, W.A., Banayo, E., Karunasiri, M.S., Lorca, S., and Evans, R.M. (2011). Exercise and PGC-1alpha-independent synchronization of type I muscle metabolism and vasculature by ERRgamma. Cell. Metab. *13,* 283-293.

50. Murray, J., Auwerx, J., and Huss, J.M. (2013). Impaired myogenesis in estrogen-related receptor gamma (ERRgamma)-deficient skeletal myocytes due to oxidative stress. Faseb j. *27,* 135-150.

51. Luo, J., Sladek, R., Carrier, J., Bader, J.A., Richard, D., and Giguere, V. (2003). Reduced fat mass in mice lacking orphan nuclear receptor estrogen-related receptor alpha. Mol. Cell. Biol. *23,* 7947-7956.

52. Gronemeyer, H., Gustafsson, J.A., and Laudet, V. (2004). Principles for modulation of the nuclear receptor superfamily. Nat. Rev. Drug Discov. *3,* 950-964.

53. Kamei, Y., Lwin, H., Saito, K., Yokoyama, T., Yoshiike, N., Ezaki, O., and Tanaka, H. (2005). The 2.3 genotype of ESRRA23 of the ERR alpha gene is associated with a higher BMI than the 2.2 genotype. Obes. Res. *13,* 1843-1844.

54. Larsen, L.H., Rose, C.S., Sparso, T., Overgaard, J., Torekov, S.S., Grarup, N., Jensen, D.P., Albrechtsen, A., Andersen, G., Ek, J., *et al.* (2007). Genetic analysis of the

estrogen-related receptor alpha and studies of association with obesity and type 2 diabetes. Int. J. Obes. (Lond) *31,* 365-370.

55. Kim, D.K., Ryu, D., Koh, M., Lee, M.W., Lim, D., Kim, M.J., Kim, Y.H., Cho, W.J., Lee, C.H., Park, S.B., Koo, S.H., and Choi, H.S. (2012). Orphan nuclear receptor estrogen-related receptor gamma (ERRgamma) is key regulator of hepatic gluconeogenesis. J. Biol. Chem. *287,* 21628-21639.

56. Kim, D.K., Gang, G.T., Ryu, D., Koh, M., Kim, Y.N., Kim, S.S., Park, J., Kim, Y.H., Sim, T., Lee, I.K., *et al.* (2013). Inverse agonist of nuclear receptor ERRgamma mediates antidiabetic effect through inhibition of hepatic gluconeogenesis. Diabetes *62,* 3093-3102.

57. Magliano, D.J., and Lyons, J.G. (2013). Bisphenol A and diabetes, insulin resistance, cardiovascular disease and obesity: controversy in a (plastic) cup? J. Clin. Endocrinol. Metab. *98,* 502-504.

58. Sun, P., Sehouli, J., Denkert, C., Mustea, A., Konsgen, D., Koch, I., Wei, L., and Lichtenegger, W. (2005). Expression of estrogen receptor-related receptors, a subfamily of orphan nuclear receptors, as new tumor biomarkers in ovarian cancer cells. J. Mol. Med. (Berl) *83,* 457-467.

59. Cavallini, A., Notarnicola, M., Giannini, R., Montemurro, S., Lorusso, D., Visconti, A., Minervini, F., and Caruso, M.G. (2005). Oestrogen receptor-related receptor alpha

(ERRalpha) and oestrogen receptors (ERalpha and ERbeta) exhibit different gene expression in human colorectal tumour progression. Eur. J. Cancer *41,* 1487-1494.

60. Ariazi, E.A., Clark, G.M., and Mertz, J.E. (2002). Estrogen-related receptor alpha and estrogen-related receptor gamma associate with unfavorable and favorable biomarkers, respectively, in human breast cancer. Cancer Res. *62,* 6510-6518.

61. Jaakkola, P., Mole, D.R., Tian, Y.M., Wilson, M.I., Gielbert, J., Gaskell, S.J., von Kriegsheim, A., Hebestreit, H.F., Mukherji, M., Schofield, C.J., *et al.* (2001). Targeting of HIF-alpha to the von Hippel-Lindau ubiquitylation complex by O2-regulated prolyl hydroxylation. Science *292,* 468-472.

62. Suzuki, T., Miki, Y., Moriya, T., Shimada, N., Ishida, T., Hirakawa, H., Ohuchi, N., and Sasano, H. (2004). Estrogen-related receptor alpha in human breast carcinoma as a potent prognostic factor. Cancer Res. *64,* 4670-4676.

63. Chang, C.Y., Kazmin, D., Jasper, J.S., Kunder, R., Zuercher, W.J., and McDonnell, D.P. (2011). The metabolic regulator ERRalpha, a downstream target of HER2/IGF-1R, as a therapeutic target in breast cancer. Cancer. Cell. *20,* 500-510.

64. Fradet, A., Sorel, H., Bouazza, L., Goehrig, D., Depalle, B., Bellahcene, A., Castronovo, V., Follet, H., Descotes, F., Aubin, J.E., Clezardin, P., and Bonnelye, E. (2011). Dual function of ERRalpha in breast cancer and bone metastasis formation: implication of VEGF and osteoprotegerin. Cancer Res. *71,* 5728-5738.

65. Zhao, Y., Li, Y., Lou, G., Zhao, L., Xu, Z., Zhang, Y., and He, F. (2012). MiR-137 targets estrogen-related receptor alpha and impairs the proliferative and migratory capacity of breast cancer cells. PLoS One *7,* e39102.

66. WARBURG, O. (1956). On respiratory impairment in cancer cells. Science *124,* 269-270.

67. Koppenol, W.H., Bounds, P.L., and Dang, C.V. (2011). Otto Warburg's contributions to current concepts of cancer metabolism. Nat. Rev. Cancer. *11,* 325-337.

68. Ao, A., Wang, H., Kamarajugadda, S., and Lu, J. (2008). Involvement of estrogen-related receptors in transcriptional response to hypoxia and growth of solid tumors. Proc. Natl. Acad. Sci. U. S. A. *105,* 7821-7826.

69. Warburg, O., Wind, F., and Negelein, E. (1927). The Metabolism of Tumors in the Body. J. Gen. Physiol. *8,* 519-530.

70. WARBURG, O. (1956). On the origin of cancer cells. Science *123,* 309-314.

71. Simonnet, H., Alazard, N., Pfeiffer, K., Gallou, C., Beroud, C., Demont, J., Bouvier, R., Schagger, H., and Godinot, C. (2002). Low mitochondrial respiratory chain content correlates with tumor aggressiveness in renal cell carcinoma. Carcinogenesis *23,* 759-768.

72. Fantin, V.R., St-Pierre, J., and Leder, P. (2006). Attenuation of LDH-A expression uncovers a link between glycolysis, mitochondrial physiology, and tumor maintenance. Cancer. Cell. *9*, 425-434.

73. Moreno-Sanchez, R., Rodriguez-Enriquez, S., Marin-Hernandez, A., and Saavedra, E. (2007). Energy metabolism in tumor cells. Febs j. *274*, 1393-1418.

74. Hsu, P.P., and Sabatini, D.M. (2008). Cancer cell metabolism: Warburg and beyond. Cell *134*, 703-707.

75. DeBerardinis, R.J., Lum, J.J., Hatzivassiliou, G., and Thompson, C.B. (2008). The biology of cancer: metabolic reprogramming fuels cell growth and proliferation. Cell. Metab. *7*, 11-20.

76. Vander Heiden, M.G., Cantley, L.C., and Thompson, C.B. (2009). Understanding the Warburg effect: the metabolic requirements of cell proliferation. Science *324*, 1029-1033.

77. DeBerardinis, R.J., Mancuso, A., Daikhin, E., Nissim, I., Yudkoff, M., Wehrli, S., and Thompson, C.B. (2007). Beyond aerobic glycolysis: transformed cells can engage in glutamine metabolism that exceeds the requirement for protein and nucleotide synthesis. Proc. Natl. Acad. Sci. U. S. A. *104*, 19345-19350.

78. Fantin, V.R., St-Pierre, J., and Leder, P. (2006). Attenuation of LDH-A expression uncovers a link between glycolysis, mitochondrial physiology, and tumor maintenance. Cancer. Cell. *9*, 425-434.

79. Baysal, B.E., Ferrell, R.E., Willett-Brozick, J.E., Lawrence, E.C., Myssiorek, D., Bosch, A., van der Mey, A., Taschner, P.E., Rubinstein, W.S., Myers, E.N., *et al.* (2000). Mutations in SDHD, a mitochondrial complex II gene, in hereditary paraganglioma. Science *287,* 848-851.

80. Pollard, P.J., Wortham, N.C., and Tomlinson, I.P. (2003). The TCA cycle and tumorigenesis: the examples of fumarate hydratase and succinate dehydrogenase. Ann. Med. *35,* 632-639.

81. Parsons, D.W., Jones, S., Zhang, X., Lin, J.C., Leary, R.J., Angenendt, P., Mankoo, P., Carter, H., Siu, I.M., Gallia, G.L., *et al.* (2008). An integrated genomic analysis of human glioblastoma multiforme. Science *321,* 1807-1812.

82. Bleeker, F.E., Lamba, S., Leenstra, S., Troost, D., Hulsebos, T., Vandertop, W.P., Frattini, M., Molinari, F., Knowles, M., Cerrato, A., *et al.* (2009). IDH1 mutations at residue p.R132 (IDH1(R132)) occur frequently in high-grade gliomas but not in other solid tumors. Hum. Mutat. *30,* 7-11.

83. Yan, H., Parsons, D.W., Jin, G., McLendon, R., Rasheed, B.A., Yuan, W., Kos, I., Batinic-Haberle, I., Jones, S., Riggins, G.J., *et al.* (2009). IDH1 and IDH2 mutations in gliomas. N. Engl. J. Med. *360,* 765-773.

84. Zhu, A., Lee, D., and Shim, H. (2011). Metabolic positron emission tomography imaging in cancer detection and therapy response. Semin. Oncol. *38,* 55-69.

85. Chisamore, M.J., Wilkinson, H.A., Flores, O., and Chen, J.D. (2009). Estrogen-related receptor-alpha antagonist inhibits both estrogen receptor-positive and estrogen receptor-negative breast tumor growth in mouse xenografts. Mol. Cancer. Ther. *8*, 672-681.

86. Eichner, L.J., Perry, M.C., Dufour, C.R., Bertos, N., Park, M., St-Pierre, J., and Giguere, V. (2010). miR-378(*) mediates metabolic shift in breast cancer cells via the PGC-1beta/ERRgamma transcriptional pathway. Cell. Metab. *12*, 352-361.

87. Tennessen, J.M., Baker, K.D., Lam, G., Evans, J., and Thummel, C.S. (2011). The Drosophila estrogen-related receptor directs a metabolic switch that supports developmental growth. Cell. Metab. *13*, 139-148.

88. Semenza, G.L. (2011). Oxygen sensing, homeostasis, and disease. N. Engl. J. Med. *365*, 537-547.

89. Schofield, C.J., and Ratcliffe, P.J. (2004). Oxygen sensing by HIF hydroxylases. Nat. Rev. Mol. Cell Biol. *5*, 343-354.

90. Murdoch, C., Muthana, M., and Lewis, C.E. (2005). Hypoxia regulates macrophage functions in inflammation. J. Immunol. *175*, 6257-6263.

91. Fine, L.G., and Norman, J.T. (2008). Chronic hypoxia as a mechanism of progression of chronic kidney diseases: from hypothesis to novel therapeutics. Kidney Int. *74*, 867-872.

92. Semenza, G.L. (2003). Targeting HIF-1 for cancer therapy. Nat. Rev. Cancer. *3,* 721-732.

93. Bruick, R.K., and McKnight, S.L. (2001). A conserved family of prolyl-4-hydroxylases that modify HIF. Science *294,* 1337-1340.

94. Yu, F., White, S.B., Zhao, Q., and Lee, F.S. (2001). HIF-1alpha binding to VHL is regulated by stimulus-sensitive proline hydroxylation. Proc. Natl. Acad. Sci. U. S. A. *98,* 9630-9635.

95. Ivan, M., Kondo, K., Yang, H., Kim, W., Valiando, J., Ohh, M., Salic, A., Asara, J.M., Lane, W.S., and Kaelin, W.G.,Jr. (2001). HIFalpha targeted for VHL-mediated destruction by proline hydroxylation: implications for O2 sensing. Science *292,* 464-468.

96. Jaakkola, P., Mole, D.R., Tian, Y.M., Wilson, M.I., Gielbert, J., Gaskell, S.J., von Kriegsheim, A., Hebestreit, H.F., Mukherji, M., Schofield, C.J., *et al.* (2001). Targeting of HIF-alpha to the von Hippel-Lindau ubiquitylation complex by O2-regulated prolyl hydroxylation. Science *292,* 468-472.

97. Lando, D., Peet, D.J., Whelan, D.A., Gorman, J.J., and Whitelaw, M.L. (2002). Asparagine hydroxylation of the HIF transactivation domain a hypoxic switch. Science *295,* 858-861.

98. Mahon, P.C., Hirota, K., and Semenza, G.L. (2001). FIH-1: a novel protein that interacts with HIF-1alpha and VHL to mediate repression of HIF-1 transcriptional activity. Genes Dev. *15,* 2675-2686.

99. Hewitson, K.S., McNeill, L.A., Riordan, M.V., Tian, Y.M., Bullock, A.N., Welford, R.W., Elkins, J.M., Oldham, N.J., Bhattacharya, S., Gleadle, J.M., *et al.* (2002). Hypoxia-inducible factor (HIF) asparagine hydroxylase is identical to factor inhibiting HIF (FIH) and is related to the cupin structural family. J. Biol. Chem. *277,* 26351-26355.

100. Carmeliet, P., Dor, Y., Herbert, J.M., Fukumura, D., Brusselmans, K., Dewerchin, M., Neeman, M., Bono, F., Abramovitch, R., Maxwell, P., *et al.* (1998). Role of HIF-1alpha in hypoxia-mediated apoptosis, cell proliferation and tumour angiogenesis. Nature *394,* 485-490.

101. Ryan, H.E., Lo, J., and Johnson, R.S. (1998). HIF-1 alpha is required for solid tumor formation and embryonic vascularization. Embo j. *17,* 3005-3015.

102. Yu, A.Y., Shimoda, L.A., Iyer, N.V., Huso, D.L., Sun, X., McWilliams, R., Beaty, T., Sham, J.S., Wiener, C.M., Sylvester, J.T., and Semenza, G.L. (1999). Impaired physiological responses to chronic hypoxia in mice partially deficient for hypoxia-inducible factor 1alpha. J. Clin. Invest. *103,* 691-696.

103. Iyer, N.V., Kotch, L.E., Agani, F., Leung, S.W., Laughner, E., Wenger, R.H., Gassmann, M., Gearhart, J.D., Lawler, A.M., Yu, A.Y., and Semenza, G.L. (1998).

Cellular and developmental control of O2 homeostasis by hypoxia-inducible factor 1 alpha. Genes Dev. *12,* 149-162.

104. Seagroves, T.N., Ryan, H.E., Lu, H., Wouters, B.G., Knapp, M., Thibault, P., Laderoute, K., and Johnson, R.S. (2001). Transcription factor HIF-1 is a necessary mediator of the pasteur effect in mammalian cells. Mol. Cell. Biol. *21,* 3436-3444.

105. Shen, C., Nettleton, D., Jiang, M., Kim, S.K., and Powell-Coffman, J.A. (2005). Roles of the HIF-1 hypoxia-inducible factor during hypoxia response in Caenorhabditis elegans. J. Biol. Chem. *280,* 20580-20588.

106. Mizukami, Y., Li, J., Zhang, X., Zimmer, M.A., Iliopoulos, O., and Chung, D.C. (2004). Hypoxia-inducible factor-1-independent regulation of vascular endothelial growth factor by hypoxia in colon cancer. Cancer Res. *64,* 1765-1772.

107. Elvidge, G.P., Glenny, L., Appelhoff, R.J., Ratcliffe, P.J., Ragoussis, J., and Gleadle, J.M. (2006). Concordant regulation of gene expression by hypoxia and 2-oxoglutarate-dependent dioxygenase inhibition: the role of HIF-1alpha, HIF-2alpha, and other pathways. J. Biol. Chem. *281,* 15215-15226.

108. Wood, S.M., Wiesener, M.S., Yeates, K.M., Okada, N., Pugh, C.W., Maxwell, P.H., and Ratcliffe, P.J. (1998). Selection and analysis of a mutant cell line defective in the hypoxia-inducible factor-1 alpha-subunit (HIF-1alpha). Characterization of hif-1alpha-

dependent and -independent hypoxia-inducible gene expression. J. Biol. Chem. *273*, 8360-8368.

109. Wingrove, J.A., and O'Farrell, P.H. (1999). Nitric oxide contributes to behavioral, cellular, and developmental responses to low oxygen in Drosophila. Cell *98*, 105-114.

110. HADDAD, G.G., WYMAN, R.J., MOHSENIN, A., SUN, Y., and KRISHNAN, S.N. (1997). Behavioral and Electrophysiologic Responses of Drosophila melanogaster to Prolonged Periods of Anoxia. J. Insect Physiol. *43*, 203-210.

111. Gorr, T.A., Gassmann, M., and Wappner, P. (2006). Sensing and responding to hypoxia via HIF in model invertebrates. J. Insect Physiol. *52*, 349-364.

112. Liu, G., Roy, J., and Johnson, E.A. (2006). Identification and function of hypoxia-response genes in Drosophila melanogaster. Physiol. Genomics *25*, 134-141.

113. Zhou, D., Xue, J., Lai, J.C., Schork, N.J., White, K.P., and Haddad, G.G. (2008). Mechanisms underlying hypoxia tolerance in Drosophila melanogaster: hairy as a metabolic switch. PLoS Genet. *4*, e1000221.

114. Centanin, L., Dekanty, A., Romero, N., Irisarri, M., Gorr, T.A., and Wappner, P. (2008). Cell autonomy of HIF effects in Drosophila: tracheal cells sense hypoxia and induce terminal branch sprouting. Dev. Cell. *14*, 547-558.

115. Mortimer, N.T., and Moberg, K.H. (2009). Regulation of Drosophila embryonic tracheogenesis by dVHL and hypoxia. Dev. Biol. *329*, 294-305.

116. Metzger, R.J., and Krasnow, M.A. (1999). Genetic control of branching morphogenesis. Science *284*, 1635-1639.

117. Feala, J.D., Coquin, L., McCulloch, A.D., and Paternostro, G. (2007). Flexibility in energy metabolism supports hypoxia tolerance in Drosophila flight muscle: metabolomic and computational systems analysis. Mol. Syst. Biol. *3*, 99.

118. Cai, Q., Lin, T., Kamarajugadda, S., and Lu, J. (2013). Regulation of glycolysis and the Warburg effect by estrogen-related receptors. Oncogene *32*, 2079-2086.

119. I. T. Jolliffe, *Principal Component Analysis*. New York: Springer, 2002

120. Centanin, L., Ratcliffe, P.J., and Wappner, P. (2005). Reversion of lethality and growth defects in Fatiga oxygen-sensor mutant flies by loss of hypoxia-inducible factor-alpha/Sima. EMBO Rep. *6*, 1070-1075.

121. Irizarry, R.A., Bolstad, B.M., Collin, F., Cope, L.M., Hobbs, B., and Speed, T.P. (2003). Summaries of Affymetrix GeneChip probe level data. Nucleic Acids Res. *31*, e15.

122. Tusher, V.G., Tibshirani, R., and Chu, G. (2001). Significance analysis of microarrays applied to the ionizing radiation response. Proc. Natl. Acad. Sci. U. S. A. *98*, 5116-5121.

123. Monserrate, J.P., Chen, M.Y., and Brachmann, C.B. (2012). Drosophila larvae lacking the bcl-2 gene, buffy, are sensitive to nutrient stress, maintain increased basal

target of rapamycin (Tor) signaling and exhibit characteristics of altered basal energy metabolism. BMC Biol. *10*, 63-7007-10-63.

124. Dehaven, C.D., Evans, A.M., Dai, H., and Lawton, K.A. (2010). Organization of GC/MS and LC/MS metabolomics data into chemical libraries. J. Cheminform *2*, 9-2946-2-9.

125. Evans A.M., DeHaven C.D., Barrett T., Mitchell M., Milgram E. (2009). Integrated, nontargeted ultrahigh performance liquid chromatography/electrospray ionization tandem mass spectrometry platform for the identification and relative quantification of the small-molecule complement of biological systems. Anal. Chem. *81*, 6656–6667.

126. Baker, K.D., Beckstead, R.B., Mangelsdorf, D.J., and Thummel, C.S. (2007). Functional interactions between the Moses corepressor and DHR78 nuclear receptor regulate growth in Drosophila. Genes Dev. *21*, 450-464.

127. Robin, E.D., Murphy, B.J., and Theodore, J. (1984). Coordinate regulation of glycolysis by hypoxia in mammalian cells. J. Cell. Physiol. *118*, 287-290.

128. Acevedo, J.M., Centanin, L., Dekanty, A., and Wappner, P. (2010). Oxygen sensing in Drosophila: multiple isoforms of the prolyl hydroxylase fatiga have different capacity to regulate HIFalpha/Sima. PLoS One *5*, e12390.

129. Lavista-Llanos, S., Centanin, L., Irisarri, M., Russo, D.M., Gleadle, J.M., Bocca, S.N., Muzzopappa, M., Ratcliffe, P.J., and Wappner, P. (2002). Control of the hypoxic

response in Drosophila melanogaster by the basic helix-loop-helix PAS protein similar. Mol. Cell. Biol. *22,* 6842-6853.

130. Beissbarth, T., and Speed, T.P. (2004). GOstat: find statistically overrepresented Gene Ontologies within a group of genes. Bioinformatics *20,* 1464-1465.

131. Zhang, H., Bosch-Marce, M., Shimoda, L.A., Tan, Y.S., Baek, J.H., Wesley, J.B., Gonzalez, F.J., and Semenza, G.L. (2008). Mitochondrial autophagy is an HIF-1-dependent adaptive metabolic response to hypoxia. J. Biol. Chem. *283,* 10892-10903.

132. Rosenfeld, M.G., Lunyak, V.V., and Glass, C.K. (2006). Sensors and signals: a coactivator/corepressor/epigenetic code for integrating signal-dependent programs of transcriptional response. Genes Dev. *20,* 1405-1428.

133. Vengellur, A., Woods, B.G., Ryan, H.E., Johnson, R.S., and LaPres, J.J. (2003). Gene expression profiling of the hypoxia signaling pathway in hypoxia-inducible factor 1alpha null mouse embryonic fibroblasts. Gene Expr. *11,* 181-197.

134. Krishnamachary, B., Berg-Dixon, S., Kelly, B., Agani, F., Feldser, D., Ferreira, G., Iyer, N., LaRusch, J., Pak, B., Taghavi, P., and Semenza, G.L. (2003). Regulation of colon carcinoma cell invasion by hypoxia-inducible factor 1. Cancer Res. *63,* 1138-1143.

135. Firth, J.D., Ebert, B.L., and Ratcliffe, P.J. (1995). Hypoxic regulation of lactate dehydrogenase A. Interaction between hypoxia-inducible factor 1 and cAMP response elements. J. Biol. Chem. *270,* 21021-21027.

136. Kaneko, K., Furuyama, K., Aburatani, H., and Shibahara, S. (2009). Hypoxia induces erythroid-specific 5-aminolevulinate synthase expression in human erythroid cells through transforming growth factor-beta signaling. Febs j. *276,* 1370-1382.

137. Suzuki, A., Kusakai, G., Shimojo, Y., Chen, J., Ogura, T., Kobayashi, M., and Esumi, H. (2005). Involvement of transforming growth factor-beta 1 signaling in hypoxia-induced tolerance to glucose starvation. J. Biol. Chem. *280,* 31557-31563.

138. Zhang, F.L., Shen, G.M., Liu, X.L., Wang, F., Zhao, H.L., Yu, J., and Zhang, J.W. (2011). Hypoxic induction of human erythroid-specific delta-aminolevulinate synthase mediated by hypoxia-inducible factor 1. Biochemistry *50,* 1194-1202.

139. Church, R.B., and Robertson, F.W. (1966). Biochemical analysis of genetic differences in the growth of Drosophila. Genet. Res. *7,* 383-407.

140. Greganova, E., Altmann, M., and Butikofer, P. (2011). Unique modifications of translation elongation factors. Febs j. *278,* 2613-2624.

141. Ortiz, P.A., Ulloque, R., Kihara, G.K., Zheng, H., and Kinzy, T.G. (2006). Translation elongation factor 2 anticodon mimicry domain mutants affect fidelity and diphtheria toxin resistance. J. Biol. Chem. *281,* 32639-32648.

142. Gupta, P.K., Liu, S., Batavia, M.P., and Leppla, S.H. (2008). The diphthamide modification on elongation factor-2 renders mammalian cells resistant to ricin. Cell. Microbiol. *10,* 1687-1694.

143. Uniacke, J., Holterman, C.E., Lachance, G., Franovic, A., Jacob, M.D., Fabian, M.R., Payette, J., Holcik, M., Pause, A., and Lee, S. (2012). An oxygen-regulated switch in the protein synthesis machinery. Nature *486*, 126-129.

144. Dekanty, A., Lavista-Llanos, S., Irisarri, M., Oldham, S., and Wappner, P. (2005). The insulin-PI3K/TOR pathway induces a HIF-dependent transcriptional response in Drosophila by promoting nuclear localization of HIF-alpha/Sima. J. Cell. Sci. *118*, 5431-5441.

145. Broughton, S.J., Piper, M.D., Ikeya, T., Bass, T.M., Jacobson, J., Driege, Y., Martinez, P., Hafen, E., Withers, D.J., Leevers, S.J., and Partridge, L. (2005). Longer lifespan, altered metabolism, and stress resistance in Drosophila from ablation of cells making insulin-like ligands. Proc. Natl. Acad. Sci. U. S. A. *102*, 3105-3110.

146. Rulifson, E.J., Kim, S.K., and Nusse, R. (2002). Ablation of insulin-producing neurons in flies: growth and diabetic phenotypes. Science *296*, 1118-1120.

147. Belgacem, Y.H., and Martin, J.R. (2006). Disruption of insulin pathways alters trehalose level and abolishes sexual dimorphism in locomotor activity in Drosophila. J. Neurobiol. *66*, 19-32.

148. Eaton, S.B., and Konner, M. (1985). Paleolithic nutrition. A consideration of its nature and current implications. N. Engl. J. Med. *312*, 283-289.

149. Schroeder, F., Petrescu, A.D., Huang, H., Atshaves, B.P., McIntosh, A.L., Martin, G.G., Hostetler, H.A., Vespa, A., Landrock, D., Landrock, K.K., Payne, H.R., and Kier, A.B. (2008). Role of fatty acid binding proteins and long chain fatty acids in modulating nuclear receptors and gene transcription. Lipids *43,* 1-17.

150. Griffin, J.L., Atherton, H., Shockcor, J., and Atzori, L. (2011). Metabolomics as a tool for cardiac research. Nat. Rev. Cardiol. *8,* 630-643.

151. Di Marzo, V. (2008). The endocannabinoid system in obesity and type 2 diabetes. Diabetologia *51,* 1356-1367.

152. McCullough, A.J. (2011). Epidemiology of the metabolic syndrome in the USA. J. Dig. Dis. *12,* 333-340.

153. Michael M. Cox and David L. Nelson, Lehninger Principles of Biochemistry. W.H.Freeman, 2008.

154. Wanders, R.J., Komen, J., and Kemp, S. (2011). Fatty acid omega-oxidation as a rescue pathway for fatty acid oxidation disorders in humans. Febs j. *278,* 182-194.

155. Xu, X., Gopalacharyulu, P., Seppanen-Laakso, T., Ruskeepaa, A.L., Aye, C.C., Carson, B.P., Mora, S., Oresic, M., and Teleman, A.A. (2012). Insulin signaling regulates fatty acid catabolism at the level of CoA activation. PLoS Genet. *8,* e1002478.

156. Allred, J.B., and Reilly, K.E. (1996). Short-term regulation of acetyl CoA carboxylase in tissues of higher animals. Prog. Lipid Res. *35,* 371-385.

157. Hardie, D.G., Corton, J., Ching, Y.P., Davies, S.P., and Hawley, S. (1997). Regulation of lipid metabolism by the AMP-activated protein kinase. Biochem. Soc. Trans. *25*, 1229-1231.

158. Mascaro, C., Acosta, E., Ortiz, J.A., Marrero, P.F., Hegardt, F.G., and Haro, D. (1998). Control of human muscle-type carnitine palmitoyltransferase I gene transcription by peroxisome proliferator-activated receptor. J. Biol. Chem. *273*, 8560-8563.

159. Brandt, J.M., Djouadi, F., and Kelly, D.P. (1998). Fatty acids activate transcription of the muscle carnitine palmitoyltransferase I gene in cardiac myocytes via the peroxisome proliferator-activated receptor alpha. J. Biol. Chem. *273*, 23786-23792.

160. Grewal, S.S. (2009). Insulin/TOR signaling in growth and homeostasis: a view from the fly world. Int. J. Biochem. Cell Biol. *41*, 1006-1010.

161. Stralfors, P., and Honnor, R.C. (1989). Insulin-induced dephosphorylation of hormone-sensitive lipase. Correlation with lipolysis and cAMP-dependent protein kinase activity. Eur. J. Biochem. *182*, 379-385.

162. Kershaw, E.E., Hamm, J.K., Verhagen, L.A., Peroni, O., Katic, M., and Flier, J.S. (2006). Adipose triglyceride lipase: function, regulation by insulin, and comparison with adiponutrin. Diabetes *55*, 148-157.

163. Sidossis, L.S., Stuart, C.A., Shulman, G.I., Lopaschuk, G.D., and Wolfe, R.R. (1996). Glucose plus insulin regulate fat oxidation by controlling the rate of fatty acid entry into the mitochondria. J. Clin. Invest. *98,* 2244-2250.

164. Bastie, C.C., Nahle, Z., McLoughlin, T., Esser, K., Zhang, W., Unterman, T., and Abumrad, N.A. (2005). FoxO1 stimulates fatty acid uptake and oxidation in muscle cells through CD36-dependent and -independent mechanisms. J. Biol. Chem. *280,* 14222-14229.

165. Xu, X., Gopalacharyulu, P., Seppanen-Laakso, T., Ruskeepaa, A.L., Aye, C.C., Carson, B.P., Mora, S., Oresic, M., and Teleman, A.A. (2012). Insulin signaling regulates fatty acid catabolism at the level of CoA activation. PLoS Genet. *8,* e1002478.

166. Rakhshandehroo, M., Knoch, B., Muller, M., and Kersten, S. (2010). Peroxisome proliferator-activated receptor alpha target genes. PPAR Res. *2010,* 10.1155/2010/612089. Epub 2010 Sep 26.

167. Lin, J., Handschin, C., and Spiegelman, B.M. (2005). Metabolic control through the PGC-1 family of transcription coactivators. Cell. Metab. *1,* 361-370.

168. Green, P.R., and Geer, B.W. (1979). Changes in the fatty acid composition of Drosophila melanogaster during development and ageing. Arch. Int. Physiol. Biochim. *87,* 485-491.

169. Oba, Y., Sato, M., Ojika, M., and Inouye, S. (2005). Enzymatic and genetic characterization of firefly luciferase and Drosophila CG6178 as a fatty acyl-CoA synthetase. Biosci. Biotechnol. Biochem. *69,* 819-828.

170. Min, K.T., and Benzer, S. (1999). Preventing neurodegeneration in the Drosophila mutant bubblegum. Science *284,* 1985-1988.

171. Pei, Z., Jia, Z., and Watkins, P.A. (2006). The second member of the human and murine bubblegum family is a testis- and brainstem-specific acyl-CoA synthetase. J. Biol. Chem. *281,* 6632-6641.

172. Steinberg, S.J., Morgenthaler, J., Heinzer, A.K., Smith, K.D., and Watkins, P.A. (2000). Very long-chain acyl-CoA synthetases. Human "bubblegum" represents a new family of proteins capable of activating very long-chain fatty acids. J. Biol. Chem. *275,* 35162-35169.

173. Sladek, R., Bader, J.A., and Giguere, V. (1997). The orphan nuclear receptor estrogen-related receptor alpha is a transcriptional regulator of the human medium-chain acyl coenzyme A dehydrogenase gene. Mol. Cell. Biol. *17,* 5400-5409.

174. Gacias, M., Perez-Marti, A., Pujol-Vidal, M., Marrero, P.F., Haro, D., and Relat, J. (2012). PGC-1beta regulates mouse carnitine-acylcarnitine translocase through estrogen-related receptor alpha. Biochem. Biophys. Res. Commun. *423,* 838-843.

175. “FlyAtlas: the Drosophila gene expression atlas”, latest news November 22, 2012. http://130.209.54.32/atlas/atlas.cgi?name=FBgn0028519.

176. Park, S.H., Gammon, S.R., Knippers, J.D., Paulsen, S.R., Rubink, D.S., and Winder, W.W. (2002). Phosphorylation-activity relationships of AMPK and acetyl-CoA carboxylase in muscle. J. Appl. Physiol. (1985) *92,* 2475-2482.

177. Heinrich, E.C., Farzin, M., Klok, C.J., and Harrison, J.F. (2011). The effect of developmental stage on the sensitivity of cell and body size to hypoxia in Drosophila melanogaster. J. Exp. Biol. *214,* 1419-1427.

178. Lee, T., and Luo, L. (1999). Mosaic analysis with a repressible cell marker for studies of gene function in neuronal morphogenesis. Neuron *22,* 451-461.

179. Suster, M.L., Seugnet, L., Bate, M., and Sokolowski, M.B. (2004). Refining GAL4-driven transgene expression in Drosophila with a GAL80 enhancer-trap. Genesis *39,* 240-245.

180. Fujikawa, K., Takahashi, A., Nishimura, A., Itoh, M., Takano-Shimizu, T., and Ozaki, M. (2009). Characteristics of genes up-regulated and down-regulated after 24 h starvation in the head of Drosophila. Gene *446,* 11-17.

181. Tiefenbock, S.K., Baltzer, C., Egli, N.A., and Frei, C. (2010). The Drosophila PGC-1 homologue Spargel coordinates mitochondrial activity to insulin signalling. Embo j. *29,* 171-183.

APPENDIX

A Appendix table 1 Hypoxia-regulated gene sets identified by microarray analysis.

B Appendix table 2 Metabolic analysis of carbohydrates by GC/MS and LC/MS.

C **Author contributions**: Keith D. Baker conceived and designed the experiments. Yan Li performed most experiments, Catherine Dumur performed all the microarray analyses, Metabolon Inc. performed the GC/LC-MS, and Keith D. Baker performed the yeast two hybrid analysis and the GST pull- down experiments. Yan Li and Keith D. Baker analyzed the data, and performed statistical analysis. Leon Avery performed the principle component analysis. Contributed reagents/materials/analysis tools: Bloomington Stock Center provided several fly strains, and Jessica Bell provided the purified GST recombinant protein.

VITA

Yan Li was born on July 3, 1983, in Beijing, P.R.China, and is a citizen of People's Republic of China. She graduated from Beijing No.5 High School, Beijing, P.R.China in 1998. She received her Bachelor of Science in Clinical Medicine from Shandong University, Jinan, Shandong province, P.R.China in 2007. She received an excellent student scholarship from Shandong University in 2002. In her last year of college, she did one year of internship in Jinan Central Hospital, Jinan, Shandong Province. She published a paper titled as "HIF- and Non-HIF-Regulated Hypoxic Responses Require the Estrogen-Related Receptor in *Drosophila melanogaster*" in PLoS Genetics in 2013.